

Neutrinoless double beta decay and neutrino mass

J.D. VERGADOS

*ARC Centre of Excellence in Particle Physics (CoEPP), Department of Physics, University of Adelaide, Adelaide SA 5005, Australia**

Center for Axion and Precision Physics Research, Institute for Basic Science (IBS), Daejeon 34141, Republic of Korea and

Board of Trustees, Technical Educational Institute, Kozani, Greece.

H. EJIRI

RCNP, Osaka University, Osaka, 567-0047, Japan and

Nuclear Science, Czech Technical University, Brehova, Prague, Czech Republic.

F Šimkovic

*Laboratory of Theoretical Physics, JINR, 141980 Dubna, Moscow region, Russia and
Department of Nuclear Physics and Biophysics, Comenius University, Mlynská dolina F1,
SK-842 15 Bratislava, Slovakia and*

Czech Technical University in Prague, 128-00 Prague, Czech Republic.

Abstract

The observation of neutrinoless double beta decay will have important consequences. First it will signal that lepton number is not conserved and the neutrinos are Majorana particles. Second, it represents our best hope for determining the absolute neutrino mass scale at the level of a few tens of meV. To achieve the last goal, however, certain hurdles have to be overcome involving particle, nuclear and experimental physics.

Particle physics is important since it provides the mechanisms for neutrinoless double beta decay. In this review we emphasize the light neutrino mass mechanism.

Nuclear physics is important for extracting the useful information from the data. One must accurately evaluate the relevant nuclear matrix elements, a formidable task. To this end, we review the recently developed sophisticated nuclear structure approaches, employing different methods and techniques of calculation. We also examine the question of quenching of the axial vector coupling constant, which may have important consequences on the size of the nuclear matrix elements.

From an experimental point of view it is challenging, since the life times are extremely long and one has to fight against formidable backgrounds. One needs large isotopically enriched sources and detectors with good energy resolution and very low background.

*Permanent address: Theoretical Physics Division, University of Ioannina, GR 451 10 Ioannina, Greece.

Keywords: Double Beta Decay, DBD, neutrino mass, neutrino mixing, Majorana neutrinos, 0- decay, 2- decay, lepton number, lepton flavor, see-saw, sterile neutrino, normal hierarchy, inverted hierarchy, Higgs, GUTs, detector sensitivity, isotope enrichment, energy threshold, life-time. background, ISM, QRPA, PHFB, IBM, nuclear NE, vector, axial, form factor, quenching, left-handed currents

1. A brief history of double beta decay

Double beta decay (DBD), namely the non exotic two-neutrino double-beta decay ($2\nu\beta\beta$ -decay)

$$(A, Z) \rightarrow (A, Z + 2) + e^- + e^- + \bar{\nu}_e + \bar{\nu}_e, \quad (1)$$

was first considered in publication¹ of Maria Goeppert-Mayer in 1935, following the suggestion of Eugene Wigner about one year after the Fermi weak interaction theory appeared. In this work an expression for the $2\nu\beta\beta$ -decay rate was derived and a half-life of 10^{17} years was estimated, assuming a Q-value of about 10 MeV.

Two years later (1937) Ettore Majorana formulated a new theory of neutrinos, whereby the neutrino ν and the antineutrino $\bar{\nu}$ are indistinguishable, and suggested antineutrino induced β^- -decay for experimental verification of this hypothesis.² In 1939, Wolfgang Furry considered for the first time neutrinoless double beta decay ($0\nu\beta\beta$ -decay),

$$(A, Z) \rightarrow (A, Z + 2) + e^- + e^-, \quad (2)$$

The available energy Δ is equal to the Q-value of the reaction, i.e. the mass difference of the ground states of the two atoms involved.

In 1952 Henry Primakoff³ calculated the electron-electron angular correlations and electron energy spectra for both the $2\nu\beta\beta$ -decay and the $0\nu\beta\beta$ -decay, producing a useful tool for distinguishing between the two processes. At that time, however, nothing was known about the chirality suppression of the $0\nu\beta\beta$ -decay. It was believed that, due to a considerable phase-space advantage, the $0\nu\beta\beta$ -decay mode dominates the double beta decay rate. Starting in 1950 this phenomenon was exploited in early geochemical, radiochemical and counter experiments. It was found that the measured lower limit on the $\beta\beta$ -decay half-life far exceeds the values expected for this process, $T_{1/2}^{0\nu} \sim 10^{12} - 10^{15}$ years. In 1955 the Raymond Davis experiment⁴ searching for the antineutrinos from reactor via nuclear reaction $\bar{\nu}_e + {}^{37}\text{Cl} \rightarrow {}^{37}\text{Ar} + e^-$, produced a zero result. The above experiments were interpreted as proof that the neutrino was not a Majorana particle, but a Dirac particle. This prompted the introduction of the lepton number to distinguish the neutrino from its antiparticle. The assumption of lepton number conservation allows the $2\nu\beta\beta$ -decay but forbids the $0\nu\beta\beta$ -decay, in which lepton number is changed by two units.

The first geochemical observation of the $\beta\beta$ -decay, with an estimated half-life $T_{1/2}(^{130}\text{Te}) = 1.4 \times 10^{21}$ years, was announced by Ingram and Reynolds in 1950.⁵ Extensive studies have been made by Gentner and Kirsten^{6,7} and others,^{8,9} on such rare-gas isotopes as ^{82}Kr , ^{128}Xe , and ^{130}Xe , which are $\beta\beta$ -decay products of ^{82}Se , ^{128}Te , and ^{130}Te , respectively, obtaining half lives around 10^{21}y for ^{130}Te .

Within the Standard Model (SM) it became apparent that the assumption of lepton number conservation led to the neutrino being strictly massless. With the development of Grand Unified Theories (GUT's) of the electroweak and strong interactions, it was realized that lepton number conservation was the result of a global symmetry not of a gauge symmetry and had to be broken at some level. In such models one could distinguish between the neutrinos produced in weak interactions (flavor neutrinos) and the eigenstates of the world Hamiltonian. The latter eigenstates can naturally be Majorana neutrinos, while Dirac type eigenstates could arise as a special case. The flavor neutrinos could still be of Dirac type, if the Majorana phases of the eigenstates are all the same, in agreement with Davis experiment.⁴ Thus, through the pioneering work of Kotani and his group,¹⁰ the interest in $0\nu\beta\beta$ -decay experiments was revived and brought it again to the attention of the nuclear physics community.

The $0\nu\beta\beta$ -decay, which involves the emission of two electrons and no neutrinos, has been found to be more than a tool in studying lepton number violating processes. Schechter and Valle proved that, if the $0\nu\beta\beta$ -decay takes place, regardless of the mechanism causing it, the neutrinos are Majorana particles with non-zero mass.^{11,12} It was also recognized that the GUT's and R-parity violating SUSY models offer a plethora of the $0\nu\beta\beta$ -decay mechanisms triggered by exchange of neutrinos, neutralinos, gluinos, leptoquarks, etc.¹³⁻¹⁵

The experimental effort concentrated on high $Q_{\beta\beta}$ isotopes, in particular on ^{48}Ca , ^{76}Ge , ^{82}Se , ^{96}Zr , ^{100}Mo , ^{116}Cd , ^{130}Te , ^{136}Xe and ^{150}Nd .¹⁶⁻¹⁹ In 1987 the first actual laboratory observation of the two neutrino double beta decay ($2\nu\beta\beta$ -decay) was done for ^{82}Se by M. Moe and collaborators,²⁰ who used a time projection chamber. Within the next few years, experiments employing counters were able to detect $2\nu\beta\beta$ -decay of many nuclei. In addition, the experiments searching for the signal of the $0\nu\beta\beta$ -decay pushed by many orders of magnitude the experimental lower limits for the $0\nu\beta\beta$ -decay half-life of different nuclei.

A great leap forward was achieved, when, early measurements of neutrinos produced in the sun, in the atmosphere, and by accelerators, suggested that neutrinos may oscillate from one "flavor" (electron, muon, and tau) to another, expected if the neutrinos are massive and non degenerate in mass. Non-zero neutrino mass can be accommodated by fairly straightforward extensions of the SM of particle physics. Thus now, starting in 1998, we have convincing evidence about the existence of non zero neutrino masses in SuperKamiokande,²¹ SNO,²² KamLAND²³ and other experiments. Such experiments, however, cannot determine the absolute scale of neutrino mass. So the determination of the scale of neutrino mass has been directed to other methods, such as cosmological observations, β -decay experiments

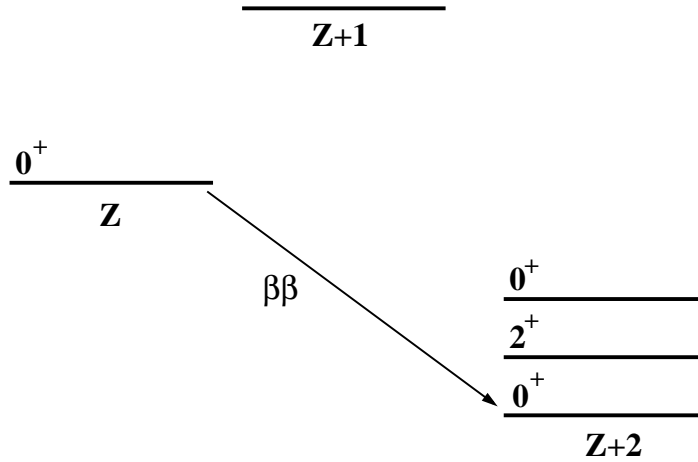


Fig. 1. Schematic diagrams of $\beta\beta$ decays in nuclear femto (10^{-15}m) laboratories, where single β -decay is forbidden, while neutrinoless double-beta decay is allowed.

and, especially if the scale happens to be in the meV range, to $0\nu\beta\beta$ -decay, see, e.g., the recent review.²⁴

So far the $2\nu\beta\beta$ -decay has been recorded for eleven nuclei (^{48}Ca , ^{76}Ge , ^{82}Se , ^{96}Zr , ^{100}Mo , ^{116}Cd , ^{128}Te , ^{130}Te , ^{150}Nd , ^{136}Xe , ^{238}U).^{16–18} In addition, the $2\nu\beta\beta$ -decay to the first 0^+ excited state of the daughter nucleus has been observed in the case of the targets ^{100}Mo and ^{150}Nd . Furthermore the two-neutrino double electron capture process in ^{130}Ba has been recorded.

Neutrinoless double beta decay has not yet been confirmed. The strongest limit recently obtained is $T_{1/2} > 1.1 \times 10^{26}\text{y}$ by Gando *et al*²⁵ (see section 6 for details).

If the neutrinos are Majorana particles other related processes in which the charge of the nucleus is decreased by two units may also occur, if they happen to be allowed by energy and angular momentum conservation laws, e.g. double positron emission, electron positron conversion, resonant neutrinoless double electron capture ($0\nu\text{ECEC}$).^{26–29} This is an interesting topic with a lot of theoretical work^{30–34} and it appears promising in view of progress in accurately determining the Q -values³⁵ needed to establish the condition of resonance employing Penning traps.^{36–38} Recently, the accuracy of Q -values at around 100 eV was achieved,^{39–50} which has already allowed to exclude some of isotopes from the list of the most promising candidates (e.g., ^{112}Sn and ^{164}Er) for searching the $0\nu\text{ECEC}$. In spite of the fact that an increased experimental activity in the field of the resonant $0\nu\text{ECEC}$ ^{51–57} in the case of ^{106}Cd ⁵⁵ and ^{112}Sn .⁵³ Resonant $0\nu\text{ECEC}$ has some im-

portant advantages with respect to experimental signatures and background conditions, but we do not know of any experiment under way in this direction and we are not going to review this field further.

Anyway $0\nu\beta\beta$ -decay (Eq. (2)), seventy five years after it was first conceived, seems to be the most likely to yield the information^{58–65} we seek.

2. Motivation for pursuing neutrinoless double beta decay

From a nuclear physics^{62,63,66–70} point of view, calculating the relevant nuclear matrix elements is indeed a challenge. First almost all nuclei, which can undergo double beta decay, are far from closed shells and some of them are even deformed. One thus faces a formidable task. Second the nuclear matrix elements are small compared to a canonical value, like the one associated with the matrix element to the (energy non allowed) double Gamow-Teller resonance or a small fraction of some appropriate sum rule. Thus, effects which are normally negligible, become important here. Third, in many models the dominant mechanism for $0\nu\beta\beta$ -decay may not involve intermediate light neutrinos, but very heavy particles. Thus one must be able to cope with the short distance behavior of the relevant operators (see section 8 for details).

It is also important from a particle physics point of view. The recent discovery of neutrino oscillations^{21,71–75} have given the first evidence of the fact that the neutrinos are massive, which necessitates to go beyond the Standard Model (SM) of particle physics. More specifically these experiments showed that the neutrinos are admixed and determined all three mixing angles (for a global analysis see, e.g.,^{76,77}). Furthermore they determined one square mass difference Δm_{21}^2 and the absolute value of the other, i.e. Δm_{32}^2 or Δm_{31}^2 . Future neutrino oscillations in matter are expected to fix the unknown sign. Neutrino oscillations, however, cannot determine:

- Whether the neutrinos are Majorana or Dirac particles.

It is obviously important to proceed further and decide on this important issue. Neutrinoless double beta decay can achieve this, even though, as we have mentioned, there might be other lepton violating processes contributing to $0\nu\beta\beta$ -decay. It is known that whatever lepton number violating process gives rise to $0\nu\beta\beta$ -decay, it can be used to generate a Majorana mass for the neutrino.¹¹

- The scale of the neutrino masses.

This task can be accomplished by astrophysical observations or via other experiments involving low energy weak decays, like triton decay or electron capture, or the $0\nu\beta\beta$ -decay. It seems that for a neutrino mass scale in meV, (10^{-3} eV), region, the best process to achieve this is the $0\nu\beta\beta$ -decay. The extraction of neutrino masses from such observations will be discussed in detail and compared with each other later (see section 4).²⁴ This mechanism, however, is not the only one, which can induce $0\nu\beta\beta$ -decay. If, however, $0\nu\beta\beta$ is ever found to occur, it will be possible to disentangle the most

important neutrino mass contribution, involving the neutrino mass scale, from the other mechanisms, provided that data on a number of targets become available.

The neutrino hierarchy, i.e. whether the neutrinos are almost degenerate, the normal hierarchy ($\Delta m_{32}^2 > 0$) or the inverted hierarchy ($\Delta m_{31}^2 < 0$), can also be inferred from double beta decay. For details on such issues see recent reviews.^{24,78–80} As we have mentioned to extract useful information from the $0\nu\beta\beta$ decay one must know the nuclear matrix elements^a. Efforts to this end can be summarized as follows:

1. Shell model calculations. These have a long history^{69,70,83–87} in double beta decay calculations. In recent years it has lead to large matrix calculations in traditional as well as Monte Carlo types of formulations.^{66–68,88–91} For a more complete set of references as well as a discussion of the appropriate effective interactions see Ref.⁶²).

2. QRPA calculations. There have been a number of such calculations covering almost all nuclear targets.^{92–104} These involve a number of collaborations, but the most extensive and complete calculations in one way or another include the Tuebingen group. We also have seen some refinements of QRPA, like proton neutron pairing, inclusion of renormalization effects due to Pauli principle corrections^{105,106} and isospin restoration.¹⁰⁷ Other less conventional approaches, like operator expansion techniques have also been employed.⁶³

3. Other nuclear models. Recently, calculations based on the Projected Hartree-Fock-Bogoliubov (PHFB) method,¹⁰⁸ the Interacting Boson Model (IBM)^{109,110} and the Energy Density Functional (EDF) method⁹¹ and relativistic EDF (REDF)¹¹¹ entered the field of such calculations.

The above schemes, in conjunction with the other improvements mentioned above, offer some optimism in our efforts for obtaining nuclear matrix elements accurate enough to allow us to extract reliable values of the lepton violating parameters from the data.

The experimental results will be examined and discussed in section 6.

3. The neutrino mass and mixing

Within the SM of elementary particles, with the particle content of the gauge bosons A_μ, Z_μ and $W_\mu^{\pm,0}$, the Higgs scalar isodoublet $\Phi = (\phi^0, \phi^-)$ (and its conjugate Φ^*) and the fermion fields arranged in:

- Isodoublets: $(u_{\alpha L}, d_{\alpha L})$ and $(\nu_{\alpha L}, e_{\alpha L})$ for quarks and leptons respectively and
- Isosinglets: $u_{\alpha R}, d_{\alpha R}$ and $e_{\alpha R}$

^aIt is not possible to deduce the expected neutrino mass from $0\nu\beta\beta$ employing Bayesian statistics⁸¹ based on a Markov chain Monte Carlo,⁸² since one cannot avoid the issue related to other possible mechanisms contributing to the process.

where α is a family index taking three values. In the context of the standard model (SM) the neutrinos are massless. They can not obtain mass after the symmetry breaking, like the quarks and the charged leptons do, since the right handed neutrino is absent.

3.1. Neutrino mass

The minimal extension of the SM that would yield mass for the neutrino is to introduce an isosinglet right handed neutrino. Then one can have a Dirac mass term arising via coupling of the leptons and Higgs.^{24,79,80} The existence of Dirac neutrinos is fine within the above minimal extension, but this is not interesting from our point of view, since the particle cannot be the same with its antiparticle and, thus, it cannot lead to neutrinoless double beta decay. Furthermore in grand unified theories one is faced with the problem that these neutrinos are going to be very heavy with a mass similar to that of up quarks, which is clearly unacceptable. So such a model is inadequate^b. The next extension of the SM is to introduce a Majorana type mass involving the isosinglet neutrinos and an additional isosinglet Higgs field, which can acquire a large vacuum expectation value, an idea essentially put forward by Weinberg¹¹³ long time ago. Thus the neutrino mass matrix becomes:²⁴

$$\mathcal{M} = (\bar{\nu}_L, \bar{\nu}_L^c) \begin{pmatrix} 0 & m^D \\ (m^D)^T & m_R \end{pmatrix} \begin{pmatrix} \nu_R \\ \nu_R^c \end{pmatrix} \quad (3)$$

Thus, provided that the Majorana mass matrix has only very large eigenvalues, one obtains an effective Majorana 3×3 matrix:

$$\mathcal{M}_\nu = -\bar{\nu}_L (m^D)^T M_R^{-1} m_D \nu_R^c, \quad (4)$$

which can provide small neutrino masses provided that the eigenvalues of the matrix M_R are sufficiently large. M_R can be arbitrarily large and is identified the total lepton number violating (LNV) scale indicated by m_{LNV} . This new scale, commonly associated with the vacuum expectation of the isosinglet, does not affect the low energy scale arising from the vacuum expectation value of the standard Higgs particles.

This is the celebrated see-saw mechanism. More precisely there exist three see-saw types (see, e.g., Abada *et al*¹¹⁴ for a summary and more recently^{115,116}). Furthermore in some of these versions¹¹⁶ new contributions to neutrinoless double beta decay are claimed. A more systematic decomposition of the neutrinoless double beta decay operator has also recently appeared.¹¹⁷

It is possible for the heavy Majorana neutrinos not to be equally heavy. By appropriately arranging the corresponding Dirac coupling, it is possible to get one

^bThere may exist light Dirac neutrinos in theories formulated in extra dimensions, see e.g. the recent review by Smirnov.¹¹² If these neutrinos do not couple to the usual leptons they are of little interest to us. If they do and it so happens that the standard neutrinos are Majorana, they also become Majorana, except in the case of very fine tuning.

Majorana neutrino in the keV scale, which couples very weakly to the three light neutrinos. This is the so called sterile neutrino.

Anyway with the see-saw mechanism the neutrino flavors get admixed, the resulting eigenstates are Majorana particles and lepton number violating interactions, like $0\nu\beta\beta$ decay, become possible.

Other extensions of the SM, which do not require the presence of right-handed neutrinos, are possible in which a light 3×3 Majorana mass matrix m_ν can be generated via an isotriplet scalar acquiring a vacuum expectation value or via its couplings to two isodoublet scalar fields at tree or at the one loop level. It is also possible to achieve this via generic diagrams involving Weinberg's idea.^{113,118} By introducing exotic isosinglet or isotriplet fermions or in the context of R-parity violating supersymmetry.¹¹⁹ We will not consider these possibilities, since they have been examined elsewhere.²⁴ We should mention, however, that there exist models which generate Majorana masses at the 2-loop level, first proposed long time ago¹²⁰ as an economic way of getting neutrino Majorana mass. In one such approach,¹²¹ reinventing the extended Majorana matrix,¹²² now coined inverse see-saw, it is claimed that, using the available neutrino oscillation data, the full Majorana matrix can be determined leading to a prediction of the Majorana phases.

3.2. Neutrino mixing

We have seen above that in general the neutrino mass matrix, Eq. (3), is a complex symmetric matrix. It can, however, be diagonalized by separate left and right unitary transformations^{58,24}

$$\begin{aligned} S_L \leftrightarrow (\nu_L^0, \nu_L^{0c}) &= \begin{pmatrix} S^{(11)} & S^{(12)} \\ S^{(21)} & S^{(11)} \end{pmatrix} \begin{pmatrix} \nu'_L \\ N'_L \end{pmatrix}, \\ S_R \leftrightarrow (\nu_R^{0c}, \nu_R^0) &= \begin{pmatrix} (S^{(11)})^* & (S^{(12)})^* \\ (S^{(21)})^* & (S^{(22)})^* \end{pmatrix} \begin{pmatrix} \nu'_R \\ N'_R \end{pmatrix} \end{aligned} \quad (5)$$

where we have added the superscript 0 to stress that they are the states entering the weak interactions. $S^{(ij)}$ are 3×3 matrices with $S^{(11)}$ and $S^{(22)}$ approximately unitary, while $S^{(12)}$ and $S^{(21)}$ are very small. (ν'_L, N'_L) and (ν'_R, N'_R) are the eigenvectors from the left and the right respectively. Thus the neutrino mass in the new basis takes the form:

$$\mathcal{M}_\nu = \sum_{j=1}^3 (m_j \bar{\nu}'_{jL} \nu'_{jR} + M_j \bar{N}'_{jL} N'_{jR}) + H.C. \quad (6)$$

This matrix can be brought into standard form by writing:

$$m_j = |m_j| e^{-i\alpha_j}, \quad M_j = |M_j| e^{-i\Phi_j}$$

and defining:

$$\nu_j = \nu'_{jL} + e^{-i\alpha_j} \nu'_{jR} \quad N_j = \nu'_{jL} + e^{-i\Phi_j} N'_{jR}$$

$$\mathcal{M}_\nu = \sum_{j=1}^3 (|m_j| \bar{\nu}_j \nu_j + |M_j| \bar{N}_j N_j) \quad (7)$$

Note, however, that:

$$\begin{aligned} \nu^c &= \nu'_{jR} + e^{i\alpha_j} \nu'_{jL} = e^{i\alpha_j} (\nu'_{jL} + e^{-i\alpha_j} \nu'_{jR}) = e^{i\alpha_j} \nu_j \\ N^c &= N'_{jR} + e^{i\Phi_j} N'_{jL} = e^{i\Phi_j} (\nu'_{jR} + e^{-i\Phi_j} N'_{jL}) = e^{i\Phi_j} N_j \end{aligned} \quad (8)$$

i.e. they are Majorana neutrinos with the given Majorana phases. Furthermore

$$\nu_{iL} = \nu'_{iL}, \quad \nu_{iR} = e^{-i\alpha_j} \nu'_{iR}, \quad N_{iL} = N'_{iL}, \quad N_{iR} = e^{-i\Phi_j} \nu'_{iR}$$

The first of Eqs. (5) remains unchanged, while the second can now be written as

$$S_R \leftrightarrow (\nu_R^0, \nu_R^0) = \begin{pmatrix} (S^{(11)})^* & (S^{(12)})^* \\ (S^{(21)})^* & (S^{(22)})^* \end{pmatrix} \begin{pmatrix} e^{i\alpha} \nu_R \\ e^{i\Phi} N_R \end{pmatrix} \quad (9)$$

where $e^{i\alpha}$ and $e^{i\Phi}$ are diagonal matrices containing the above Majorana phases.

The full parametrization of matrix \mathcal{U} includes 15 rotational angles and 10 Dirac and 5 Majorana CP violating phases.

The neutrinos interact with the charged leptons via the charged current (see below). So the effective coupling of the neutrinos to the charged leptons involves the mixing of the electrons S^e . Thus the standard mixing matrix appearing in the absence of right-handed neutrinos is:

$$U_{PMNS} = U = U^{(11)} = (S^{(e)})^+ S^{(11)} \quad (10)$$

The other entries are defined analogously:

$$U^{(ij)} = (S^{(e)})^+ S^{(ij)}, \quad (ij) = (12), (21), (22) \quad (11)$$

In particular the usual electronic neutrino is written as:

$$\nu_{eL} = \sum_j (U_{ej}^{(11)} \nu_{jL} + U_{ej}^{(12)} N_{jL}), \quad \nu_{eL}^c = \sum_j (U_{ej}^{(21)} \nu_{jL} + U_{ej}^{(22)} N_{jL}) \quad (12)$$

$$\begin{aligned} \nu_{eR}^c &= \sum_j (U_{ej}^{(11)})^* e^{\alpha_j} \nu_{jR} + (U_{ej}^{(12)})^* e^{\Phi_j} N_{jR}, \\ \nu_{eR} &= \sum_j (U_{ej}^{(21)})^* e^{\alpha_j} \nu_{jR} + (U_{ej}^{(22)})^* e^{\Phi_j} N_{jR} \end{aligned} \quad (13)$$

In other words the left handed neutrino may have a small heavy component, while the right handed neutrino may have a small light component. Note also that the neutrinos appearing in weak interactions can be Majorana particles in the special case that all Majorana phases are the same.

Unfortunately the above notation is not unique. For the reader's convenience we mention that sometimes the notation

$$U^{(11)} \rightarrow U, U^{(12)} \rightarrow S, U^{(21)} \rightarrow T, U^{(22)} \rightarrow V \quad (14)$$

is employed.¹²³ It is also possible to decompose the 6×6 mixing matrix as follows¹²³

$$\mathcal{U} = \begin{pmatrix} \mathbf{1} & \mathbf{0} \\ \mathbf{0} & U_0 \end{pmatrix} \begin{pmatrix} A & R \\ S & B \end{pmatrix} \begin{pmatrix} V_0 & \mathbf{0} \\ \mathbf{0} & \mathbf{1} \end{pmatrix}, \quad (15)$$

where $\mathbf{0}$ and $\mathbf{1}$ are the 3×3 zero and identity matrices, respectively. The parametrization of matrices A, B, R and S and corresponding orthogonality relations are given in.¹²³ In the limit case $A = \mathbf{1}$, $B = \mathbf{1}$, $R = \mathbf{0}$ and $S = \mathbf{0}$ there would be a separate mixing of heavy and light neutrinos, which would participate only in left and right-handed currents, respectively. In that case only the neutrino mass mechanism of the $0\nu\beta\beta$ -decay would be allowed and exchange neutrino momentum dependent mechanisms associated with the W_L - W_R exchange and W_L - W_R mixing would be forbidden. If masses of heavy neutrinos are above the TeV scale, the mixing angles responsible for mixing of light and heavy neutrinos are small. By neglecting the mixing between different generations of light and heavy neutrinos A, B, R and S matrices can be approximated as follows:

$$A \approx \mathbf{1}, B \approx \mathbf{1}, R \approx \frac{m_D}{m_{LNV}} \mathbf{1}, S \approx -\frac{m_D}{m_{LNV}} \mathbf{1}. \quad (16)$$

Here, m_D represents energy scale of charged leptons and m_{LNV} is the total lepton number violating scale, which corresponds to masses of heavy neutrinos. For sake of simplicity the same mixing angle is assumed for each generation of mixing of light and heavy neutrinos. We see that U_0 can be identified to a good approximation with the PMNS matrix and V_0 is its analogue for heavy neutrino sector. Both of them are almost unitary matrices of order 1, but unrelated to each other. Since V_0 is unknown, sometimes it is assumed that the structure of V_0 is the same one as U_0 .

The situation is very much simplified, if the mixing between the light and heavy neutrinos is small²⁴ by diagonalizing the matrix given by Eq. (4). Then the mixing is described by the Pontecorvo-Maki-Nakagawa-Sakata neutrino mixing matrix U_{PMNS} , which is parametrized by

$$U_{PMNS} = \begin{pmatrix} c_{12}c_{13} & c_{13}s_{12} & e^{-i\delta}s_{13} \\ -c_{23}s_{12} - e^{i\delta}c_{12}s_{13}s_{23} & c_{12}c_{23} - e^{i\delta}s_{12}s_{13}s_{23} & c_{13}s_{23} \\ s_{12}s_{23} - e^{i\delta}c_{12}c_{23}s_{13} & -e^{i\delta}c_{23}s_{12}s_{13} - c_{12}s_{23} & c_{13}c_{23} \end{pmatrix}, \quad (17)$$

where

$$c_{ij} \equiv \cos(\theta_{ij}), \quad s_{ij} \equiv \sin(\theta_{ij}). \quad (18)$$

θ_{12} , θ_{13} and θ_{23} and three mixing angles and δ is the CP-violating phase. Sometimes the Majorana phases are absorbed into the mixing matrix. Then the above matrix is multiplied from the right by the diagonal matrix, e.g. $\text{diag}(e^{i\alpha_1}, e^{i\alpha_2}, 1)$.

The theoretical goal is to drive the above matrix on the basis of suitable extensions of the Standard Model (SM) as mentioned above,²⁴ which are not going to be discussed here. In recent years, especially after the first neutrino oscillation experiments, a different approach based on symmetries has been adopted. In this approach one extends the symmetry G_s of the SM to a larger symmetry $G \supset G_s \times G_f$, where G_f is called flavor or horizontal symmetry. Since there exist only three generations a natural candidate $G_f = SU_f(3)$. This leads to the phenomenologically successful discrete symmetry A_4 ,¹²⁴ which is isomorphic to the set of the even permutations of 4 objects, which has 12 generators. An avalanche of papers involving this symmetry as well as its subsequent extensions and breaking, when θ_{13} was found to be non zero, followed, see e.g. the recent article¹²⁵ and the reviews^{126–128} with relevance to $0\nu\beta\beta$ -decay. Applications of this approach to neutrino masses relevant to $0\nu\beta\beta$ have recently begun to develop. e.g.^{129–131}

One therefore would like to see the SU_f as a gauge symmetry, spontaneously broken without surviving Goldstone bosons. The first step in this direction has been made.¹³² In fact this has been shown to be possible by considering quadratic and quartic scalar potentials, which are $SU(3)$ and $SO(3)$ invariant, constructed by exploiting the full symmetry chain $SU(3) \supset SO(4) \subset A_4$. There are sufficient A_4 singlets, $\underline{1}$ (A_4 invariant) as well as of the type $\underline{1}'$ and $\underline{1}''$, which can cause the spontaneous symmetry breaking down to A_4 . The minimum set of an $SU(3)$ $\underline{10}$ (decouplet) and $\underline{10}^*$ together with the adjointed $\underline{8}$ (octet) is sufficient for this purpose. Attempts to embed the $G_s \times SU_f(3)$ to a higher Grand Unified Symmetry (GUT) are also currently under way.

4. Attempts at measuring the absolute scale of the neutrino mass

The neutrino oscillation data, accumulated over many years, converge towards a minimal three-neutrino framework, where known flavor states (ν_e, ν_μ, ν_τ) are expressed as a quantum superpositions of three massive states ν_i ($i=1,2,3$) with masses m_i . With the discovery of neutrino oscillations quite a lot of information regarding the neutrino sector has become available (e.g., for recent reviews see^{78, 133}). More specifically we know:

- The mixing angles θ_{12} and θ_{23} and θ_{13} .
- We know the two independent mass-squared differences, which can be chosen as follows: $\delta m^2 = m_2^2 - m_1^2$ and $\Delta m^2 = m_3^2 - (m_1^2 + m_2^2)/2$.
- A limited information is available also about the Dirac CP-violating phase δ .¹³⁴

Neutrino oscillation experiments cannot tell us about the absolute scale of neutrino masses. The measured two neutrino mass squared differences suggest two scenarios

for neutrino mass pattern: i) *Normal Spectrum-NS*: $m_1 < m_2 < m_3$:

$$m_1 = m_0, \quad m_2 = \sqrt{m_0^2 + \delta m^2}, \quad m_3 = \sqrt{m_0^2 + \Delta m^2 + \frac{\delta m^2}{2}}; \quad (19)$$

ii) *Inverted Spectrum-IS*, $m_3 < m_1 < m_2$:

$$m_1 = \sqrt{m_0^2 + \Delta m^2 - \frac{\delta m^2}{2}}, \quad m_2 = \sqrt{m_0^2 + \Delta m^2 + \frac{\delta m^2}{2}}, \quad m_3 = m_0. \quad (20)$$

Here, $m_0 = m_1(m_3)$ is the lightest neutrino mass. Given the type of neutrino mass

The current values of neutrino oscillations parameters obtained by a global fit of results coming from experiments using neutrinos from solar, atmospheric, accelerator and reactor sources are presented in Ref.¹³⁴ This combined analysis allows to constrain the previously unknown CP phase δ . Concerning the type of spectrum ($\text{sign}(\Delta m^2)$), there is no indication in favor of normal or inverted mass ordering. However, assuming NS there is a hint about the other unknown, namely a preference is found in favor of the first θ_{23} octant ($\theta_{23} < \pi/4$ at $\sim 95\%$ C.L.). We note that a similar results were obtained also by a global fit performed by Gonzalez-Garcia et al.,¹³⁵ who considered a different definition of two mass squared differences.

The absolute scale m_0 of neutrino mass can in principle be determined by the following observations:

- Neutrinoless double beta decay.

As we shall see later (section 5) the effective light neutrino mass $m_{\beta\beta}$ (sometimes denoted as Majorana neutrino mass) extracted in such experiments is given as follows:^{24, 58, 79, 80, 136}

$$m_{\beta\beta} = \left| \sum_k^3 (U_{ek}^{(11)})^2 m_k \right| = |c_{12}^2 c_{13}^2 e^{2i\alpha_1} m_1 + c_{13}^2 s_{12}^2 e^{2i\alpha_2} m_2 + s_{13}^2 m_3|. \quad (21)$$

- The neutrino mass extracted from ordinary beta decay, e.g. from triton decay.^{137–139}

$$m_\beta = \sqrt{\sum_k^3 |U_{ek}^{(11)}|^2 m_k^2} = \sqrt{c_{12}^2 c_{13}^2 m_1^2 + c_{13}^2 s_{12}^2 m_2^2 + s_{13}^2 m_3^2}. \quad (22)$$

assuming, of course, that the three neutrino states cannot be resolved.

- From astrophysical and cosmological observations (see, e.g., the recent summary¹⁴⁰).

$$\Sigma = \sum_k^3 m_k \leq m_{\text{astro}} \quad (23)$$

The current limit on Σ depends on the type of observation.¹⁴⁰ In our previous report²⁴ we used the CMB primordial spectrum which gives 1.3 eV,

CMB+distance 0.58 eV, galaxy distribution and lensing of galaxies 0.6 eV. On the other hand the largest photometric red shift survey yields 0.28 eV.¹⁴¹ Since then various analysis have been performed. It is worth stressing the following 2σ C. L. upper limits: 0.17 eV obtained in Ref.¹⁴² by combining CMB data of the Wilkinson Microwave Anisotropy Probe, galaxy clustering and the Lyman-alpha forest of the Sloan Digital Sky Survey (SDSS); 0.18 eV of Ref.¹⁴³ using Planck and Wiggle Z galaxy clustering data; 0.14 eV obtained in Ref.¹⁴⁴ by combining Lyman-alpha SDSS data with Planck; 0.153 eV obtained in Ref.¹⁴⁵ by using Planck temperature and polarization measurements including a prior on the Hubble parameter, Supernovae and Baryonic Acoustic Oscillations (BAOs). It has recently been shown in Ref.¹⁴⁶ that the variation of the astrophysical data affects the range of the expected neutrino mass of the $0\nu\beta\beta$ -decay.

The above mass combinations entering triton decay and cosmological constraints are not going to be discussed here, since they can be found in an earlier review.²⁴ We will discuss here only those relevant for $0\nu\beta\beta$ decay.

The value Majorana neutrino mass $m_{\beta\beta}$ can be predicted in the limit of the normal and inverted hierarchies:

- (1) Normal Hierarchy (NH): $m_1 \ll m_2 \ll m_3$:

In this case for the neutrino masses we have

$$m_1 \ll \sqrt{\delta m^2}, \quad m_2 \simeq \sqrt{\delta m^2}, \quad m_3 \simeq \sqrt{\Delta m^2}.$$

Neglecting a small contribution of m_1 to $m_{\beta\beta}$ we find

$$|s_{12}^2 c_{13}^2 \sqrt{\delta m^2} - s_{13}^2 \sqrt{\Delta m^2}| \leq m_{\beta\beta} \leq s_{12}^2 c_{13}^2 \sqrt{\delta m^2} + s_{13}^2 \sqrt{\Delta m^2}. \quad (24)$$

Using the best-fit values of the mass squared differences and the mixing angles we find

$$1.4 \text{ meV} \leq m_{\beta\beta} \leq 3.6 \text{ meV}. \quad (25)$$

- (2) Inverted Hierarchy (IH): $m_3 \ll m_1 < m_2$:

In the IH scenario

$$m_3 \ll \sqrt{\Delta m^2}, \quad m_1 \simeq m_2 \simeq \sqrt{\Delta m^2}.$$

We find

$$|1 - 2s_{12}^2 c_{13}^2 \sqrt{\Delta m^2}| \leq m_{\beta\beta} \leq c_{13}^2 \sqrt{\Delta m^2}. \quad (26)$$

Using the best-fit values of the parameters we find the following range for $m_{\beta\beta}$ in the case of the IH:

$$20 \text{ meV} \leq m_{\beta\beta} \leq 49 \text{ meV}. \quad (27)$$

In Fig. 2 the updated prediction on the Majorana neutrino mass is plotted as function of the lightest neutrino mass m_0 . The 3σ values of neutrino oscillations

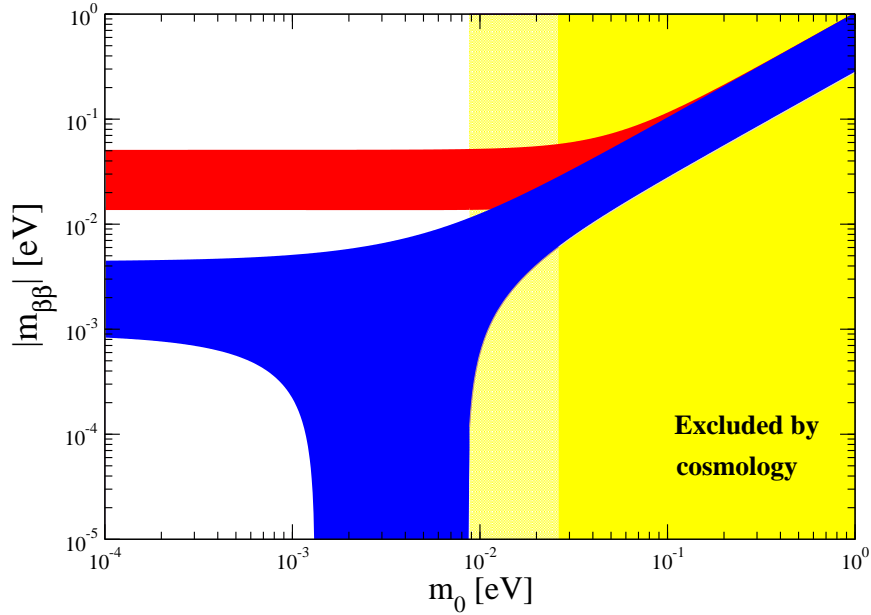


Fig. 2. (Color online) Updated predictions on $m_{\beta\beta}$ from neutrino oscillations versus the lightest neutrino mass m_0 in the two cases of normal (the blue region) and inverted (the red region) spectra. The 3σ values of neutrino oscillation parameters are considered.¹³⁴ The excluded region by cosmological data ($\Sigma < 110$ meV¹⁴⁷) is ($m_0 > 26$ meV (NS), 87 meV (IS)) presented in yellow.

parameters θ_{12} , θ_{13} , δm^2 and Δm^2 are taken into account.¹³⁴ The two Majorana phases $\alpha_{1,2}$ are assumed to be arbitrary. The constraint from the cosmological data ($\Sigma < 110$ meV¹⁴⁷) on the lightest neutrino mass ($m_0 > 26$ meV (NS), 87 meV (IS)) is displayed.

4.1. The effect of nuclear environment on Majorana neutrino mass

It has recently been proposed that the neutrino mixing and masses in a nucleus can differ significantly from those in vacuum, if there exist exotic particles, preferably scalars, which do interact with neutrinos. The related nuclear matter effect on the $0\nu\beta\beta$ -decay rate can be calculated in the mean field approach.¹⁴⁸

The effective four-fermion neutrino-quark lepton number violating Lagrangian with the operators of the lowest dimension can be written as

$$\mathcal{L}_{\text{eff}} = \frac{1}{\Lambda_{LNV}^2} \sum_{i,j,q} \left(g_{ij}^q \bar{\nu}_{Li}^C \nu_{Lj} \bar{q}q + \text{H.c.} \right), \quad (28)$$

where the fields ν_{Li} are the active neutrino left-handed flavor states, g_{ij}^q are their

dimensionless couplings to the scalar quark currents with $i, j = e, \mu, \tau$.

For sake of simplicity we consider case of scalar coupling. In this case the effective Majorana mass¹⁴⁸ is

$$m_{\beta\beta} = \left| \sum_{i=1}^3 (U_{ei})^2 \xi_i |m_i - \langle \bar{q}q \rangle g| \right|. \quad (29)$$

The Majorana phase factor ξ_i is given in.¹⁴⁸

With the above simplification the quantity $m_{\beta\beta}$ in nuclear medium in comparison with the one in vacuum depends on the new unknown parameter g . The unknown phases in Eq. (29) are varied in the interval $[0, 2\pi]$. In Figure 3 $m_{\beta\beta}$ is expressed as a function of a directly observable parameters, namely m_β and Σ . The best-fit values of vacuum mixing angles and the neutrino mass squared differences are taken from.¹³⁴ In upper and lower panels green, blue and red bands refer to values $\langle \bar{q}q \rangle g = 0$ (vacuum), 0.1, and -0.05 eV, respectively. We see that in-medium ($g \neq 0$) values of $m_{\beta\beta}$ differ significantly from those for a vacuum ($g = 0$).

If in the future the gradually improving limits on m_β and Σ will come into conflict with the possible evidence of the $0\nu\beta\beta$ -decay represented by $m_{\beta\beta}$ in vacuum, new physics would be mandatory. A possible explanation could be a generation of in-medium Majorana neutrino mass due to nonstandard interactions of neutrinos with nuclear matter of decaying nuclei.

The limit on Majorana neutrino mass from the $0\nu\beta\beta$ -decay experiments depends on the value of nuclear matrix elements (NMEs). Taking as an experimental limit the value $|m_{\beta\beta}| < 0.2$ eV and combining it with the cosmological and tritium limits one finds¹⁴⁸

$$\Lambda_{LNV} \geq 2.4 \text{ TeV (Planck), } 1.1 \text{ TeV (} ^3\text{H)}. \quad (30)$$

For convenience the above limits can be expressed in terms of a dimensionless parameter ε_{ij} defined as $\varepsilon_{ij} G_F / \sqrt{2} = g_{ij}^q / \Lambda_{LNV}^2$. The quantity ε_{ij} characterizes the relative strength of the 4-fermion lepton number violating operators in (28) with respect to the Fermi constant G_F . We find $\varepsilon_{ij} \leq 0.02$ (Planck), 0.1 (Tritium).

5. The intermediate Majorana neutrino mechanism.

We have seen that the determination of the scale of the neutrino mass is an urgent issue of current physics. To proceed further, however, on this goal, i.e. in our study of the neutrino mediated $0\nu\beta\beta$ -decay process, it is necessary to study the structure the effective weak beta decay Hamiltonian. In general it has both left handed and right handed components. Within the $SU(2)_L \times SU(2)_R \times U(1)$ we encounter the following situations:

5.1. The light neutrino mass mechanism

The $0\nu\beta\beta$ -decay is a process of second order in the perturbation theory of weak interactions. In the case of the light neutrino mass mechanism of the $0\nu\beta\beta$ -decay

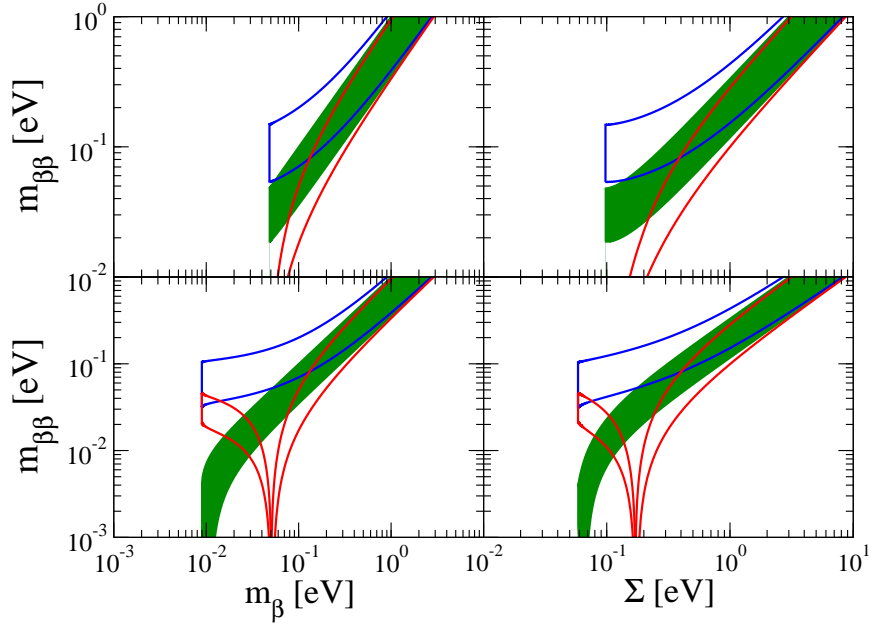


Fig. 3. (Color online) The allowed range of values for effective Majorana mass $m_{\beta\beta}$ as a function of the effective electron neutrino mass m_{β} (left panels) and sum of neutrino masses Σ (right panels). The upper and lower panels correspond to the cases of the inverted and normal spectrum of neutrino masses. In panels green, blue and red bands refer to values $\langle \bar{q}q \rangle g = 0$ (vacuum), 0.1, and -0.05 eV, respectively.

the weak β -decay Hamiltonian has the standard form,

$$H^{\beta} = \frac{G_{\beta}}{\sqrt{2}} \left[(\bar{e}\gamma_{\rho}(1 - \gamma_5)\nu_e) J_L^{\rho\dagger} + h.c. \right] \quad (31)$$

$e_L(e_R)$ and $\nu_{eL}^0(\nu_{eR}^0)$ are field operators representing the left (right) handed electrons and electron neutrinos in a weak interaction basis in which the charged leptons are diagonal. We have seen above the the weak neutrino eigenstates can be expressed in terms of the propagating mass eigenstates⁵⁸ (see Eqs. (12) and (13)). Thus omitting the subscript zero we write

$$\nu_e = \sum_{k=1}^3 U_{ek}\nu_k, \quad (32)$$

with ν_k the light neutrino mass eigenstates. Here, $G_{\beta} = G_F \cos \theta_C$, where G_F and θ_C are Fermi constant and Cabbibo angle, respectively. ν_k is the Majorana neutrino

$$\begin{aligned} \langle p(P') | J^{\mu\dagger} | n(P) \rangle = & \bar{u}_p(P') \left[g_V \gamma^\mu + i g_M \frac{\sigma^{\mu\nu}}{2m_N} (P' - P)_\nu \right. \\ & \left. - g_A \gamma^\mu \gamma_5 - g_P \gamma_5 (P' - P)^\mu \right] u_n(P'), \end{aligned} \quad (33)$$

where the $u_p(P')$ and $u_n(P)$ are the spinors describing the proton and neutron with corresponding four-momenta $P'^\mu = (E', \mathbf{p}')$ and $P^\mu = (E, \mathbf{p})$, respectively. m_N is the nucleon mass, $q = P' - P$ is the momentum transfer and $q_V \equiv q_V(q^2)$, $q_M \equiv q_M(q^2)$, $q_A \equiv q_A(q^2)$ and $q_P \equiv q_P(q^2)$ are the vector, weak-magnetism, axial-vector and induced pseudoscalar form-factors, respectively. m_N is the nucleon mass.

Within the non-relativistic impulse approximation, the hadronic current can be written as⁶⁰

$$\begin{aligned} J_L^{\rho\dagger}(\mathbf{x}) = & \sum_n \tau_n^+ \delta(\mathbf{x} - \mathbf{r}_n) \left[(g_V - g_A C_n) g^{\rho 0} \right. \\ & \left. + g^{\rho k} \left(g_A \sigma_n^k - g_V D_n^k - g_P q_n^k \frac{\vec{\sigma}_n \cdot \mathbf{q}_n}{2m_N} \right) \right]. \end{aligned} \quad (34)$$

Here, $\mathbf{q}_n = \mathbf{p}_n - \mathbf{p}'_n$ is the momentum transfer between the nucleons. The final proton (initial neutron) possesses energy E'_n (E_n) and momentum \mathbf{p}'_n (\mathbf{p}_n). $\vec{\sigma}_n$, τ_n^+ and \mathbf{r}_n are the Pauli matrix, the isospin raising operator and the position operator, respectively. These operators act on the n -th nucleon.

The nucleon recoil operators C_n and \mathbf{D}_n are given by

$$\begin{aligned} C_n = & \frac{\vec{\sigma} \cdot (\mathbf{p}_n + \mathbf{p}'_n)}{2m_N} - \frac{g_P}{g_A} (E_n - E'_n) \frac{\vec{\sigma} \cdot \mathbf{q}_n}{2m_N}, \\ \mathbf{D}_n = & \frac{(\mathbf{p}_n + \mathbf{p}'_n)}{2m_N} - i \left(1 + \frac{g_M}{g_V} \right) \frac{\vec{\sigma} \times \mathbf{q}_n}{2m_N}. \end{aligned} \quad (35)$$

Here, $q_M \equiv q_M(q^2)$ and $q_P \equiv q_P(q^2)$ are, respectively, the weak-magnetism and induced pseudoscalar form-factors in the case of left-handed hadronic currents.

5.2. The V-A mechanism with sterile neutrino(s)

Here by the term sterile we do not mean only the usual sterile neutrino discussed in section 3.1, which is heavier than the standard neutrino but lighter than a few keV and is often included in discussions of cosmology and neutrino oscillations. In other words here we assume that in addition to the three conventional light neutrinos there exist other Majorana neutrino mass eigenstates N of an arbitrary mass m_N , dominated by the sterile neutrino species ν_s and with some admixture of the active neutrino weak eigenstates, $\nu_{e,\mu,\tau}$ as

$$N = \sum_{\alpha=s,e,\mu,\tau} U_{N\alpha} \nu_\alpha. \quad (36)$$

Massive neutrinos N have been considered in the literature in different contexts with the masses m_N ranging from the eV to the Planck scale, in particular with neutrino mass at keV (hot dark mater), Fermi (~ 200 MeV), TeV (physics at LHC), GUT (10^{16} GeV) or Planck (10^{16} GeV) scale.¹⁴⁹ Their phenomenology have been actively studied from various perspectives including their contribution to particle decays and production in collider experiments.^{150, 151} The corresponding searches for N have been carried out in various experiments.¹⁵²

5.3. The mechanisms within the left-right symmetric model

The left-right symmetric models (LRSM)^{153, 154} provide a natural framework to understand the origin of neutrino Majorana masses. In general one cannot predict the scale where the left-right symmetry is realized, but it is natural to assume that it could be as low as \sim a few TeV which can affect the $0\nu\beta\beta$ decay rate significantly.^{155–157} In the left-right symmetric theories in addition to the left-handed V-A weak currents also leptonic and hadronic right-handed V+A weak currents are present.

The effective current-current interaction at low energies, which can trigger the $0\nu\beta\beta$ -decay,

$$H^\beta = \frac{G_\beta}{\sqrt{2}} \left[j_L^\rho J_{L\rho}^\dagger - \epsilon j_L^\rho J_{R\rho}^\dagger + \epsilon j_R^\rho J_{L\rho}^\dagger + \kappa j_R^\rho J_{R\rho}^\dagger + h.c. \right]. \quad (37)$$

Here, ϵ is the mixing of W_L and W_R gauge bosons

$$W_L = \cos \epsilon W_1 - \sin \epsilon W_2, \quad W_R = \sin \epsilon W_1 + \cos \epsilon W_2 \quad (38)$$

where W_1 and W_2 are the mass eigenstates of the gauge bosons with masses M_{W_1} and M_{W_2} , respectively. The mixing is assumed to be small, $\sin \epsilon \approx \epsilon$, $\cos \epsilon \approx 1$, and $M_{W_1} \approx m_{W_L}$, $M_{W_2} \approx m_{W_R}$. κ is the mass squared ratio $\kappa = \frac{M_{W_1}^2}{M_{W_2}^2}$. The left-handed hadron current is given Eq. (34) and right-handed hadron current takes the form

$$J_R^{\rho\dagger}(\mathbf{x}) = \sum_n \tau_n^+ \delta(\mathbf{x} - \mathbf{r}_n) \left[(g'_V + g'_A C_n) g^{\rho 0} + g^{\rho k} \left(-g'_A \sigma_n^k - g'_V D_n^k + g'_P q_n^k \frac{\vec{\sigma}_n \cdot \mathbf{q}_n}{2m_N} \right) \right]. \quad (39)$$

As the strong and electromagnetic interactions conserves parity there are relations among form-factors entering the left-handed and right-handed hadronic currents:⁶⁰

$$\frac{g_A}{g_V} = \frac{g'_A}{g'_V}, \quad \frac{g_M}{g_V} = \frac{g'_M}{g'_V}, \quad \frac{g_P}{g_V} = \frac{g'_P}{g'_V}. \quad (40)$$

The left- and right-handed leptonic currents are given by

$$j_L^\rho = \bar{e} \gamma_\rho (1 - \gamma_5) \nu_{eL}, \quad j_R^\rho = \bar{e} \gamma_\rho (1 + \gamma_5) \nu_{eR}. \quad (41)$$

The ν_{eL} and ν_{eR} are the weak eigenstate electron neutrinos, which are expressed as superpositions of the light and heavy mass eigenstate Majorana neutrinos ν_j and N_j , respectively. The electron neutrinos eigenstates can be expressed as

$$\begin{aligned}\nu_{eL} &= \sum_{j=1}^3 (U_{ej}\nu_{jL} + S_{ej}(N_{jR})^C), \\ \nu_{eR} &= \sum_{j=1}^3 (T_{ej}^*(\nu_{jL})^C + V_{ej}^*N_{jR}).\end{aligned}\quad (42)$$

Before proceeding further we should mention that in the context of the above $0\nu\beta\beta$ -decay is a two step process. The neutrino is produced via the lepton current in one vertex and propagates in the other vertex. If the two current helicities are the same one picks out of the neutrino propagator the term:

$$\frac{m_j}{q^2 - m_j^2} \rightarrow \begin{cases} m_j/q^2, & m_j^2 \ll q^2 \\ -1/m_j, & m_j^2 \gg q^2 \end{cases}\quad (43)$$

where q is the momentum transferred by the neutrino. In other words the amplitude for light neutrino becomes proportional to its mass, but for a heavy neutrino inversely proportional to its mass.

If the leptonic currents have opposite chirality the one picks out of the neutrino propagator the term:

$$\frac{q}{q^2 - m_j^2} \rightarrow \frac{q}{q^2}, \quad m_j^2 \ll q^2\quad (44)$$

i.e. in the interesting case of light neutrino the amplitude does not explicitly depend on the neutrino mass. The kinematics becomes different than that for the mass term.

At this point we should note that, in general, there can be several coexisting mechanisms for the $0\nu\beta\beta$ decay. In addition to the light Majorana ν exchange and heavy Majorana ν exchange, with or without right handed currents, just discussed, one can have contributions from R parity breaking super symmetry etc. In order to extract the most interesting information related to the light neutrino mass in the presence of two or more competing mechanisms, we need to measure the $0\nu\beta\beta$ decay rates for several isotopes. In order to determine the relative contributions of each mechanism, we need for each one of them very precisely known NMEs for the isotopes involved.²⁴

Before proceeding further with theoretical issues we will review the current status and the future prospects of double beta decay searches.

6. Experiments of neutrinoless double beta decay

In this section we briefly describe experimental aspects of DBD and recent DBD experiments. Details of DBD experiments are given in reviews.^{17, 18, 24, 158}

6.1. *Experimental methods and detectors*

The $0\nu\beta\beta$ decay rate is of the order of or less than 10^{-27} and 10^{-29} per year (y) in cases of inverted (IH) and normal (NH) neutrino hierarchy spectra, respectively. Actually the decay rate depends quadratically on the nuclear matrix element (NME) $M_\nu^{0\nu}$. The energy of the $0\nu\beta\beta$ signal is only a few MeV. This is in the same energy region as backgrounds (BGs). The size of DBD isotope required in the target is of the order of multi ton (t) and multi k-ton scales for the IH and NH masses. Then BGs rates have to be necessarily reduced to the order of a few $\times 10^{-1}$ and a few $\times 10^{-3}$ events per year per ton of the DBD isotopes (yt).

The DBD nuclei are used as femto (femto m scale) laboratories where the $0\nu\beta\beta$ signal is enhanced and the single β BGs are suppressed. The luminosity of the ton-scale DBD nuclear ensemble is of the order of $L \approx 10^{77} \text{sec}^{-1} \text{cm}^{-2}$, while the $0\nu\beta\beta$ cross section for the IH ν -mass process is of order of $\sigma \approx 10^{-84} \text{cm}^2$. Thus one may expect the signal rate of the order of $L\sigma T \approx 3$ in a year of $T=3 \times 10^7$ s.

DBD processes are studied by measuring the sum-energy spectrum of the two β rays. The $0\nu\beta\beta$ process, which can occur beyond the SM, is identified by the sharp peak of the 2 body kinematics at $Q_{\beta\beta}$, and the neutrino-less process accompanied by a Majoron boson ($0\nu M\beta\beta$) is characterized²⁴ by the broad peak of the 3 body kinematics.

The $0\nu\beta\beta$ process may be due to the left-handed weak current (LHC) and the right-handed weak current (RHC). The LHC includes the light Majorana ν -mass mode, the heavy Majorana ν mode, the SUSY modes, and others beyond SM. The RHC by itself includes mainly heavy neutrino mass contributions. One additional possible mechanism involves the interference of left handed and right handed leptonic currents and is due to the light neutrino component (see section 5.3), but it leads to neutrino mass independent lepton violating parameters $\langle \eta \rangle$ and $\langle \lambda \rangle$ (for more details see section 7.3). This processes picks out the intermediate neutrino momentum rather than the neutrino mass (see Eq. (44)), and is characterized by different kinematics. It may thus be experimentally distinguished from the mass terms by measuring the angular and energy correlations of the two β rays. The modes (light ν , heavy ν , SUSY, etc) involved in the LHC are investigated by measuring the $0\nu\beta\beta$ rates in various nuclei.

6.2. *DBD detectors and sensitivities*

We discuss the $0\nu\beta\beta$ process with the light Majorana- ν exchange. Then the transition rate $T^{0\nu}$ per year ton (yt) is expressed in terms of the nuclear sensitivity S_N in units of meV^{-2} and the Majorana neutrino mass $m_{\beta\beta}$ as.^{17, 24}

$$(T^{0\nu})^{-1} = m_{\beta\beta}^2 S_N, \quad S_N^{1/2} = (78)^{-1} |M_\nu^{0\nu}| g_A^2 (G^{0\nu}/0.01A)^{1/2}, \quad (45)$$

where $M_\nu^{0\nu}$ is the NME, $G^{0\nu}$ is the phase space volume in units of $10^{-14}/\text{y}$, and A is the mass number.

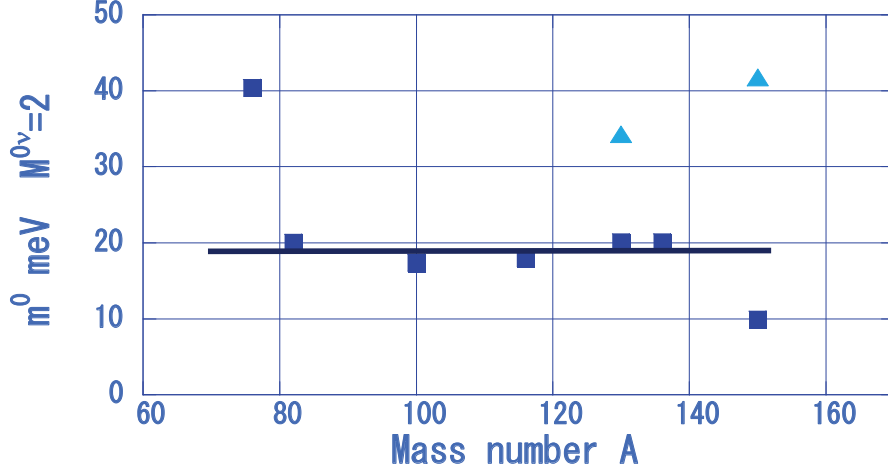


Fig. 4. Unit mass sensitivities m^0 (squares) in case of $M_{\nu}^{0\nu}=2$ for ^{76}Ge , ^{82}Se , ^{100}Mo , ^{116}Cd , ^{130}Te , ^{136}Xe and ^{150}Nd and those (triangles) for natural ^nTe and ^nNd .

The mass sensitivity m_m is defined as the minimum mass required to identify the $0\nu\beta\beta$ signal. It is expressed in terms of S_N and the detector sensitivity D as

$$m_m = S_N^{-1/2} D^{-1/2}, \quad D = (\epsilon NT)(\delta)^{-1}, \quad (46)$$

where ϵ is the $0\nu\beta\beta$ peak efficiency, N is the number of the DBD isotopes in units of ton, T is the run time in unit of year and δ is the minimum number of counts for the peak identification with 90 % CL (confidence level). Since BNT is much larger than 1 in most DBD experiments, we use $\delta \approx 1.7 \times (BNT)^{1/2}$. Then m_m is

$$m_m \approx m^0 D^{-1/2}, \quad (47)$$

$$m^0 = 39 G^{-1/2} (2/M_{\nu}^{0\nu}) 1/g_A^2, \quad D^{-1/2} = 1.3 \epsilon^{-1/2} [B/NT]^{1/4}, \quad (48)$$

where $G = (G^{0\nu}/0.01A)$, m^0 is the unit mass sensitivity in units of meV, i.e. the mass sensitivity in case of a detector with $D=1$ ($\epsilon=1$, $NT=3$ t y and BG rate of $B=1/(t y)$).

The nuclear sensitivity S_n is proportional to the phase space factor $G^{0\nu}$ and $|M_{\nu}^{0\nu}|^2$. The DBD isotopes used for realistic high-sensitivity experiments include ^{76}Ge , ^{82}Se , ^{100}Mo , ^{116}Cd , ^{130}Te , and ^{136}Xe . These isotopes have the large phase space factor around $G^{0\nu} \approx 1.5$ in units of 10^{-14} y^{-1} and multi-ton scale enriched isotopes obtained by means of the centrifugal isotope separation. ^{76}Ge detectors are used because of the high energy-resolution although $G^{0\nu} \approx 0.25$ is much smaller than the others. The unit mass sensitivities m^0 for typical DBD nuclei are plotted in Fig.4.

Actually, the sensitivity depends on the enrichment of the isotope. If natural isotopes with the same total mass (N ton) as the enriched one are used, the $0\nu\beta\beta$

efficiency ϵ is reduced effectively by the abundance ratio r , while the BG rate B remains same. Thus the mass sensitivity gets larger by the factor $r^{-1/2}$. The unit mass sensitivities for ${}^n\text{Te}$ with $r=0.34$ and ${}^n\text{Nd}$ with $r=0.056$ are as shown in Fig.4.

The detector-sensitivity factor $D^{-1/2}$ is proportional to the factor $[B/NT]^{1/4}$. Then one needs low-BG large-volume detectors. In the case of $m^0 \approx 20$ meV, detectors with $B \leq 0.3/(\text{t y})$, $\epsilon=0.5$, and $N \geq 3$ t may be used to access the IH ν mass of around 15 meV for $T=4$ y, while those with, for instance, $B \leq 0.01/(\text{y t})$ and $N \geq 1$ kt are required to explore the NH ν mass of $m_{\beta\beta} \approx 1.5$ meV for $T=4$ y.

The BG sources to be considered are natural RIs as ${}^{208}\text{Tl}$, ${}^{214}\text{Bi}$ and other Ur-Th chain RIs, cosmogenic RIs, as ${}^{68}\text{Ga}$ in the case of Ge detectors, muon and neutron interactions, solar- ν CC and NC interactions, the high-energy tail of the $2\nu\beta\beta$ spectrum and others. Then DBD experiments are made by using high purity (RI-free) DBD detectors with good energy resolution at a deep underground laboratory.

The energy resolution is very important to select the $0\nu\beta\beta$ signal at the ROI and to reduce the BG contributions since the BG spectra are mostly continuum. Thus Ge detectors and cryogenic (scintillation) bolometers are very sensitive detectors. SSSC (single site spacial correlation) analysis is used to reduce RI BGs associated with γ rays since γ rays deposit their energies at multi-sites through Compton scatterings. PSD (pulse shape discrimination) is effective for single site time correlation (SSTC). SSTC analysis is used to reduce RI BGs from ${}^{214}\text{Bi}$, ${}^{68}\text{Ga}$ and others by delayed anti-coincidence with the preceding β or X rays.^{17, 18, 24, 158}

The solar neutrinos are omnipresent, and the solar- ν CC and NC interactions with nuclei and atoms in DBD detectors are serious BG sources for high-sensitivity DBD experiments. The solar- ν CC interaction with the DBD nucleus A excite $\text{GT}(1^+)$ states in the intermediate nucleus B and the β decay from B to the final nucleus C contributes to BGs at the ROI in the $0\nu\beta\beta$ of $\text{A} \rightarrow \text{C}$. The contributions¹⁵⁹ are appreciable even for IH ν -mass studies with medium energy-resolution (\approx a few %) experiments unless they are reduced by SSSC, SSTC and others.

The ${}^8\text{B}$ solar- ν CC and NC interactions with atomic electrons in DBD isotopes and those in liquid scintillators used for DBD experiments¹⁶⁰⁻¹⁶³ are also BG sources for medium energy-resolution experiments^{164, 165} The BG contribution for the liquid scintillator loaded with DBD isotopes of interest is expressed as

$$B_e \approx 0.15 \times Ef/(\text{t y}) \quad f = w/R, \quad (49)$$

where E is the Q value in units of MeV, w the energy resolution in FWHM, and R is the concentration of the DBD isotopes in the scintillator. The BG rate is $B_e \approx 2-3/(\text{t y})$ in a typical case of $E \approx 3$ MeV and $f \approx 5$, i.e. $w \approx 5$ % and $R \approx 1$ %. Thus the contribution from the solar ν interaction needs to be well considered.

The ν -mass sensitivities for ${}^{130}\text{Te}$ with $M_{\nu}^{0\nu}=2$ and $\epsilon=0.5$ are shown as a function of the exposure NT in cases of $B=1/(\text{t y})$ and $B=0.01/(\text{t y})$ in Fig.5. Exposures required for studies of the IH and NH mass regions are $NT=1-10$ y t and $NT=100-1000$ y t in cases of $B=1/(\text{t y})$ and $B=0.01/(\text{t y})$, respectively. These are similar for ${}^{82}\text{Se}$, ${}^{100}\text{Mo}$, ${}^{116}\text{Cd}$, ${}^{130}\text{Te}$, ${}^{136}\text{Xe}$.

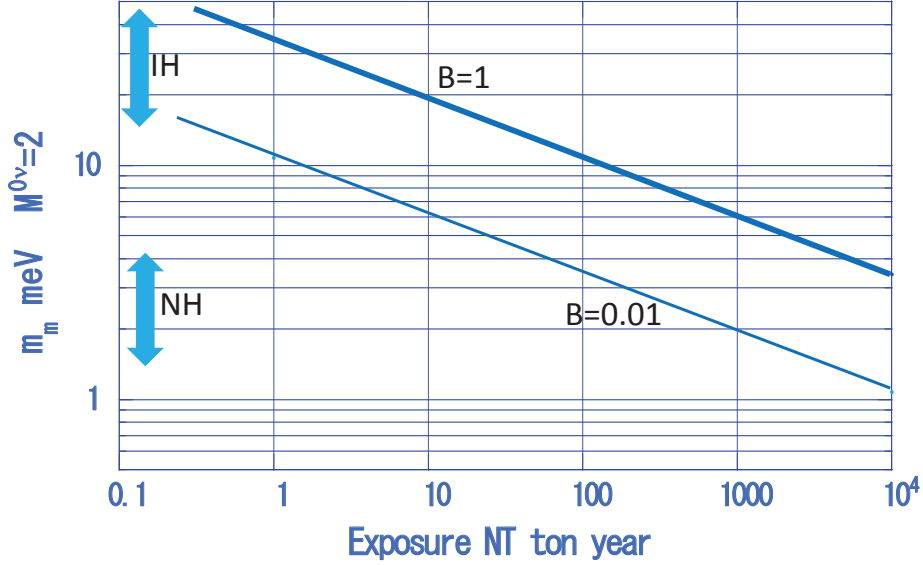


Fig. 5. Neutrino-mass sensitivities m_m for ^{130}Te with $M'^{0\nu}=2$ (i.e. $m_m \times M'^{0\nu}/2$) and $\epsilon=0.5$ as a function of the exposure NT in cases of the BG rates of $B=1/(\text{t y})$ and $0.01/(\text{t y})$, respectively.

6.3. The present status of neutrinoless double beta decay experiments

Experimental $0\nu\beta\beta$ studies with the QD (quasi-degenerate mass hierarchy sub eV) mass sensitivity have been carried out extensively as given in other reviews.^{17,18,24,158} The ^{76}Ge experiments with ^{76}Ge semiconductors (HM,¹⁶⁶IGEX¹⁶⁷), the ^{130}Te experiment with TeO_2 cryogenic bolometers (CUORETINO^{168,169}) and the large volume ^{136}Xe experiments (EXO,^{170,171} KanLAND-Zen¹⁶⁰) have been carried out to study the $\beta\beta$ decays. Tracking detectors (ELEGANT V¹⁷² and NEMO-3¹⁷³) have been used for studying $\beta\beta$ decays from ^{82}Se , ^{100}Mo , ^{116}Cd and other isotopes with large $Q_{\beta\beta}$ values.

Recently stringent lower limits were obtained on $T_{1/2}^{0\nu}$ of ^{76}Ge , ^{100}Mo , ^{130}Te and ^{136}Xe , as given in Table 1. The upper limit on the effective ν -mass was derived from the half-life limit by using the calculated $M'^{0\nu}$, as given in the 4th column of Table 1. The mass range reflects the range of the $M'^{0\nu}$ values, depending on the model and the effective coupling constant g_A^{eff} used for the calculation. Accurate theoretical evaluations for g_A^{eff} are not easy. The ν -mass limit may become approximately 50 % larger if one uses a 30% smaller value for g_A^{eff} . Recent experiments on neutrino-less $\beta\beta$ decays give also lower limits on the half lives $T_{1/2}^{0\nu M}$ for the Majoron emitting process and the Majoron neutrino coupling $\langle g_{ee} \rangle$, e.g. in¹⁷⁴ for ^{100}Mo . Such limits

Table 1. Limits on $T_{1/2}^{0\nu}$, $Q_{\beta\beta}$: Q value for the $0^+ \rightarrow 0^+$ ground state transition. $G^{0\nu}$: phase volume with $g_A = 1.25$ and $R = 1.2$ fm $A^{1/3}$. $m_{\beta\beta}$: the range of the upper limit on the effective Majorana $\nu\nu$ -mass. See text.

Isotope	$Q_{\beta\beta}$ [MeV]	$T_{1/2}^{0\nu}$ [10^{24} y]	$m_{\beta\beta}$ [meV]	Experiment
^{76}Ge	2.039	52	160-260	GERDA Ge semiconductor ^a
^{100}Mo	3.034	1	900 - 300	NEMO-3 Tracking chamber ^b
^{130}Te	2.528	4	760 - 270	CUORE Bolometer ^c
^{136}Xe	2.459	11	450 - 190	EXO ionization-scintillation ^d
^{136}Xe	2.459	110	161-60	KamLAND-Zen Scintillator ^e

a:;¹⁷⁵ b:;¹⁷⁶ c:;¹⁷⁷ d:;¹⁷⁸ e:;²⁵

exist for a number of other targets, but we do not discuss them in this work (see the earlier report²⁴).

GERDA phase I aims at high energy-resolution studies of ^{76}Ge by using ^{76}Ge detectors (17.7 kg +3.6 kg) immersed into liquid scintillator.¹⁷⁹ The BG level is 0.01 / (keV kg y) at ROI. The phase I data with 21.6 kg y exposure gives a half-life limit of 2.1×10^{25} y with 90% CL. The limit obtained by combining the previous data¹⁶⁶ is 3×10^{25} y with 90 % CL. Thus the claim of the $0\nu\beta\beta$ evidence¹⁸⁰ is strongly disfavored with 99 % probability. The combined data set an upper limit on the effective ν mass as 200-400 meV. Recently a new limit of 5.2×10^{25} y (160-260 meV) with 90% CL was derived.¹⁷⁵

A new value for $2\nu\beta\beta$ half life is $T_{1/2}^{2\nu} = (1.926 \pm 0.095) \times 10^{21}$ y and the $0\nu M\beta\beta$ half-life limit¹⁸¹ is $T^{0\nu M} = 4.3 \times 10^{23}$ y, corresponding to $\langle g_{ee} \rangle = (3.4-8.7) \times 10^{-5}$

NEMO-3 with the tracking chambers and the PL scintillation detectors gives half-life limits of 1.1×10^{24} y on ^{100}Mo .¹⁷⁶ The corresponding ν -mass limit is 300-900 meV. The half-life limits on the one Majoron emitting process are $T^{0\nu M} = 2.7 \times 10^{22}$ y for ^{100}Mo .¹⁷⁴ The limits on the Majoron coupling is $\langle g_{ee} \rangle = (0.4-1.9) \times 10^{-4}$.

CUORE0 is one module of CUORE, which is an expansion of CUORICINO.¹⁶⁹ It is a high energy-resolution bolometer array to study ^{130}Te $0\nu\beta\beta$ decays at LNGS by using 39 kg TeO_2 (10.9 kg ^{130}Te). The CUORE0 experiment reports the result of the 9.8 kg y exposure¹⁷⁷ with the energy resolution of 4.9 keV in FWHM and the BG level is 0.058 / (keV kg y). The obtained half-life limit is 2.7×10^{24} y with 90% CL, and the limit derived by combining the previous CUORITINO experiment is 4×10^{24} y. The corresponding ν -mass limit is 270-760 meV.

EXO-200 is the 80%-enriched ^{136}Xe TPC experiment (150 kg in the detector proper) at WIPP. The energy-resolution of around 3.5 % in FWHM is achieved by measuring both the ionization and scintillation signals.^{170,178} A lower limit on $T_{1/2}^{0\nu\beta\beta}$ was derived as 1.1×10^{25} y (ν -mass limit is 190 meV - 450 meV) with 90 % CL.¹⁷⁸ The BG rate at ROI is 1.7×10^{-3} / (keV kg y).¹⁷⁸ A lower limit of 1.2×10^{24} with 90% CL was derived for $T_{1/2}^{0\nu M}$.¹⁸² This limit corresponds to the upper limit of $\langle g_{ee} \rangle = (0.8-1.6) \times 10^{-5}$. The precise $2\nu\beta\beta$ half life of $T_{1/2}^{2\nu} = 2.165 \times 10^{21}$ y

was obtained.¹⁸³

KamLAND-Zen studies the ^{136}Xe DBD by means of the KamLAND detector with the 1 kt liquid scintillator at Kamioka.¹⁶⁰ A mini balloon is set at the center for the ^{136}Xe -loaded liquid scintillator with ^{136}Xe isotopes around 320-380 kg. The energy resolution is 9.5 % in FWHM. The $2\nu\beta\beta$ half life of $T_{1/2}^{2\nu}=2.38 \times 10^{21}$ y¹⁶⁰ is in consistent with the value by EXO.¹⁸³ A half-life limit on the $0\nu\beta\beta$ was derived as 1.9×10^{25} y.¹⁸⁴ The limit by combining the EXO experiment is 3.4×10^{25} y.¹⁸⁴ The lower limit¹⁸⁵ on the $T_{1/2}^{0\nu M}$ is $2.6 \cdot 10^{24}$ y, corresponding to the upper limit of $\langle g_{ee} \rangle = (0.8-1.6) \cdot 10^{-5}$. Recently, a stringent limit of 1.1×10^{26} y was derived by combining the new data with the previous ones. It corresponds to the ν mass limit of 60-161 meV.²⁵

It is noted that the HM claim for the $0\nu\beta\beta$ peak^{180,186} is strongly disfavored not only by the GERDA experiment,¹⁷⁹ but also by the ^{136}Xe experiments^{170,184} if one may use relative matrix elements of ^{76}Ge and ^{136}Xe given by various models.

The $2\nu\beta\beta$ -decay rates have been observed in 12 nuclides (^{48}Ca , ^{76}Ge , ^{82}Se , ^{96}Zr , ^{100}Mo , ^{116}Cd , ^{128}Te , ^{130}Te , ^{136}Xe , ^{150}Nd , ^{130}Ba and ^{238}U) and in two excited states. The recommended half lives can be found in ref.¹⁸⁷ These half lives give $2\nu\beta\beta$ NMEs $M^{2\nu}$.

The recent stringent limits on $T_{1/2}^{0\nu}$ give the upper limit of $m_{\beta\beta} \approx 60-400$ meV in the QD region. Here the ν -mass depends strongly on $M_{\nu}^{0\nu}$. In order to search for the full IH-mass region of 15-45 meV, one needs to improve the mass sensitivity by one order of magnitude, i.e. the half-life sensitivity by 2 orders of magnitude. The limits on $T_{1/2}^{0\nu M}$ give the upper limit of the Majoron neutrino coupling $\langle g_{ee} \rangle \approx 0.8-1.6$, depending on $M_{\nu}^{0\nu M}$. It is very crucial to get right NMEs $M_{\nu}^{0\nu}$ and $M^{0\nu M}$.

6.4. Future high-sensitivity experiments

Experimental DBD groups are extensively working for future high-sensitivity experiments. Some of them are listed in Table 2. We briefly describe them below.

GERDA Phase II studies the $0\nu\beta\beta$ of ^{76}Ge by introducing additional 20 kg Ge detectors.¹⁸⁸ The energy resolution, the PSD and others are improved to get the very low BG level around $1/(\text{keV y t})$. The expected sensitivity is 1.4×10^{26} y after 100 kg y exposure, which corresponds to 100-200 meV.

MJD (MAJORANA DEMONSTRATOR) is the 44 kg Ge (29 kg ^{76}Ge and 15 kg ^{76}Ge) experiment to study ^{76}Ge at SURF.¹⁸⁹ It uses PPC (p-type point contact) Ge detectors, and the expected BG rate at ROI is $B \leq 3.5 /(\text{y t})$. It is envisioned to demonstrate a path forward to achieve the BG rate $1/\text{yt}$ for the next generation ton-scale experiment to study the ν -mass in the IH mass region. The module 1 (23 kg) and 2 (21 kg) are taking data. The Majorana and GERDA collaborations will be merged for one ton-scale future experiment by selecting the best techniques.

MOON is an extension of ELEGANT V.¹⁷² It is a hybrid $\beta\beta$ and solar ν experiment with ^{100}Mo to study the QD/IH ν -mass sensitivity and the low energy solar neutrinos.¹⁹⁰⁻¹⁹² Super-module of PL plates and wire chambers are being

Table 2. High-sensitivity DBD experiments in futures. A : natural abundance. $Q_{\beta\beta}$: Q value for the $0^+ \rightarrow 0^+$ and low BG ground state transition. $G^{0\nu}$: kinematic (phase space volume) factor ($g_A = 1.25$ and $R = 1.2$ fm $A^{1/3}$).

isotope	A [%]	$Q_{\beta\beta}$ [MeV]	$G^{0\nu}$ [$10^{-15} y^{-1}$]	Future experiments experiments
^{76}Ge	7.8	2.039	2.36	GERDA, Majorana Demonstrator
^{82}Se	9.2	2.992	10.2	SuperNEMO, MOON
^{100}Mo	9.6	3.034	15.9	AMoRE, LUMINEU, CUPID, MOON
^{116}Cd	7.5	2.804	16.7	AURORA COBRA
^{130}Te	34.5	2.529	14.2	CUORE
^{136}Xe	8.9	2.467	14.6	EXO, KamLAND-Zen, NEXT, Panda X-III
^{150}Nd	5.6	3.368	63.0	SuperNEMO, SON+, DCBA

developed.

SuperNEMO studies the IH mass region by large tracking chambers and PL scintillation detectors with 100 kg ^{82}Se isotopes.¹⁹³⁻¹⁹⁵ It uses 20 modules, each module with 5 kg $\beta\beta$ isotopes. The detector is based on NEMO-3, but the energy resolution and the BG level have been much improved. The expected sensitivity with the BG rate 12/(t y) is $T_{1/2} = 1 \times 10^{26}$ y, corresponding to the ν mass of 50-140 meV. SuperNEMO demonstrator with 7 kg ^{82}Se is in preparation. The sensitivity is $T_{1/2}=6 \times 10^{24}$ y (200-500 meV). The energy resolution is around 4% at $E=3$ MeV.

AMoRE aims to study ^{100}Mo in the region of IH mass (5×10^{26} y) by using 200 kg $^{40}\text{Ca}^{100}\text{MoO}_4$ low-temperature detectors at Y2L.¹⁹⁶ PSD with the phonon and photon signals is used to separate α BGs from electron signals. The pilot experiment with a 1.5 kg $^{48dep}\text{Ca}^{100}\text{MoO}_4$ detector is going on at Y2L.

LUMINEU is developing cryogenic scintillation bolometers of Li_2MoO_4 and ZnMoO_4 to study ^{100}Mo .¹⁹⁷⁻¹⁹⁹ High purity crystals with PSD make it possible to get low BG level of around 0.3 / (keV t y) and good energy resolution of around 5 keV.

CUPID (CUORE Upgrade with PI) is a proposed ton-scale bolometer experiment with the ν -mass sensitivity of the order of 10 meV.²⁰⁰ The collaboration is starting 40 crystals of Li_2MoO_4 with 6 kg ^{100}Mo .²⁰¹

COBRA and AURORA study ^{116}Cd . COBRA uses a large amount of high energy-resolution CZT(CdZnTe) semiconductors at room temperature.²⁰² The COBRA collaboration tests 64 CZT 1 cm³ detectors at LNGS. The energy resolution is $\Delta E=1.1\%$ at 2.6 MeV. Pixelization is a major step forward. Recent results of the COBRA demonstrator has been reported.²⁰³ AURORA uses a $^{116}\text{CdWO}_4$ and the current half-life limit is 1.9×10^{23} y.²⁰⁴

CUORE uses 988 natural TeO_2 crystals with the natural Te isotopes (741 kg TeO_2 , 206 kg ^{130}Te) to study ^{130}Te at the IH ν -mass region.^{177,205} By improving

the BG level to be $0.01/(\text{keV kg y})$, the expected sensitivity is 9.5×10^{25} y. This corresponds to the ν -mass sensitivity around 50 meV-150 meV.

nEXO is an expansion of EXO-200 by using a low BG and 2.3% energy-resolution TPC with scintillation and ionization readouts.^{182,206} The expected half-life sensitivity is around 10^{28} (6-15 meV) by using 5 ton ^{136}Xe isotopes for 5 y run..

KamLAND-Zen aims at the higher-sensitivity ^{136}Xe experiment by using 0.75 ton enriched ^{136}Xe isotopes.^{207,208} The energy resolution and the BG rate will be same as those of the previous phases. The expected half-life sensitivity is around 5×10^{26} , which corresponds to the IH ν -mass region. NEXT-100 uses a high pressure TPC with 100 kg enriched ^{136}Xe to study the QD ν mass (≤ 100 meV) at LSC.^{209,210} It is a low BG and good energy resolution TPC with separate readout planes for tracking and energy. NEXT-DEM is a demonstrator.

SNO+ uses the 1 kt scintillation detector with 0.3 % loading of natural Te isotopes (800 kg ^{130}Te) to study the ^{130}Te decays and plan 0.5 % loading.^{211,212}

Current DBD experiments are mostly on high $Q_{\beta\beta}$ $\beta^-\beta^-$ decays because of the large phase volume. CANDELS ^{48}Ca , DCBA-MTD ^{150}Nd , Panda X-III and others are under development as discussed in the reviews^{17,18,24} and NEUTRINO 2016. CANDLES III with 300 kg natural Ca will be enlarged to IV and V with enriched isotopes in future.²¹³ Panda X-III is a high pressure Xe TPC with 200 kg ^{136}Xe source at CJPL.²¹⁴ The $0\nu\beta^+\beta^+$, $0\nu\beta+\text{EC}$ and $0\nu\text{EC}$ EC decays are studied by measuring the β^+ annihilation γ rays and K X-rays.

6.5. *Experimental studies of DBD matrix elements*

At this point we should mention the progress towards using other experiments,^{17,158,215} mainly charge exchange reactions (CERs) and single β decays^{216,217} to help evaluate DBD NMEs needed in extracting the neutrino mass from $0\nu\beta\beta$ experiments.

One direct way to get the weak response is to use the ν CER of (ν_e, e) . Since the ν nuclear cross section is as small as $\sigma \approx 10^{-42}$ cm², one needs high-flux ν beams and large-volume detectors.^{17,158} The ν beams may be obtained from pion decays and the pions are obtained from GeV proton beams from SNS at ORNL²¹⁸ and J-PARC.²¹⁹

Muon (μ^-) CERs of (μ, ν_μ) ^{220,221} give β^+ strengths for $J = 0.1.2$ states in the wide excitation region of $E = 0-70$ MeV. Recently $(\mu^-, xn\gamma)$ reactions on Mo isotopes were studied by using DC and pulsed μ beams at RCNP and MLF J-PARC.²²² The μ CER of ^{100}Mo (μ, xn) $^{100-x}\text{Nb}$ was studied by measuring delayed $\beta - \gamma$ rays from $^{100-x}\text{Nb}$ isotopes. The weak strength distribution for the μ CER was deduced from the observed Nb RI distribution by using the statistical model for the neutron emission. The μ capture shows a giant resonance around $E = 10-15$ MeV. The μ capture life time gives the absolute weak strength and the NMEs with effective g_A .

Weak responses for β^+ decays are studied by using photo-nuclear (γ, x) reactions

through isobaric analogue states (IAS).²²³ The polarization of the photon can be used to study E1 and M1 matrix elements separately.²²⁴

Nuclear CERs with medium energy nuclear beams were used to study single β^\pm NMEs at IUCF, KVI, MSU, RCNP, Triumf and others.^{17, 24, 215} The ($^3\text{He}, t$) reactions with the high energy-resolution of $\Delta E \approx 25$ keV were studied extensively on DBD nuclei by using the 420 MeV ^3He beam at RCNP.²²⁵⁻²³¹ Recently spin dipole (2^-) NMEs, which may be relevant to $0\nu\beta\beta$ NMEs, have been studied by using ($^3\text{He}, t$) reactions at RCNP.²³² Double charge exchange reactions DCER provide useful information on DBD NMEs. The RCNP DCER ($^{11}\text{B}, ^{11}\text{Li}$) at $E/A=80$ MeV shows that the DCE strengths are not located at the low lying states, but mostly concentrated at the high excitation region.²³³ Furthermore the DCER of ($^{18}\text{O}, ^{18}\text{Ne}$) on ^{40}Ca was measured to get the DCER strength for the ground state $0^+ \rightarrow 0^+$ transitions.²³⁴ Nucleon transfer reactions have been used to get nucleon vacancy and occupation probabilities of DBD initial and final nuclei.²³⁵

The Fermi Surface Quasi Particle model (FSQP) based on experimental single- β^\pm NMEs reproduces well the $2\nu\beta\beta$ NMEs $M^{2\nu}$ for the $A(Z, N) \leftrightarrow C(Z+2, N-2)$ ground-state to ground state $0^+ \leftrightarrow 0^+$ transition.²³⁶⁻²³⁸ The initial, intermediate and final state nucleons involved in the ground state transition must necessarily be on the diffused Fermi surface. Thus $M^{2\nu}$ is given by the sum of the products of the single β^\pm matrix elements via the FSQP intermediate states.^{17, 24, 237} The agreement of $M^{2\nu}(EXP)$ and $M^{2\nu}(FSQP)$ shows that $M^{2\nu}$ is very small due to the nuclear medium and correlation effects given by $k^-k^+ \approx 0.06$ with $k^- \approx k^+ \approx 0.25$ for the single β^\pm decay NMEs. FSQP may be used also for evaluating $M_{\nu}^{0\nu}$ by using CERs and single β/EC rates to intermediate $1^\pm, 2^\pm$, and other states.

A recent analysis of β^\pm -EC NMEs in medium heavy nuclei shows that the axial vector GT(Gamow-Teller 1^+) and SD (spin dipole 2^-) NMEs are reduced with respect to the single quasi-particle NMEs by the coefficient $k^\pm \approx 0.20-0.25$.^{216, 217} The reduction may be inferred to be partly due to the nucleon spin isospin correlation of $k_{\sigma\tau} \approx 0.4-0.5$ and partly due to the non-nucleon (isobar) and nuclear medium effect of $k_{NM} \approx 0.5-0.6$.^{216, 217} Here the effect of $k_{\sigma\tau} \approx 0.4-0.5$ is included in QRPA with $\sigma\tau$ correlation, while the isobar and nuclear medium effect is a sort of the renormalization (quenching) of the axial-vector weak coupling. The renormalization effect may be incorporated by the effective coupling of $(g_A^{\text{eff}}/g_A) \approx 0.5-0.6$. Accordingly the axial vector components of the DBD NME is reduced with respect to the QRPA model calculations by the coefficient $(g_A^{\text{eff}}/g_A)^2 \approx 0.3$.

So far no experimental data on $2\nu\beta^+/EC$ NMEs are available mainly due to the small phase space. One possible candidate is ^{106}Cd . FSQP predicts a large NME of $M^{2\nu}(FSQP) = 0.10$ in unit of m_e^{-1} . The FSQP half lives for ECEC, $EC\beta^+$ and $\beta^+\beta^+$ are 5.2×10^{21} y, 4.4×10^{22} y and 1.7×10^{27} y, respectively, They are longer than experimental limits of 4.2×10^{20} y, 1.1×10^{21} y and 2.3×10^{21} y, respectively.²³⁹ The decays are also being studied by Ge detectors.²⁴⁰

7. Expression for the lifetime of neutrinoless double beta decay

We briefly review half-lives associated with $0\nu\beta\beta$ -decay mechanisms including exchange of light and heavy Majorana neutrinos. We shall pay attention only to the $0^+ \rightarrow 0^+$ ground state to ground state $0\nu\beta\beta$ -decays transitions.

7.1. The light Majorana neutrino mass mechanism

The expression for the lifetime of $0\nu\beta\beta$ decay is simplified by the fact that it is factorized into three factors: The phase-space factor, the nuclear matrix elements and the lepton violating neutrino parameters.

Indeed the inverse value of the $0\nu\beta\beta$ -decay half-life can be written as²⁴

$$\left(T_{1/2}^{0\nu}\right)^{-1} = \frac{m_{\beta\beta}^2}{m_e^2} g_A^4 \left|M_{\nu}^{0\nu}(g_A^{\text{eff}})\right|^2 G^{0\nu}(E_0, Z), \quad (50)$$

where the first term $m_{\beta\beta}^2$ is the lepton violating parameter and $G^{0\nu}(E_0, Z)$, with $E_0 = E_i - E_f$ being the energy release, is the phase-space integral given by:

$$G^{0\nu}(E_0, Z) = \frac{G_{\beta\beta}^4 m_e^9}{32\pi^5 R^2 \ln(2)} \times \frac{1}{m_e^5} \int_{m_e}^{E_i - E_f - m_e} (g_{-1}^2(\varepsilon_1) + f_{+1}^2(\varepsilon_1)) (g_{-1}^2(\varepsilon_2) + f_{+1}^2(\varepsilon_2)) \varepsilon_1 p_1 \varepsilon_2 p_2 d\varepsilon_1$$

with $\varepsilon_2 = E_i - E_f - \varepsilon_1$, $p_i = \sqrt{\varepsilon_i^2 - m_e^2}$ ($i=1,2$).

Unlike in previous derivation⁶⁰ the exact Dirac wave functions with finite nuclear size and electron screening of the emitted electrons in the $s_{1/2}$ and $p_{1/2}$ wave states,

$$\begin{aligned} \psi(\mathbf{r}, p, s) &\simeq \psi_{s_{1/2}}(\mathbf{r}, p, s) + \psi_{p_{1/2}}(\mathbf{r}, p, s) \\ &= \begin{pmatrix} g_{-1}(\varepsilon, r) \chi_s \\ f_{+1}(\varepsilon, r) (\vec{\sigma} \cdot \hat{\mathbf{p}}) \chi_s \end{pmatrix} + \begin{pmatrix} i g_{+1}(\varepsilon, r) (\vec{\sigma} \cdot \hat{\mathbf{r}}) (\vec{\sigma} \cdot \hat{\mathbf{p}}) \chi_s \\ -i f_{-1}(\varepsilon, r) (\vec{\sigma} \cdot \hat{\mathbf{r}}) \chi_s \end{pmatrix}. \end{aligned} \quad (51)$$

were taken into account. The relativistic electron wave function $\psi(\mathbf{r}, p, s)$ in the central symmetric Coulomb field of a uniform charge distribution of a nucleus can be decomposed in partial waves. In the case of the light neutrino mass mechanism of the $0\nu\beta\beta$ -decay only the dominant $s_{1/2}$ -waves of emitted electrons were taken into account:

$$\psi(\mathbf{r}, p, s) \simeq \psi_{s_{1/2}}(\mathbf{r}, p, s). \quad (52)$$

Given the Coulomb potential of the daughter nucleus and the screening potential of bound electrons in atom $g_{\pm 1}(\varepsilon, r)$ and $f_{\pm 1}(\varepsilon, r)$ are solutions of the radial Dirac equations.

Furthermore the electron wave functions including relativistic effect, $g_{\pm 1}(\varepsilon, r)$, and $f_{\pm 1}(\varepsilon, r)$ are replaced by their values at the nuclear radius R . We have

$$g_{\pm 1}(\varepsilon, r) = g_{\pm 1}(\varepsilon, R), \quad f_{\pm 1}(\varepsilon, r) = f_{\pm 1}(\varepsilon, R). \quad (53)$$

Table 3. The current experimental lower limit on the $0\nu\beta\beta$ -decay half-life for 10 isotopes with largest $Q_{\beta\beta}$ -value and theoretical predictions for the half-life by assuming the cases of normal (NH) and inverted (IH) hierarchies in evaluation of effective Majorana neutrino mass $m_{\beta\beta}$. The averaged values of nuclear matrix elements with variances from Table 6 are taken into account. The non-quenched value of the weak-axial coupling constant is assumed. The constraints on $T_{1/2}^{0\nu-exp}$ are from NEMO3 (^{48}Ca , $^{243}\text{ }^{82}\text{Se}$, $^{173}\text{ }^{100}\text{Mo}$, $^{244}\text{ }^{150}\text{Nd}^{245}$), GERDA ($^{76}\text{Ge}^{175}$), CAMEO (^{116}Cd , $^{246}\text{ CUORE}$ ($^{130}\text{Te}^{247}$) and Kamlandzen ($^{136}\text{Xe}^{25}$) experiments.

Nucl.	$G^{0\nu}$ [10^{-15}yr^{-1}]	$T_{1/2}^{0\nu-exp}$ [yr]	$T_{1/2}^{0\nu-theor}$ [yr]	
			IH	NH
^{48}Ca	24.81	$> 2.0 \times 10^{22}$	$(0.37, 36.) \times 10^{27}$	$(0.68, 74.) \times 10^{29}$
^{76}Ge	2.363	$> 5.2 \times 10^{25}$	$(0.54, 9.5) \times 10^{27}$	$(0.99, 19.) \times 10^{29}$
^{82}Se	10.16	$> 2.5 \times 10^{23}$	$(0.17, 2.6) \times 10^{27}$	$(0.31, 5.2) \times 10^{29}$
^{96}Zr	20.58	-	$(0.52, 74.) \times 10^{26}$	$(0.96, 150) \times 10^{28}$
^{100}Mo	15.92	$> 1.1 \times 10^{24}$	$(0.70, 6.4) \times 10^{26}$	$(0.13, 1.3) \times 10^{29}$
^{110}Pd	4.815	-	$(0.14, 2.8) \times 10^{27}$	$(0.26, 5.7) \times 10^{29}$
^{116}Cd	16.70	$> 1.7 \times 10^{23}$	$(0.95, 12.) \times 10^{26}$	$(0.18, 2.4) \times 10^{29}$
^{124}Sn	9.040	-	$(0.28, 6.6) \times 10^{27}$	$(0.52, 13.) \times 10^{29}$
^{130}Te	14.22	$> 4.0 \times 10^{24}$	$(0.11, 5.8) \times 10^{27}$	$(0.21, 12.) \times 10^{29}$
^{136}Xe	14.58	$> 1.1 \times 10^{26}$	$(0.21, 7.8) \times 10^{27}$	$(0.39, 16.) \times 10^{29}$
^{150}Nd	63.03	$> 2.0 \times 10^{22}$	$(0.35, 14.) \times 10^{26}$	$(0.65, 29.) \times 10^{28}$

The improved values of $G^{0\nu}$ calculated by taking into account the Dirac electron wave functions with finite nuclear size and electron screening are tabulated in Ref.²⁴¹

The nuclear matrix element $M'_{\nu}{}^{0\nu}$ takes the form

$$M'_{\nu}{}^{0\nu}(g_A^{\text{eff}}) = \frac{R}{2\pi^2 g_A^2} \sum_n \int e^{i\mathbf{p}\cdot(\mathbf{x}-\mathbf{y})} \frac{\langle 0_f^+ | J_L^{\mu\dagger}(\mathbf{x}) | n \rangle \langle n | J_{L\mu}^{\dagger}(\mathbf{y}) | 0_i^+ \rangle}{p(p + E_n - \frac{E_i - E_f}{2})} d^3p d^3x d^3y, \quad (54)$$

where $\mathbf{r}_{ij} \equiv \mathbf{r}_i - \mathbf{r}_j$. Initial and final nuclear ground states with energies E_i and E_f are denoted by $|0_i^+\rangle$ and $|0_f^+\rangle$, respectively. The summation index runs over intermediate nuclear states $|n\rangle$ with energies E_n . Details on the evaluation of the NME in Eq. (54) appear, e.g., in Ref.²⁴² and will be discussed in Sec. 8. We note that the axial-vector $g_A^{\text{eff}}(p^2)$ and induced pseudoscalar $g_P^{\text{eff}}(p^2)$ form factors of nuclear hadron currents $J^{\mu\dagger}$ are “renormalized in nuclear medium”. The magnitude and origin of this renormalization is the subject of the analysis of many works, since it tends to increase the $0\nu\beta\beta$ -decay half-life in comparison with the case in which this effect is absent. This issue will be addressed in Sec. 8.

In Table 3 we show predicted lifetimes of the $0\nu\beta\beta$ -decay, obtained with a Majorana neutrino mass corresponding to the NH and IH (see Eqs. (25) and (27)) and by assuming averaged values and variances of $M'_{\nu}{}^{0\nu}$ given in Table 6. They are compared with the best experimental limits on the $0\nu\beta\beta$ -decay half-life. We see

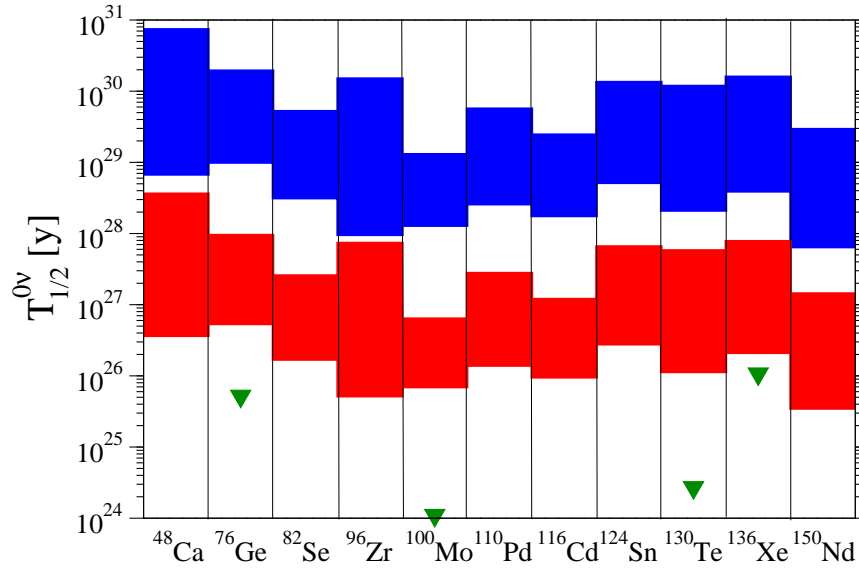


Fig. 6. (Color online.) The $0\nu\beta\beta$ -decay half-lives of nuclei of experimental interest calculated for the case of the NH (blue region) and IH (red region) (see Eqs. (25) and (27)). The averaged values with their variances for a given isotope from Table 6 are considered. The non-quenched value of weak-axial coupling constant is assumed. The current experimental constraints on the $0\nu\beta\beta$ -decay half-life are shown with filled green triangles.

that in the case of ^{136}Xe the current constraint is close to the range corresponding to the IH. This situation is displayed also in Fig. 6.

7.2. The neutrinoless double beta decay with sterile neutrinos

In our treatment sterile means a neutrino species, which does not participate in weak interactions. The mass of the sterile neutrinos is not known, so they could be light, but much heavier than the standard neutrinos or very heavy.

The contribution of such a neutrino to the $0\nu\beta\beta$ -decay amplitude is due to its nonzero admixture to ν_e weak eigenstate and as a result is described by the standard neutrino exchange diagram between the two β -decaying neutrons. Assuming LNV dominance the $0\nu\beta\beta$ decay half-life for a transition to the ground state of final nucleus takes the form²⁴⁸

$$[T_{1/2}^{0\nu}]^{-1} = G^{0\nu}(E_0, Z)g_A^4 \left| \sum_N (U_{eN}^2 m_N) m_p M'^{0\nu}(m_N, g_A^{\text{eff}}) \right|^2, \quad (55)$$

with m_p the proton mass. In the above formula g_A and g_A^{eff} stand respectively for the standard and "quenched" values of the nucleon axial-vector coupling constants.

The relevant nuclear matrix element $M'^{0\nu}$ is given by

$$M'^{0\nu}(m_N, g_A^{\text{eff}}) = \frac{1}{m_p m_e} \frac{R}{2\pi^2 g_A^2} \sum_n \int d^3x d^3y d^3p \times e^{i\mathbf{p}\cdot(\mathbf{x}-\mathbf{y})} \frac{\langle 0_F^+ | J_L^{\mu\dagger}(\mathbf{x}) | n \rangle \langle n | J_{L\mu}^\dagger(\mathbf{y}) | 0_I^+ \rangle}{\sqrt{p^2 + m_N^2} (\sqrt{p^2 + m_N^2} + E_n - \frac{E_I - E_F}{2})}. \quad (56)$$

The dependence on g_A^{eff} has been incorporated into the weak one-body charged current J_μ^\dagger .

Two conventional limiting cases are of interest, namely light, $m_N \ll p_F$, and the heavy, $m_N \gg p_F$, Majorana neutrino exchange mechanisms, where $p_F \sim 200$ MeV is the characteristic momentum carried via the virtual neutrino. In such cases the half-life in Eq. (55) can be written as

$$[T_{1/2}^{0\nu}]^{-1} = G^{0\nu}(E_0, Z) g_A^4 \begin{cases} \left| \frac{\langle m_\nu \rangle}{m_e} \right|^2 |M_\nu'^{0\nu}(g_A^{\text{eff}})|^2, & \text{for } m_N \ll p_F, \\ \left| \left\langle \frac{1}{m_N} \right\rangle m_p \right|^2 |M_N'^{0\nu}(g_A^{\text{eff}})|^2, & \text{for } m_N \gg p_F, \end{cases} \quad (57)$$

with

$$\langle m_\nu \rangle = \sum_N U_{eN}^2 m_N, \quad \left\langle \frac{1}{m_N} \right\rangle = \sum_N \frac{U_{eN}^2}{m_N}. \quad (58)$$

Here, p_F is identified with the Fermi momentum. The NMEs $M_\nu'^{0\nu}$, $M_N'^{0\nu}$ are obtained from $M'^{0\nu}$ appearing in Eq. (56) as follows

$$M'^{0\nu}(m_N \rightarrow 0, g_A^{\text{eff}}) = \frac{1}{m_p m_e} M_\nu'^{0\nu}(g_A^{\text{eff}}), \quad (59)$$

$$M'^{0\nu}(m_N \rightarrow \infty, g_A^{\text{eff}}) = \frac{1}{m_N^2} M_N'^{0\nu}(g_A^{\text{eff}}). \quad (60)$$

The NMEs of $M_\nu'^{0\nu}(g_A^{\text{eff}})$ and $M_N'^{0\nu}(g_A^{\text{eff}})$ associated with exchange of light and very heavy neutrinos can be found in Tables 6 and 7.

It has been shown in Ref.²⁴⁹ that, with the use of the above NMEs corresponding to the two limiting-cases, the half-life given by Eq. (56) can be obtained with a reasonably good accuracy using an "interpolating formula" given by

$$[T_{1/2}^{0\nu}]^{-1} = \mathcal{A} \left| m_p \sum_N U_{eN}^2 \frac{m_N}{\langle p^2 \rangle + m_N^2} \right|^2, \quad (61)$$

where

$$\mathcal{A} = G^{0\nu}(E_0, Z) g_A^4 |M_N'^{0\nu}(g_A^{\text{eff}})|^2, \quad (62)$$

$$\langle p^2 \rangle = m_p m_e \left| \frac{M_N'^{0\nu}(g_A^{\text{eff}})}{M_\nu'^{0\nu}(g_A^{\text{eff}})} \right| \quad (63)$$

Table 4. The values of the parameter $\langle p^2 \rangle$ of the interpolating formula specified in Eq. (63) calculated within different nuclear structure approaches: interacting shell model (ISM) (Strasbourg-Madrid (StMa)²⁵⁰ and Central Michigan University (CMU)²⁵¹ groups), interacting boson model (IBM),²⁵² quasiparticle random phase approximation (QRPA) (Tuebingen-Bratislava-Caltech (TBC)^{107, 253} and Jyväskylä (Jy)²⁵⁴ groups), projected Hartree-Fock Bogoliubov approach (PHFB).²⁵⁵ The Argonne, CD-Bonn and UCOM two-nucleon short-range correlations are taken into account. The non-quenched value of weak axial-vector coupling g_A is assumed.

Method	g_A	src	$\sqrt{\langle p^2 \rangle}$ [MeV]					
			⁴⁸ Ca	⁷⁶ Ge	⁸² Se	⁹⁶ Zr	¹⁰⁰ Mo	¹¹⁰ Pd
ISM-StMa	1.25	UCOM	178	150	149			
ISM-CMU	1.27	Argonne	178	134	138			
		CD-Bonn	203	165	162			
IBM	1.27	Argonne	113	103	103	129	136	135
QRPA-TBC	1.27	Argonne	189	163	164	180	174	166
		CD-Bonn	231	193	194	211	204	194
QRPA-Jy	1.26	CD-Bonn		191	192	217	207	187
PHFB	1.25	Argonne				130	127	124
		CD-Bonn				150	145	143

Method	g_A	src	$\sqrt{\langle p^2 \rangle}$ [MeV]					
			¹¹⁶ Cd	¹²⁴ Sn	¹²⁸ Te	¹³⁰ Te	¹³⁶ Xe	¹⁵⁰ Nd
ISM-StMa	1.25	UCOM		160		161	159	
ISM-CMU	1.27	Argonne		153		159	170	
		CD-Bonn		177		184	197	
IBM	1.27	Argonne	130	109	109	109	107	155
QRPA-TBC	1.27	Argonne	157	186	178	180	183	
		CD-Bonn	182	214	207	209	211	
QRPA-Jy	1.26	CD-Bonn	177	202	196	201	175	
PHFB	1.27	Argonne			131	132		121
		CD-Bonn			150	150		139

The values parameters $\langle p^2 \rangle$ obtained from $M_{\nu}^{\prime 0\nu}(g_A^{\text{eff}})$ and $M_{\text{N}}^{\prime 0\nu}(g_A^{\text{eff}})$, in the context of various nuclear structure methods, are given Table 4. A numerical comparison of the "exact" results, obtained within the QRPA with isospin restoration,¹⁰⁴ with those calculated with the interpolating formula (61) showed a rather good agreement, with the possible exception of the transition region where the accuracy is about 20% - 25%.²⁴⁸ By glancing the Table 4 one can see that there is a significant difference in the values of $\sqrt{\langle p^2 \rangle}$ calculated by different methods, using different short range two nucleon correlations. We note that the parameter $\sqrt{\langle p^2 \rangle}$ with typical values ~ 150 -200 MeV can be interpreted as the mean Fermi momentum p_F of the nucleons in the nucleus, as suggested by the structure of the NME in Eq. (56).

The apparent advantage of the formula (61) is the fact that it exhibits explicitly the m_{N} dependence of the $0\nu\beta\beta$ amplitude or the half-life. It can be conveniently

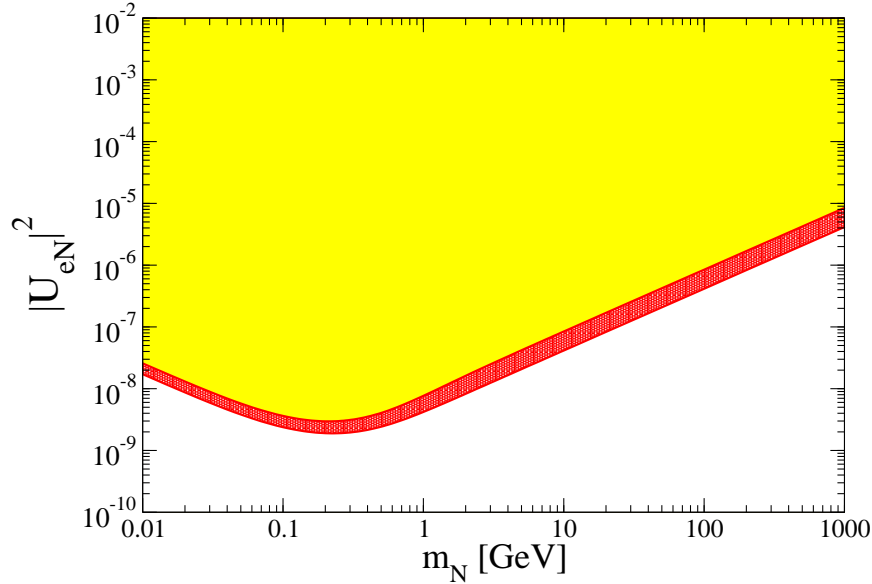


Fig. 7. The exclusion plot in the $|U_{eN}|^2 - m_N$ plane (yellow region) derived from the lower limit on the $0\nu\beta\beta$ -decay half-life of ^{136}Xe ($T_{1/2}^{0\nu\text{-exp}}(^{136}\text{Xe}) > 3.4 \cdot 10^{25}$ yr, combined EXO+KamlandZEN).¹⁸⁴ The weakest (strongest) limit is obtained for $M^{0\nu}(m_N)$ calculated with Argonne potential (CD-Bonn potential) within the QRPA with isospin restoration¹⁰⁴ and assuming $g_A^{\text{eff}} = 1.00$ ($g_A^{\text{eff}} = 1.269$).

used for an analysis of the neutrino sector without relying on the sophisticated machinery of the nuclear structure calculations. Also any upgrade in the nuclear structure approach typically brings out asymptotic NMEs for $m_N \ll p_F$ and $m_N \gg p_F$. This method allows one to immediately reconstruct with a good accuracy upgraded NMEs for any value of m_N .

The role of the intermediate mass sterile neutrinos N in various LNV processes has been extensively studied in the literature (for a recent review, c.f.^{150, 151}) and suitable limits in the $|U_{\alpha N}|^2 - m_N$ -plane have been derived. In fact it has been shown that $0\nu\beta\beta$ -decay limits for $|U_{eN}|^2 - m_N$ are the most stringent compared to those derived from other LNV processes, with the possible exception of a narrow region of the parametric plane.^{150, 256, 257} In Fig. 7 we present the exclusion plot $|U_{eN}|^2$ vs m_N . The most stringent half-life limit $T_{1/2}^{0\nu\text{-exp}} > 1.07 \times 10^{26}$ yr²⁵ has been used in the analysis.

In Ref.²⁴⁸ the $0\nu\beta\beta$ -decay half-life formula for a generic neutrino spectrum has been presented. It incorporates a popular scenario νMSM ^{258, 259} and offers a solution of the DM and baryon asymmetry problems utilizing massive Majorana neutrinos.

It contains the following ingredients:

- i) three light neutrinos $\nu_{k=1,2,3}$ with the masses $m_{\nu(k)} \ll p_F \sim 200$ MeV dominated by $\nu_{e,\mu,\tau}$;
- ii) a number of neutrinos ν_i^{DM} as dark matter (DM) candidates with the masses m_i^{DM} at the keV scale;
- iii) a number of heavy neutrinos N with the masses $m_N \gg p_F$,
- (iv) several intermediate mass m_h neutrinos h including a pair highly degenerate in mass, which is needed for the generation of the baryon asymmetry via leptogenesis.²⁵⁹

Taking the advantage of the "interpolating" formula (61) the $0\nu\beta\beta$ -decay half-life is given by²⁴⁸

$$\begin{aligned}
 [T_{1/2}^{0\nu}]^{-1} = \mathcal{A} & \left[\frac{m_p}{\langle p^2 \rangle} \sum_{k=1}^3 U_{ek}^2 m_k + \frac{m_p}{\langle p^2 \rangle} \sum_i (U_{ei}^{DM})^2 m_i^{DM} \right. \\
 & \left. + m_p \sum_N \frac{U_{eN}^2}{m_N} + m_p \sum_h \frac{U_{eh}^2 m_h}{\langle p^2 \rangle + m_h^2} \right]^2. \quad (64)
 \end{aligned}$$

Here, since the expected mixing $|U_{ei}^{DM}|, |U_{eN}|, |U_{eh}| \ll |U_{ek}|$ between the sterile and the standard neutrinos is very small, the mixing between the light neutrinos ν_k to a good accuracy can be identified with the PMNS mixing matrix $U_{ek} \approx U^{PMNS}$.

7.3. The right-handed current mechanisms of light neutrinos

Recently, the description of $0\nu\beta\beta$ -decay mechanisms due to the interference of the the left handed and right handed leptonic currents (see section 5.3), restricted to light neutrino exchange, has been revived and improved.²⁶⁰ Furthermore the effect of the induced pseudoscalar term of nucleon current was considered. Then, within the standard approximations the $0\nu\beta\beta$ -decay half-life takes the form

$$\begin{aligned}
 [T_{1/2}^{0\nu}]^{-1} = g_A^4 |M_{GT}|^2 & \left\{ C_{mm} \left(\frac{|m_{\beta\beta}|}{m_e} \right)^2 \right. \\
 & + C_{m\lambda} \frac{|m_{\beta\beta}|}{m_e} \langle \lambda \rangle \cos \psi_1 + C_{m\eta} \frac{|m_{\beta\beta}|}{m_e} \langle \eta \rangle \cos \psi_2 \\
 & \left. + C_{\lambda\lambda} \langle \lambda \rangle^2 + C_{\eta\eta} \langle \eta \rangle^2 + C_{\lambda\eta} \langle \lambda \rangle \langle \eta \rangle \cos(\psi_1 - \psi_2) \right\}. \quad (65)
 \end{aligned}$$

The effective lepton number violating parameters and the relative phases appearing in the previous equation are given by

$$\begin{aligned}
\langle \lambda \rangle &= \kappa \left| \sum_{j=1}^3 U_{ej} T_{ej}^* (g'_V/g_V) \right|, & \langle \eta \rangle &= \epsilon \left| \sum_{j=1}^3 U_{ej} T_{ej}^* \right|, \\
\psi_1 &= \arg \left[\left(\sum_{j=1}^3 m_j U_{ej}^2 \right) \left(\sum_{j=1}^3 U_{ej} T_{ej}^* (g'_V/g_V) \right)^* \right], \\
\psi_2 &= \arg \left[\left(\sum_{j=1}^3 m_j U_{ej}^2 \right) \left(\sum_{j=1}^3 U_{ej} T_{ej}^* \right)^* \right].
\end{aligned} \tag{66}$$

With help of (66) and by assuming (16), $U_0 \simeq V_0$ and $(g'_V/g_V) \simeq 1$ we get

$$\langle \lambda \rangle \approx (M_{W_1}/M_{W_2})^2 \frac{m_D}{m_{LNV}} |\xi|, \quad \langle \eta \rangle \approx \epsilon \frac{m_D}{m_{LNV}} |\xi|, \tag{67}$$

with

$$\begin{aligned}
|\xi| &= |c_{23}c_{12}c_{13}s_{13}^2 - c_{12}^3c_{13}^3 - c_{13}c_{23}c_{12}^2s_{13}^2 - c_{12}c_{13}(c_{13}^2s_{12}^2 + s_{13}^2)| \\
&\simeq 0.82
\end{aligned} \tag{68}$$

The experimental upper bound on the mixing angle of left and right vector bosons is $\epsilon < 0.013$ and, provided that the CP-violating phases in the mixing matrix for right-handed quarks are small, one gets $\epsilon < 0.0025$. Flavor and CP-violating processes of kaons and B-mesons allow one to deduce lower bound on the mass of the heavy vector boson $M_{W_2} > 2.9$ TeV.²⁶¹ In left right symmetric models (LRSM) there could be additional contributions to $0\nu\beta\beta$ -decay due to the doubly charged Higgs triplet. This triplet, also considered in the case of type-I seesaw mechanism, as pointed in Ref.,²⁶¹ was found to make a negligible contribution in this case.

The coefficients C_I ($I=mm, m\lambda, m\eta, \lambda\lambda, \eta\eta$ and $\lambda\eta$) can be expressed as appro-

appropriate combinations of nuclear matrix elements and phase-space factors as follows:

$$\begin{aligned}
C_{mm} &= (1 - \chi_F + \chi_T)^2 G_{01}^{0\nu}, \\
C_{m\lambda} &= -(1 - \chi_F + \chi_T) [\chi_{2-} G_{03}^{0\nu} - \chi_{1+} G_{04}^{0\nu}], \\
C_{m\eta} &= (1 - \chi_F + \chi_T) \\
&\quad \times [\chi_{2+} G_{03}^{0\nu} - \chi_{1-} G_{04}^{0\nu} - \chi_P G_{05}^{0\nu} + \chi_R G_{06}^{0\nu}], \\
C_{\lambda\lambda} &= \chi_{2-}^2 G_{02}^{0\nu} + \frac{1}{9} \chi_{1+}^2 G_{011}^{0\nu} - \frac{2}{9} \chi_{1+} \chi_{2-} G_{010}^{0\nu}, \\
C_{\eta\eta} &= \chi_{2+}^2 G_{02}^{0\nu} + \frac{1}{9} \chi_{1-}^2 G_{011}^{0\nu} - \frac{2}{9} \chi_{1-} \chi_{2+} G_{010}^{0\nu} + \chi_P^2 G_{08}^{0\nu} \\
&\quad - \chi_P \chi_R G_{07}^{0\nu} + \chi_R^2 G_{09}^{0\nu}, \\
C_{\lambda\eta} &= -2[\chi_{2-} \chi_{2+} G_{02}^{0\nu} - \frac{1}{9} (\chi_{1+} \chi_{2+} + \chi_{2-} \chi_{1-}) G_{010}^{0\nu} \\
&\quad + \frac{1}{9} \chi_{1+} \chi_{1-} G_{011}^{0\nu}].
\end{aligned} \tag{69}$$

The explicit form of nuclear matrix elements M_{GT} and the ratios χ_I of the other matrix elements over this one is given in.²⁶⁰ The integrated kinematical factors as recently improved are given in Table 5.

In this case the $0\nu\beta\beta$ -decay rate (65) depends on a number of parameters, $\langle\lambda\rangle$, $\langle\eta\rangle$, ψ_1 and ψ_2 , whose values are unknown. Their importance also depends on the value of the coefficients C_I ($I=mm, m\lambda, m\eta, \lambda\lambda, \eta\eta$ and $\lambda\eta$), which can be calculated. The corresponding quantity is a superposition of contributions C_I^{0k} associated with phase space factors $G_{0k}^{0\nu}$ ($k=1, \dots, 11$). In Fig. 8 ratios C_I^{0k}/C_I for the $0\nu\beta\beta$ -decay ^{76}Ge and ^{136}Xe are displayed. They were obtained by using the quasiparticle random phase approximation (QRPA)²⁶² and the interacting shell-model (ISM)⁶⁸ nuclear matrix elements. We should mention that the coefficients C_{mm} , $C_{\lambda\lambda}$, $C_{\eta\eta}$, and $C_{m\eta}$ are dominated by a single contribution. In the case of $C_{m\lambda}$ and $C_{\lambda\eta}$, however, there may exist a competition between two contributions.

Using these nuclear matrix elements^{68, 262} and the phase-space factors from Table 5 one can deduce from the experimental data $T_{1/2}^{0\nu-exp} > 1.07 \times 10^{26} \text{ yr}^{25}$ for ^{136}Xe decay²⁵ in the case of left-right symmetric theories constraints on the parameters as follows:²⁶⁰

$$\begin{aligned}
\langle\eta\rangle &\leq 1.2 \times 10^{-9} \text{ (QRPA)}, \quad 1.7 \times 10^{-9} \text{ (ISM)}, \\
\langle\lambda\rangle &\leq 2.4 \times 10^{-7} \text{ (QRPA)}, \quad 1.9 \times 10^{-7} \text{ (ISM)}.
\end{aligned} \tag{70}$$

Furthermore by assuming the values $\epsilon = 0.013$ and 0.0025 mentioned earlier as well as the current limit - $\langle\eta\rangle \leq 1.7 \times 10^{-9}$ (^{136}Xe , ISM) we end up with $m_D/m_{LNV} < 1.6 \times 10^{-7}$ and $< 8.3 \times 10^{-7}$, respectively. For $M_{W_2} = 2.9 \text{ TeV}$ and $\langle\lambda\rangle \leq 1.9 \times 10^{-7}$ (^{136}Xe , ISM) we get $m_D/m_{LNV} = 3.0 \times 10^{-4}$. Thus, from the more stringent limits on $\langle\eta\rangle$ we obtain $m_{LNV}/\text{TeV} > (1.2 - 6.3) m_D/\text{MeV}$, in agreement with the assumption that the basic scale of LRSM is $\text{O}(\text{TeV})$. It is therefore obvious

Table 5. Phase-space factors $G_{0j}^{0\nu}$ ($j=1, \dots, 11$) in units yr^{-1} obtained using screened exact finite-size Coulomb wave functions for $s_{1/2}$ and $p_{1/2}$ states of electron.

	^{48}Ca	^{76}Ge	^{82}Se	^{96}Zr	^{100}Mo	^{110}Pd
$10^{14}G_{01}^{0\nu}$	2.483	0.237	1.018	2.062	1.595	0.483
$10^{14}G_{02}^{0\nu}$	16.229	0.391	3.529	8.959	5.787	0.814
$10^{15}G_{03}^{0\nu}$	18.907	1.305	6.913	14.777	10.974	2.672
$10^{15}G_{04}^{0\nu}$	5.327	0.470	2.141	4.429	3.400	0.978
$10^{13}G_{05}^{0\nu}$	3.007	0.566	2.004	4.120	3.484	1.400
$10^{12}G_{06}^{0\nu}$	3.984	0.531	1.733	3.043	2.478	0.934
$10^{10}G_{07}^{0\nu}$	2.682	0.270	1.163	2.459	1.927	0.599
$10^{11}G_{08}^{0\nu}$	1.109	0.149	0.708	1.755	1.420	0.462
$10^{10}G_{09}^{0\nu}$	16.246	1.223	4.779	8.619	6.540	1.939
$10^{14}G_{010}^{0\nu}$	2.116	0.141	0.801	1.855	1.359	0.309
$10^{15}G_{011}^{0\nu}$	5.376	0.476	2.183	4.557	3.502	1.010
	^{116}Cd	^{124}Sn	^{130}Te	^{136}Xe	^{150}Nd	
$10^{14}G_{01}^{0\nu}$	1.673	0.906	1.425	1.462	6.316	
$10^{14}G_{02}^{0\nu}$	5.349	1.967	3.761	3.679	29.187	
$10^{15}G_{03}^{0\nu}$	11.128	5.403	8.967	9.047	45.130	
$10^{15}G_{04}^{0\nu}$	3.569	1.886	3.021	3.099	14.066	
$10^{13}G_{05}^{0\nu}$	4.060	2.517	3.790	4.015	14.873	
$10^{12}G_{06}^{0\nu}$	2.563	1.543	2.227	2.275	7.497	
$10^{10}G_{07}^{0\nu}$	2.062	1.113	1.755	1.812	8.085	
$10^{11}G_{08}^{0\nu}$	1.703	0.939	1.549	1.657	8.405	
$10^{10}G_{09}^{0\nu}$	6.243	3.301	4.972	4.956	19.454	
$10^{14}G_{010}^{0\nu}$	1.418	0.660	1.146	1.165	7.115	
$10^{15}G_{011}^{0\nu}$	3.704	1.955	3.148	3.238	15.055	

that already the present limits of $0\nu\beta\beta$ -decay half-lives can be used to constrain the allowed parameter space of LRSM. Furthermore the present mechanism associated with right-handed currents, somewhat forgotten in recent years, can, in principle, compete with the one based on $m_{\beta\beta}$ that is commonly used.

Before concluding this section we should mention again that the contributions discussed in this section can involve different kinematics, since due to the chiralities involved the neutrino momentum is picked in the propagator (see Eq. (44)) rather than the neutrino mass. It can thus, in principle, be distinguished from the left handed ν - mass contribution by measuring energy and angular correlations of the two β rays as discussed in more detail in earlier reviews.^{17, 24} To this end dedicated tracking detectors such as ELEGANT/MOON and NEMO-3/SuperNEMO can be

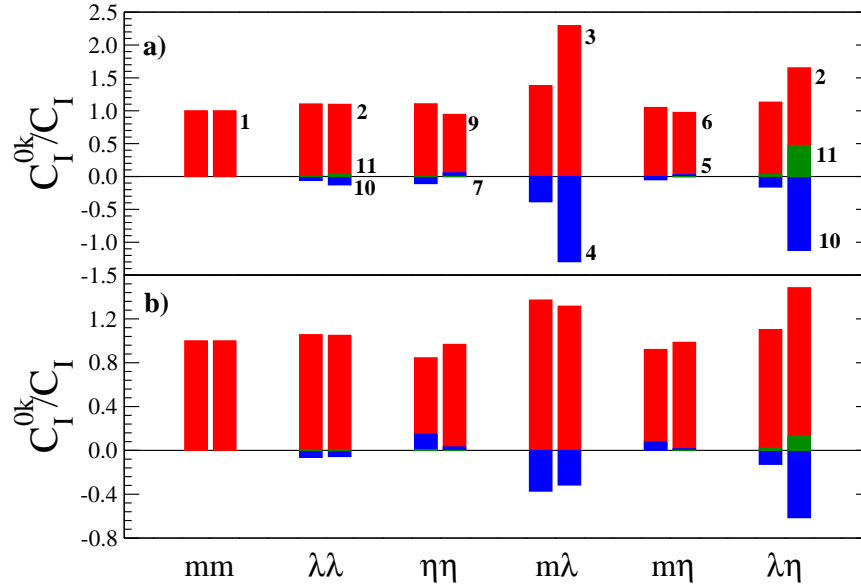


Fig. 8. (Color online) The decomposition of coefficients C_I ($I=mm, m\lambda, m\eta, \lambda\lambda, \eta\eta$ and $\lambda\eta$, see Eqs. (65) and (69)) on partial contributions C_I^{0k} associated with phase space factors $G_{0k}^{0\nu}$ ($k=1, \dots, 11$). The symbols standing for index I are shown on the x-axis. The partial contributions are identified by index k , whose value is shown by the corresponding bar. The contributions from largest to the third largest are displayed in red, blue and orange colors, respectively. Ratios C_I^{0k}/C_I calculated with the ISM and QRPA matrix elements are presented with left and right bars for each value of index I , respectively. Results for ^{76}Ge and ^{136}Xe are presented in the lower b) and upper a) panels, respectively.

used for the correlation studies (see section 6).

7.4. Mechanism with heavy neutrinos within LR symmetric models

In connection with LHC facility at CERN there is a frequently addressed question whether the origin of neutrino masses is due to physics at the TeV scale. A brief overview of a class of TeV scale theories for neutrino masses based on the LR extension of the standard model can be found e.g. in Ref.²⁶³

By considering only those $0\nu\beta\beta$ -decay mechanisms within the LR theories, which amplitudes are proportional to light light neutrino masses m_i or inverse proportional to heavy neutrino masses M_i , for the half-life we get

$$\left(T_{1/2}^{0\nu} G^{0\nu} g_A^4\right)^{-1} = \left|\eta_\nu M'^{0\nu}_\nu(g_A^{\text{eff}}) + \eta_N^L M'^{0\nu}_N(g_A^{\text{eff}})\right|^2 + \left|\eta_N^R M'^{0\nu}_N(g_A^{\text{eff}})\right|^2 \quad (71)$$

$$\begin{aligned}\eta_\nu &= \frac{m_{\beta\beta}^2}{m_e^2} = \sum_i (U_{ei}^{(11)})^2 \frac{m_i}{m_e} \approx \frac{m_p}{m_{LNV}} \frac{m_D^2}{m_e m_p} \sum_i (U_0)_{ei}^2 \frac{m_i}{m_D^2} m_{LNV}, \\ \eta_N^L &= \frac{m_p}{m_{LNV}} \sum_i (U_{ei}^{(12)})^2 \frac{m_{LNV}}{M_i} \approx \frac{m_p}{m_{LNV}} \left(\frac{m_D}{m_{LNV}} \right)^2 \sum_i \frac{m_{LNV}}{M_i}, \\ \eta_N^R &= \frac{m_p}{m_{LNV}} \left(\frac{M_{W_1}}{M_{W_2}} \right)^2 \sum_i (U_{ei}^{(22)})^2 \frac{m_{LNV}}{M_i} \approx \frac{m_p}{m_{LNV}} \left(\frac{M_{W_1}}{M_{W_2}} \right)^2 \sum_i (V_0)_{ei}^2 \frac{m_{LNV}}{M_i}.\end{aligned}\quad (72)$$

We note that the negligible interference term between left and right handed contributions is not taken into account. From the qualitative analysis in Eq. (72) it follows that if $M_{W_1}/M_{W_2} \gg m_D/m_{LNV}$ the heavy neutrino mass contribution due to right-handed currents to the $0\nu\beta\beta$ -decay (η_N^R mechanism) dominates over the heavy neutrino mass contribution determined by only left handed currents (η_N^L mechanism) unless there is some strong suppression due to mixing among heavy neutrinos. Further, the η_ν and η_N^R mechanisms could be of a comparable importance, if we could write

$$\begin{aligned}\sum_i (U_0)_{ei}^2 \frac{m_i}{m_D^2} m_{LNV} &\simeq \sum_i (V_0)_{ei}^2 \frac{m_{LNV}}{M_i} \\ \frac{m_D^2}{m_e m_p} M'_\nu &\simeq \left(\frac{M_{W_1}}{M_{W_2}} \right)^2 M'_N.\end{aligned}\quad (73)$$

In such a case a competition between these two mechanism can play an important role.

There is a general consensus that a measurement of the $0\nu\beta\beta$ -decay in one isotope does not allow us to determine the underlying physics mechanism. Complementary measurements in different isotopes is very important especially for the case there are competing mechanisms of the $0\nu\beta\beta$ -decay. Different cases of competing $0\nu\beta\beta$ -decay mechanisms were discussed in Ref.²⁴ and more recently in Refs.²⁶⁴⁻²⁶⁶

If the $0\nu\beta\beta$ -decay is induced by two “non-interfering” mechanisms η_ν and η_N^R one can determine the absolute values of these two fundamental parameters from data on the half-lives of two nuclear isotopes.^{265,266} Given a pair of nuclei, $|\eta_\nu|^2$ and $|\eta_N^R|^2$ are solutions of a system of two linear equations

$$\left(T_{1/2}^{0\nu}(i) G^{0\nu}(i) g_A^4 \right)^{-1} = |\eta_\nu M'_\nu(i)|^2 + |\eta_N^R M'_N(i)|^2, \quad (74)$$

where the index i denotes the isotope. From the “positivity” conditions ($|\eta_\nu|^2 > 0$ and $|\eta_N^R|^2 > 0$) it follows that the ratio of half-lives is within the range^{265,266}

$$\frac{G^{0\nu}(i) |M_N^{0\nu}(i)|^2}{G^{0\nu}(j) |M_N^{0\nu}(j)|^2} \leq \frac{T_{1/2}^{0\nu}(j)}{T_{1/2}^{0\nu}(i)} \leq \frac{G^{0\nu}(i) |M_\nu^{0\nu}(i)|^2}{G^{0\nu}(j) |M_\nu^{0\nu}(j)|^2}. \quad (75)$$

Surprisingly, the physical solutions are possible only if the ratio of the half-lives takes values in narrow intervals.²⁶⁵ This also is true in the case of other

competing mechanisms.²⁴ Often the non physical solutions can be eliminated by already existing data.²⁴

In Fig. 9 the allowed ranges of $m_{\beta\beta}$ and η_N^R parameters obtained as solution of Eq. (75) are presented as function of half-life of ^{76}Ge , ^{76}Se and ^{76}Te by assuming $T_{1/2}^{0\nu\text{-exp}}(^{136}\text{Xe}) = 1.0 \cdot 10^{27}$ y, what is compatible with inverted hierarchy of neutrino masses. In the case of a dominance of a single mechanism we have $m_{\beta\beta} = 38$ meV and $\eta_N^R = 1.1 \cdot 10^{-9}$. We notice that linear set of equations in Eq. (75) has solution for a very narrow interval for $T_{1/2}^{0\nu\text{-exp}}(^{130}\text{Te})$ and that by assuming co-existence of both mechanisms the values of parameters $m_{\beta\beta}$ and η_N^R are smaller.

8. The neutrinoless double-beta decay nuclear matrix elements

The nuclear matrix elements for the $0\nu\beta\beta$ decay must be evaluated using nuclear structure methods. There are no observables that could be directly related to the magnitude of $0\nu\beta\beta$ nuclear matrix elements and that could be used to determine them in a model independent way.

The nuclear matrix elements $M_{\nu}^{0\nu}$ and $M_N^{0\nu}$ associated with exchange of light (sub eV scale) and heavy (TeV scale) neutrinos, respectively, can be written as

$$M_{\nu,N}^{0\nu} = \left(\frac{g_A^{\text{eff}}}{g_A} \right)^2 M_{\nu,N}^{0\nu}(g_A^{\text{eff}}), \quad (76)$$

where $M_{\nu,N}^{0\nu}$ consists of Fermi, Gamow-Teller and tensor parts as

$$M_{\nu,N}^{0\nu}(g_A^{\text{eff}}) = -\frac{M_F^{(\nu,N)}}{(g_A^{\text{eff}})^2} + M_{GT}^{(\nu,N)}(g_A^{\text{eff}}) + M_T^{(\nu,N)}(g_A^{\text{eff}}). \quad (77)$$

This definition of $M_{\nu,N}^{0\nu}$ allows to display the effects of uncertainties in g_A^{eff} .

There is a common practice to calculate $0\nu\beta\beta$ -decay NMEs by taking advantage of relative coordinates of two decaying nucleons. For $0^+ \rightarrow 0^+$ transition we have

$$M_K^{(\nu,N)} = \sum_{J_m^{\pi}, \mathcal{J}} \sum_{pn p' n'} (-1)^{j_n + j_{p'} + J + \mathcal{J}} \sqrt{2\mathcal{J} + 1} \left\{ \begin{matrix} j_p & j_n & J \\ j_{n'} & j_{p'} & \mathcal{J} \end{matrix} \right\} \times \quad (78)$$

$$\langle p(1), p'(2); \mathcal{J} \parallel \mathcal{O}_K^{(\nu,N)} \parallel n(1), n'(2); \mathcal{J} \rangle \langle 0_f^+ \parallel [c_{p'}^+ \tilde{c}_{n'}]_J \parallel J_m^{\pi} \rangle \langle J_m^{\pi} \parallel [c_p^+ \tilde{c}_n]_J \parallel 0_i^+ \rangle .$$

The reduced matrix elements of the one-body proton-neutron operators $c_p^+ \tilde{c}_n$ (\tilde{c}_n denotes the time-reversed state) in the Eq. (79)

The two-body operators $O_K^{(\nu,N)}$, $K = \text{Fermi (F), Gamow-Teller (GT), and Tensor (T)}$ in (79) contain neutrino potentials and spin and isospin operators, and energies of excited states $E_{J\pi}^m$:

$$\begin{aligned} O_F^{(\nu,N)}(r_{12}, E_{J\pi}^k) &= \tau^+(1)\tau^+(2) H_F^{(\nu,N)}(r_{12}, E_{J\pi}^m), \\ O_{GT}^{(\nu,N)}(r_{12}, E_{J\pi}^k) &= \tau^+(1)\tau^+(2) H_{GT}^{(\nu,N)}(r_{12}, E_{J\pi}^m) \sigma_{12}, \\ O_T^{(\nu,N)}(r_{12}, E_{J\pi}^k) &= \tau^+(1)\tau^+(2) H_T^{(\nu,N)}(r_{12}, E_{J\pi}^m) S_{12}. \end{aligned} \quad (79)$$

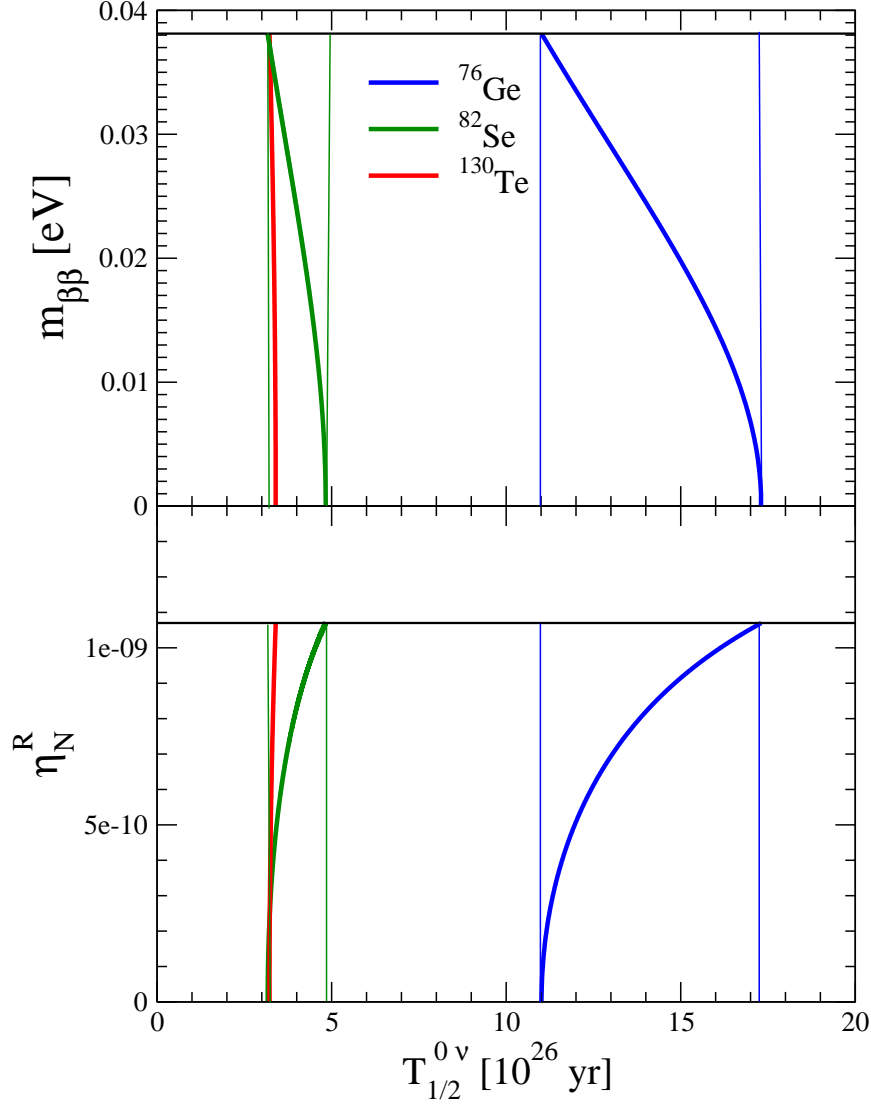


Fig. 9. (Color online) The parameters $m_{\beta\beta}$ and η_N^R versus the $0\nu\beta\beta$ -decay half-life of ^{76}Ge (blue), ^{82}Se (green) and ^{130}Te (red) for $T_{1/2}^{0\nu-e\text{xp}}(^{136}\text{Xe}) = 1.0 \cdot 10^{27}$ yr. The horizontal lines correspond to values of $m_{\beta\beta}$ and η_N^R , if there is a dominance of single mechanism. The QRPA NMEs (TBC, Argonne src) and the non-quenched value of g_A^{eff} are considered (see Tables 6 and 7).

with

$$\begin{aligned}
 \mathbf{r}_{12} &= \mathbf{r}_1 - \mathbf{r}_2, & r_{12} &= |\mathbf{r}_{12}|, & \hat{\mathbf{r}}_{12} &= \frac{\mathbf{r}_{12}}{r_{12}}, \\
 \sigma_{12} &= \vec{\sigma}_1 \cdot \vec{\sigma}_2, & S_{12} &= 3(\vec{\sigma}_1 \cdot \hat{\mathbf{r}}_{12})(\vec{\sigma}_2 \cdot \hat{\mathbf{r}}_{12}) - \sigma_{12}.
 \end{aligned} \tag{80}$$

Here, \mathbf{r}_1 and \mathbf{r}_2 are the coordinates of the nucleons undergoing beta decay.

The neutrino potentials are integrals over the exchanged momentum q ,

$$H_K^{(\nu, N)}(r_{12}, E_{J\pi}^k) = \frac{2}{\pi} R \int_0^\infty f_K(qr_{12}) F^{(\nu, N)}(q^2) h_K(q^2) q^2 dq \quad (81)$$

The functions $f_{F,GT}(qr_{12}) = j_0(qr_{12})$ and $f_T(qr_{12}) = -j_2(qr_{12})$ are spherical Bessel functions. The functions $h_K(q^2)$ that enter the H_K 's through the integrals over q in Eq. (81) are

$$\begin{aligned} h_F(q^2) &= g_V^2(q^2) & (82) \\ h_{GT}(q^2) &= \frac{g_A^2(q^2)}{g_A^2} \left[1 - \frac{2}{3} \frac{q^2}{q^2 + m_\pi^2} + \frac{1}{3} \left(\frac{q^2}{q^2 + m_\pi^2} \right)^2 \right] + \frac{2}{3} \frac{g_M^2(q^2)}{(g_A^{\text{eff}})^2} \frac{q^2}{4m_p^2}, \\ h_T(q^2) &= \frac{g_A^2(q^2)}{g_A^2} \left[\frac{2}{3} \frac{q^2}{q^2 + m_\pi^2} - \frac{1}{3} \left(\frac{q^2}{q^2 + m_\pi^2} \right)^2 \right] + \frac{1}{3} \frac{g_M^2(q^2)}{(g_A^{\text{eff}})^2} \frac{q^2}{4m_p^2} \end{aligned}$$

Here, the Partially Conserved Axial Current (PCAC) hypothesis has been employed. The finite nucleon size is taken into account via momentum dependence of the nucleon form-factors. For the vector, weak-magnetism and axial-vector form factors we adopt the usual dipole approximation as follows:

$$g_V(q^2) = \frac{g_V}{(1 + q^2/M_V^2)^2}, \quad g_M(q^2) = (\mu_p - \mu_n)g_V(q^2), \quad g_A(q^2) = \frac{g_A^{\text{eff}}}{(1 + q^2/M_A^2)^2}, \quad (83)$$

where $g_V = 1$, $(\mu_p - \mu_n) = 3.70$. The parameters $M_V = 850 \text{ MeV}$ and $M_A = 1086 \text{ MeV}$ come from electron scattering and neutrino charged-current scattering experiments.

The difference in the calculation of $M_\nu^{0\nu}(g_A^{\text{eff}})$ and $M_N^{0\nu}(g_A^{\text{eff}})$ has origin in factors $F^{(\nu, N)}(q^2)$. We have

$$F^{(\nu)}(q^2) = \frac{1}{q (q + E_{J\pi}^m - (E_i + E_f)/2)}, \quad F^{(\nu, N)}(q^2) = \frac{1}{m_e m_p}. \quad (84)$$

From the form of $F^{(\nu)}(q^2)$ it follows that corresponding potentials (81) depend weakly on the energies of the virtual intermediate states, $E_{J\pi}^m$ as the mean neutrino momentum is large about 100-200 MeV. As $F^{(\nu, N)}(q^2)$ does not depend on the energy of intermediate states, the summation over these states by using completeness relation

$$1 = \sum_{J_m^\pi} |J_m^\pi\rangle \langle J_m^\pi|. \quad (85)$$

Then the calculation of $M_N^{0\nu}(g_A^{\text{eff}})$ requires only the knowledge of initial and final ground state wave functions. The same is valid also for calculation of $M_\nu^{0\nu}(g_A^{\text{eff}})$ once the closure approximation for intermediate nuclear states is considered by replacing energies of intermediate states $[E_{J\pi}^m - (E_i + E_f)/2]$ by an average value $\bar{E} \approx 10 \text{ MeV}$.

However, we note that a construction of reliable ground state wave functions requires diagonalization procedure by which all states of the intermediate nucleus are calculated. The problem with the averaged energy \overline{E} is that its value is unknown and there is no good way to calculate it.

The nuclear structure approaches do not allow one to introduce the short-range correlations into the two-nucleon relative wave function. The traditional way to take them into account is to introduce an explicit Jastrow-type correlation function $f(r_{12})$ into the involved two-body transition matrix elements

$$\langle \Psi_{\mathcal{J}} \| f(r_{12}) \mathcal{O}_K(r_{12}) f(r_{12}) \| \Psi_{\mathcal{J}} \rangle. \quad (86)$$

Here,

$$|\overline{\Psi}_{\mathcal{J}}\rangle = f(r_{12}) |\Psi_{\mathcal{J}}\rangle, \quad |\Psi_{\mathcal{J}}\rangle \equiv |n(1), n'(2); \mathcal{J}\rangle \quad (87)$$

are the relative wave function with and without the short-range correlations, respectively. Currently, for purpose of numerical calculation of the $0\nu\beta\beta$ -decay NMEs the coupled cluster method short-range correlation functions in an analytic form of Jastrow-like function are used,

$$f(r_{12}) = 1 - c e^{-ar^2} (1 - br^2). \quad (88)$$

The set of parameters for Argonne and CD-Bonn NN interactions is given by

$$\begin{aligned} \text{set A: } & a = 1.59 \text{ fm}^{-2}, \quad b = 1.45 \text{ fm}^{-2}, \quad c = 0.92, \\ \text{set B: } & a = 1.52 \text{ fm}^{-2}, \quad b = 1.88 \text{ fm}^{-2}, \quad c = 0.46. \end{aligned} \quad (89)$$

Another option is to adopt the the unitary correlation operator method (UCOM) approach for description of the two-body correlated wave function.²⁶⁷

8.1. Nuclear matrix elements for non-quenched value of axial vector coupling constant

There is a variety of nuclear structure methods used for the calculation of the $0\nu\beta\beta$ -decay NMEs. The differences among them are due to construction of the mean field, the ways residual interaction is fixed, the size of the considered single nucleon model space, the many-body approximations are used in the diagonalization of the nuclear Hamiltonian and the type considered short-range correlations.

In the last few years there is a lot of activity in the field of calculation of the $0\nu\beta\beta$ -decay NMEs and significant progress has been achieved. Five different many-body approximate methods have been applied for the calculation as follows:

- (1) The Interacting Shell Model (ISM) (Strasbourg-Madrid (StMa)²⁵⁰ and Central Michigan University (CMU)²⁵¹ groups).

The disadvantage of the ISM is that only a limited number of orbits close to the Fermi level is considered. The advantage is that all possible correlations within

the space are included. As a result a good spectroscopy of low-lying excited states for parent and daughter nuclei is achieved. This approach has been applied only for six double beta decay systems with $A=48, 76, 82, 124, 130$ and 136 . The CMU group managed to perform calculation without consideration of the closure approximation.^{251,268-270} In addition, useful multipole decomposition of the $0\nu\beta\beta$ -decay nuclear matrix element was presented.

For a given choice of harmonic single particle states it can allow a large number of nucleons to be put in these orbitals leading to large configuration mixing. Unfortunately, however, even with the most advanced computers, in order to get a manageable size of the resulting shell model matrices, the number of orbitals is restricted, usually ≤ 4 .

This limitation can be somewhat overcome by considering doorway states in perturbation theory. Suppose that the double beta decay operator for light neutrinos in the case of the closure approximation is given by

$$T_0 = \sum_{i<j} \tau_i^+ \tau_j^+ (f_V^2 - g_A^2 \sigma_i \cdot \sigma_j), \quad T_1 = \sum_{i<j} \tau_i^+ \tau_j^+ (f_V^2 - g_A^2 \sigma_i \cdot \sigma_j) \frac{1}{r_{ij}} \quad (90)$$

Suppose now that the ground state of the initial nucleus (N, Z) obtained in the ISM is $|i\rangle$ and that of the final $(N-2, Z+2)$ nucleus is $|f\rangle$. Consider now the doorway states d_i and d_f built on the initial and final states respectively, namely

$$d_i = T_0|i\rangle, \quad d_f = T_0^\dagger|f\rangle. \quad (91)$$

Suppose further that the states d_i and d_f are normalized and orthogonalized to the final and initial ISM states respectively, i.e. :

$$\langle d_i|f\rangle = 0, \quad \langle d_f|i\rangle = 0, \quad \langle d_i|d_i\rangle = 1, \quad \langle d_f|d_f\rangle = 1. \quad (92)$$

Then using the employed nucleon-nucleon interaction one computes the mixing to the final and initial states as follows:

$$C_f = \frac{\langle d_i|V|f\rangle}{E_{d_i} - E_f}, \quad C_i = \frac{\langle d_f|V|i\rangle}{E_{d_f} - E_i} \quad (93)$$

where E_{d_i}, E_{d_f} are the energies of the doorway states and E_i and E_f are the energies of the initial and final states obtained in the ISM.

The neutrinoless double beta decay nuclear matrix element can be given as:

$$M_\nu^{0\nu} = \langle f|T|i\rangle + C_f \langle d_i|T|i\rangle + C_i \langle f|T|d_f\rangle \quad (94)$$

where T is the transition operator, as described in section 7, with the first ME as obtained in the ISM. In this approach one will manage to include any missing the spin-orbit partner in the ISM, which guarantees that the Ikeda sum rule is fulfilled.

If one wants to be more ambitious one may use the operator T_1 instead of T_0 .

It is clear that this treatment does not avoid the number of operations involved in the full Hilbert space. The only great advantage is that it does not lead to an increase of the already large matrix dimensions involved in the ISM.

- (2) Quasiparticle Random Phase Approximation (QRPA) (Tuebingen-Bratislava-Caltech (TBC),^{107, 253} Jyväskylä (Jy),²⁵⁴ and Noth-Caroline University (NC)²⁷¹ groups).

The formalism of the spherical¹⁰⁷ and deformed²⁵³ QRPA has been improved by the TBC group by achieving partial restoration of the isospin symmetry by the requirement that $2\nu\beta\beta$ -decay Fermi matrix element vanishes, as it should, unlike in previous version of the method. It was achieved by separating the renormalization parameter g_{pp} of the particle-particle proton-neutron interaction into isovector and isoscalar parts. The isovector parameter $g_{pp}^{T=1}$ was chosen to be essentially equal to the constant g_{pair} used to renormalize the nucleon pairing interactions. So, no new parameter was needed. As a result in the case of $0\nu\beta\beta$ -decay the Fermi matrix element is substantially reduced, while the full matrix element $M_\nu^{0\nu}$ is reduced by $\approx 10\%$. The Jy group improved their calculation²⁵⁴ by following the calculation procedure of the TBC group apart from the isospin restoration. Unlike in their previous calculations²⁷²⁻²⁷⁴ the tensor contribution to $M_\nu^{0\nu}$ has been found to be non-negligible in agreement with the TBC results.¹⁰⁷ In both, TBC and Jy calculations the pairing and residual interactions of the nuclear Hamiltonian and the two-nucleon short-range correlations (SRC) are derived from the same realistic nucleon-nucleon interaction (CD-Bonn and Argonne potentials) by exploiting the Brueckner-Hartree-Fock and coupled cluster methods. Contrary, calculation of the NC group are performed within the deformed QRPA approach by exploiting the Skyrme interaction. We note that there is a new QRPA approach developed by Terasaki in which the $0\nu\beta\beta$ -decay NME is calculated with particle-particle QRPA by two particle transfer to the intermediate nucleus (A+2,Z+2) nucleus under the closure approximation, instead the true double-beta path through (A,Z+1) nucleus.²⁷⁵ The obtained result for ^{150}Nd are in a rather good agreement with that of the TBC group within deformed QRPA approach.²⁵³

- (3) Interacting Boson Model (IBM).²⁵²

In the IBM the low lying states of the nucleus are modeled in terms of either L=0 (s boson) or L=2 (d boson) states. Recently, the IBM-2 approach has been also improved by considering isospin restoration in the calculation of the $0\nu\beta\beta$ -decay NMEs.²⁵² It affected slightly the Fermi contribution to $M_\nu^{0\nu}$, which become smaller.

- (4) The Projected Hartree-Fock-Bogoliubov Method (PHFB)²⁷⁶ and non-relativistic²⁷⁷ and relativistic¹¹¹ the Energy Density Functional Method (EDF) methods.

Recently, within the PHFB approach a systematic study of the uncertainties in calculated $0\nu\beta\beta$ -decay matrix elements has been performed by considering different sets of schematic residual interaction and Jastrow-like short-range

correlations.²⁷⁶ The advantage of the PHFB is that the PHFB wave functions possess good particle number and angular momentum obtained by projection on the axially symmetric intrinsic HFB states. The EDF is considered to be an improvement with respect to the PHFB. Compared with the PHFB, the EDF includes additional correlations connected with particle number projection, as well as fluctuations in quadrupole shapes and pairing gaps. Recently, a systematic study of the $0\nu\beta\beta$ -decay matrix elements was presented in the framework of the relativistic EDF (REDF) method.¹¹¹ For sake of simplicity often calculations are performed without taking into account two-body short-range correlations.

- (5) The ab initio methods.^{278–281} The issue of ab initio methods is the description of nuclei starting from the constituent nucleons and the realistic interactions among them. The nuclear forces include two-, three- and possibly higher many-nucleon components. This approach has so far been applied successfully for nuclear structure properties of light nuclei. Thus up to now there have been no results for double beta transitions apart for some toy model calculations. It might be that the ab initio $0\nu\beta\beta$ -decay results for ^{48}Ca will appear soon.

It goes without saying that each of the applied methods has some advantages and drawbacks and that there is space for further improvement of each of them.

In Table 6, recent results of the different methods for $M_{\nu}^{0\nu}$ are summarized. The presented numbers have been obtained with the non-quenched value of the axial coupling constant ($g_A^{\text{eff}} = g_A$)^c. Thus, the discrepancies among the results of different approaches are mostly related to the approximations on which a given nuclear many-body method is based. From Table 6 it follows that there exists significant difference between the results of the ISM and other approaches. The UCOM and Brueckner (CD-Bonn and Argonne) short-range correlations were considered. The impact of the choice of the short-range correlations on the NME is not large, about 10%. The spread of values for a given isotope is mostly given by factor 2 and for ^{48}Ca about factor 5. The spread for a given isotope is affected by the presence of results calculated with the ISM and the REDF approaches, which usually offer the smallest and largest value of calculated NME. In order to estimate the current uncertainty in NMEs for a given isotope we take advantage of calculation of mean values and variances following Refs.^{282,283} We see that the smallest uncertainty is reported by ^{128}Te , ^{100}Mo (not calculated within the ISM) and ^{82}Se and the largest by ^{48}Ca .

In Table 7, recent results of different methods for $M_N^{0\nu}$ are presented. They have been achieved within the ISM, IBM, QRPA and PHFB methods but not in the EDF approach. This fact is probably a reason of small spread of results for ^{48}Ca . The results with the CD-Bonn short-range correlations are significantly

^c A modern value of the axial-vector coupling constant is $g_A = 1.269$. We note that in the referred calculations of the $0\nu\beta\beta$ -decay NMEs the previously accepted value $g_A^{\text{eff}} = g_A = 1.25$ was assumed.

Table 6. The NME of the $0\nu\beta\beta$ -decay $M_{\nu}^{0\nu}$ calculated in the framework of different approaches: interacting shell model (ISM) (Strasbourg-Madrid (StMa)²⁵⁰ and Central Michigan University (CMU)^{250, 251} groups), interacting boson model (IBM),²⁵² quasiparticle random phase approximation (QRPA) (Tuebingen-Bratislava-Caltech (TBC),^{107, 253} Jyväskylä (Jy),²⁵⁴ and North-Caroline University²⁷¹ groups), projected Hartree-Fock Bogoliubov approach (PHFB),²⁷⁶ non-relativistic²⁷⁷ energy density functional method.¹¹¹ The Argonne, CD-Bonn and UCOM two-nucleon short-range correlations are taken into account. Averaged nuclear matrix element of different approaches and its variances for a given isotope are calculated following Refs.^{282, 283} The non-quenched value of weak axial-vector coupling g_A and $R = 1.2$ fm $A^{1/3}$ are assumed.

Method	g_A	src	$M_{\nu}^{0\nu}$					
			⁴⁸ Ca	⁷⁶ Ge	⁸² Se	⁹⁶ Zr	¹⁰⁰ Mo	¹¹⁰ Pd
ISM-StMa	1.25	UCOM	0.85	2.81	2.64			
ISM-CMU	1.27	Argonne	0.80	3.37	3.19			
		CD-Bonn	0.88	3.57	3.39			
IBM	1.27	Argonne	1.75	4.68	3.73	2.83	4.22	4.05
QRPA-TBC	1.27	Argonne	0.54	5.16	4.64	2.72	5.40	5.76
		CD-Bonn	0.59	5.57	5.02	2.96	5.85	6.26
QRPA-Jy	1.26	CD-Bonn		5.26	3.73	3.14	3.90	6.52
dQRPA-NC	1.25	without		5.09				
PHFB	1.25	Argonne				2.84	5.82	7.12
		CD-Bonn				2.98	6.07	7.42
NREDF	1.25	UCOM	2.37	4.60	4.22	5.65	5.08	
REDF	1.25	without	2.94	6.13	5.40	6.47	6.58	
Mean value			1.34	4.55	4.02	3.78	5.57	6.12
variance			0.81	1.20	0.91	2.49	0.58	1.78

Method	g_A	src	$M_{\nu}^{0\nu}$					
			¹¹⁶ Cd	¹²⁴ Sn	¹²⁸ Te	¹³⁰ Te	¹³⁶ Xe	¹⁵⁰ Nd
ISM-StMa	1.25	UCOM		2.62		2.65	2.19	
ISM-CMU	1.27	Argonne		2.00		1.79	1.63	
		CD-Bonn		2.15		1.93	1.76	
IBM	1.27	Argonne	3.10	3.19	4.10	3.70	3.05	2.67
QRPA-TBC	1.27	Argonne	4.04	2.56	4.56	3.89	2.18	
		CD-Bonn	4.34	2.91	5.08	4.37	2.46	3.37
QRPA-Jy	1.26	CD-Bonn	4.26	5.30	4.92	4.00	2.91	
dQRPA-NC	1.25	without				1.37	1.55	2.71
PHFB	1.27	Argonne			3.90	3.81		2.58
		CD-Bonn			4.08	3.98		2.68
NREDF	1.25	UCOM	4.72	4.81	4.11	5.13	4.20	1.71
REDF	1.25	without	5.52	4.33		4.98	4.32	5.60
Mean value			4.34	3.07	4.34	3.42	2.59	3.01
variance			0.79	1.01	0.23	1.67	1.10	1.34

larger in comparison with those using Argonne short-range correlations. The largest values are reported by the QRPA. The explanation might be that there is larger momentum transfer between nucleons by the heavy neutrino in comparison with light neutrino exchange. Therefore, the role of transitions through higher multipoles is expected to be important. But, these states are not described within the ISM and the IBM and as result the value of $M_N^{0\nu}$ is reduced.

The range of results produced within different nuclear models for a given isotope (see Tables 6 and 7) means that some of them, or generally all of them, are deficient in the way they incorporate some important physics. It is not clear which nuclear physics observables and/or nuclear models need be reproduced to give a reliable prediction for the $0\nu\beta\beta$ -decay NME, apart from the $2\nu\beta\beta$ -decay NMEs deduced from the measured half-lives. But, none of the discussed models can do it reliably now. Complementary experimental information from processes like charge-exchange and particle transfer reactions, muon capture and charged current (anti)neutrino-nucleus reactions is assumed to be also relevant (see section 6.5). The occupancies of valence neutron and proton orbits have been extracted by accurate measurements of one nucleon adding and removing transfer reactions by J. Schiffer and collaborators²⁸⁴ for double beta decay systems with $A=76$ (protons and neutrons^{235, 285}), 100 (neutrons²⁸⁶), 130 (neutrons²⁸⁷ and protons²⁸⁸) and 136 (proton²⁸⁸). The Gamow-Teller strengths to intermediate nucleus have been investigated via charge-exchange reactions for $A=48$ (β^{-289} and β^{+289}), 76 (β^{-228}), 96 (β^{-230}), 100 (β^{-229}), 128 (β^{-227}), 130 (β^{-227}), 130 (β^{-226}) and 150 (β^{-225} and β^{+225}). Unfortunately, there is no available or useful information about the β^+ strengths connecting intermediate and final nuclei for many double beta decaying systems. These transitions might be probed not only by charge-exchange reactions, but with muon capture as well.

There are two important questions in the context of the calculation of the $0\nu\beta\beta$ -decay NME: i) What is behind the smallness of both $2\nu\beta\beta$ - and $0\nu\beta\beta$ -decay matrix elements? ii) Is the sensitivity the QRPA to the renormalization of particle-particle interaction of nuclear Hamiltonian an artifact of the QRPA? Vogel and Zirnbauer discussed a possibility that the underlying symmetry is the spin-isospin Wigner SU(4) symmetry.^{92, 290} The main argument against it was the fact that in medium-heavy and heavy nuclei the SU(4) symmetry is badly broken by spin-orbit splitting. Recently, the $2\nu\beta\beta$ -decay Gamow-Teller and Fermi transitions were studied within an exactly model, which allows a violation of both spin-isospin SU(4) and isospin SU(2) symmetries.²⁹¹ It was found that the model reproduces the main features of realistic calculation within the QRPA with isospin symmetry restoration, in particular the dependence of the $2\nu\beta\beta$ -decay decay matrix elements on the vector and isoscalar particle-particle interactions. By using perturbation theory an explicit dependence of the $2\nu\beta\beta$ -decay matrix elements on the like-nucleon pairing, particle-particle proton-neutron interaction was obtained. It was found that these matrix elements do not depend on the mean field part of Hamiltonian and that they are governed by a weak violation of both SU(2) and SU(4) symmetries by the particle-

Table 7. The NME of the $0\nu\beta\beta$ -decay $M_N^{0\nu}$ calculated in the framework of different approaches: interacting shell model (ISM) (Strasbourg-Madrid (StMa)²⁵⁰ and Central Michigan University (CMU)²⁵¹ groups), interacting boson model (IBM),²⁵² quasiparticle random phase approximation (QRPA) (Tuebingen-Bratislava-Caltech (TBC)^{107,253} and Jyväskylä (Jy)²⁵⁴ groups), projected Hartree-Fock Bogoliubov approach (PHFB).²⁵⁵ The Argonne, CD-Bonn and UCOM two-nucleon short-range correlations are taken into account. The non-quenched value of weak axial-vector coupling g_A and $R = 1.2 \text{ fm } A^{1/3}$ are assumed.

Method	g_A	src	$M_N^{0\nu}$					
			⁴⁸ Ca	⁷⁶ Ge	⁸² Se	⁹⁶ Zr	¹⁰⁰ Mo	¹¹⁰ Pd
ISM-StMa	1.25	UCOM	56.5	133	122			
ISM-CMU	1.27	Argonne	52.9	126	127			
		CD-Bonn	75.5	202	187			
IBM	1.27	Argonne	47	104	83	99	164	154
QRPA-TBC	1.27	Argonne	40.3	287	262	184	342	333
		CD-Bonn	66.3	433	394	276	508	492
QRPA-Jy	1.26	CD-Bonn		401	287	308	350	476
PHFB	1.25	Argonne				101	195	230
		CD-Bonn				141	267	316

Method	g_A	src	$M_N^{0\nu}$					
			¹¹⁶ Cd	¹²⁴ Sn	¹²⁸ Te	¹³⁰ Te	¹³⁶ Xe	¹⁵⁰ Nd
ISM-StMa	1.25	UCOM		141		144	115	
ISM-CMU	1.27	Argonne		97.4		94.5	98.8	
		CD-Bonn		141		136	143	
IBM	1.27	Argonne	110	79	101	92	73	116
QRPA-TBC	1.27	Argonne	209	184	302	264	152	
		CD-Bonn	302	279	454	400	228	
QRPA-Jy	1.26	CD-Bonn	278	453	396	338	186	
PHFB	1.27	Argonne			139	138		78.5
		CD-Bonn			191	188		108

particle interaction of Hamiltonian.²⁹¹ The fact that mean field, which breaks the SU(4) symmetry, plays only secondary role in the evaluation of double beta decay NMEs might be an explanation of both of the above posed questions. In order to prove it is desired to perform beyond closure calculation of $2\nu\beta\beta$ -decay NMEs within nuclear structure models of interest (ISM, (R)EDF, IBM etc) and to study sensitivity of obtained results to proton-neutron residual interaction.

8.2. Impact of quenching of weak axial-vector coupling constant on the NMEs

One important source of uncertainty in $M'_{\nu,N}{}^{0\nu}(g_A^{\text{eff}})$ (see Eq. 76) comes from the fact that the effective value of the axial-vector coupling constant g_A^{eff} is not well known. The axial-vector coupling constant is renormalized due to nuclear medium effects

and, unfortunately, it is reduced, i.e. quenched. The vector coupling constant, which is not expected to be renormalized due to conserved vector current (CVC) hypothesis, yields a smaller contribution to the nuclear matrix element. To a good accuracy $M'_{\nu,N}{}^{0\nu}(g_A^{\text{eff}})$ is proportional to the squared value of g_A^{eff} and correspondingly the decay-rate to its the fourth power. Thus, quenching of axial-vector coupling constant is very important for double beta decay. The origin of the quenching is not completely known. This effect is usually attributed to the Δ -isobar admixture in the nuclear wave function or to the shift of the GT strength to higher excitation energies due to the short-range tensor correlations.

It has been shown that the axial vector single β -decay NMEs for GT 1^+ , SD 2^- and others, which may affect the DBD NMEs, are reduced with respect to pnQRPA calculations due to the non-nuclear and nuclear medium effects which are not included in pnQRPA,^{216,217} but it is not clear what is the most important part, i.e. the fraction to nuclear medium effects, which will affect the NME obtained in other nuclear models, e.g. in the context of ISM.

Different observations and nuclear structure calculations predict various values of g_A^{eff} :

- $(g_A)^4 = (1.269)^4 = 2.59$. A modern value of axial-vector coupling constant of a free nucleon is $g_A=1.269$ (previously, $g_A = 1.254$ was considered). This non-quenched value ($g_A^{\text{eff}} = g_A$) is often adopted in the calculation of $M'_{\nu,N}{}^{0\nu}(g_A^{\text{eff}})$ and offers its largest value.
- $(g_A^{\text{eff}})^4 \simeq 1.00$ (Experimental prediction). It is well known that sum of Gamow-Teller β^- -strengths to individual final states estimated by the IKEDA sum rule is significantly larger than the experimental ones. That effect is known as the axial-vector current matrix elements quenching. In order to account for this, it is customary to quench the calculated GT matrix elements up to 70%. Formally, this is accomplished by replacing the true value of the coupling constant $g_A = 1.269$ by a quenched value $g_A^{\text{eff}} = 1.0$.
- $(g_A^{\text{eff}})^4 \simeq 0.66$ (^{48}Ca), 0.66 (^{76}Ge), 0.30 (^{76}Se), 0.20 (^{130}Te) and 0.11 (^{136}Xe) (The ISM calculation^{292,293}). The shell model, which describes qualitatively well energy spectra, does reproduce experimental values of $M^{2\nu}$ only by consideration of significant quenching of the Gamow-Teller operator, typically by 0.45 to 70%.
- $(g_A^{\text{eff}})^4 \simeq (1.269 A^{-0.18})^4 = 0.063$ (The IBM prediction²⁹³). This is an incredible result. The quenching of the axial-vector coupling within the IBM-2 is more like 60%.²⁹³ It has been determined by theoretical prediction for the $2\nu\beta\beta$ -decay half-lives, which were based on within closure approximation calculated corresponding NMEs, with the measured half-lives.

- $(g_A^{\text{eff}})^4 \simeq 0.30$ and 0.50 for ^{100}Mo and ^{116}Cd , respectively (The QRPA prediction). In Ref.²⁹⁴ g_A^{eff} was treated as a completely free parameter alongside g_{pp} (used to renormalize particle-particle interaction) by performing calculations within the QRPA and RQRPA. It was found that a least-squares fit of g_A^{eff} and g_{pp} , where possible, to the β -decay rate and β^+ /EC rate of the $J^\pi = 1^+$ ground state in the intermediate nuclei involved in double-beta decay in addition to the $2\nu\beta\beta$ rates of the initial nuclei, leads to an effective g_A^{eff} of about 0.7 or 0.8. This value, which is comparable to that needed in the shell model to reproduce $2\nu\beta\beta$ -decay rates is significantly smaller than 1.0 - 1.27, the range usually used in the QRPA.¹⁰⁴ The above statistical approach has been extended also for analysis of 47 isobaric triplets 28 more extended isobaric chains of nuclei to extract values and uncertainties for g_A^{eff} in calculations performed within the QRPA. A comparatively small value of g_A^{eff} was found.²⁹⁵

We see that the uncertainty in the calculated $0\nu\beta\beta$ -decay half-life due to quenching is quite large.

The quenching of axial-vector coupling constant is assumed to have different sources like the truncation of the many-nucleon Hilbert space and the many-body currents, which reduce matrix elements by amounts that are still in dispute. The effect of two-body currents can be isolated by defining new *effective* one-body current with the factor $g_A(p^2)$ replaced by an effective coupling $g_A^{\text{eff}}(p^2)$, given by

$$g_A^{\text{eff}}(p^2) = g_A(p^2) \left(1 - \frac{\rho}{F_\pi^2} \left[\frac{c_D}{g_a \Lambda_\chi} + \frac{2}{3} c_3 \frac{p^2}{4m_\pi^2 + p^2} + I(\rho, 0) \left(\frac{1}{3} (2c_4 - c_3) + \frac{1}{6m} \right) \right] \right), \quad (95)$$

with

$$I(\rho, P) = 1 - \frac{3m_\pi^2}{2k_F^2} + \frac{3m_\pi^3}{2k_F^3} \text{acot} \left[\frac{m_\pi^2 + \frac{P^2}{4} - k_F^2}{2m_\pi k_F} \right] + \frac{3m_\pi^2}{4k_F^3 P} \left(k_F^2 + m_\pi^2 - \frac{P^2}{4} \right) \ln \left[\frac{m_\pi^2 + (k_F - \frac{P}{2})^2}{m_\pi^2 + (k_F + \frac{P}{2})^2} \right]. \quad (96)$$

Here, k_F is the Fermi momentum and P is the center-of-mass momentum of the decaying nucleons, which can be set to zero without altering $I(\rho, P)$ significantly.²⁹⁶ The constants c_3 , c_4 , and c_D are the effective field theory parameters, fit to data in light nuclei.²⁹⁶

The $0\nu\beta\beta$ -decay matrix element has a different form than does the $2\nu\beta\beta$ matrix element and it might be that the quenching $2\nu\beta\beta$ decay has a smaller effect on $0\nu\beta\beta$ -decay. First, this issue was discussed in the context of the two-body currents and the ISM in Ref.²⁹⁶ It was found that the effect of the two-body currents decreases as the momentum transfer increases, and so such currents will quench $2\nu\beta\beta$ -decay NME, for which the momentum transfer is essentially zero, more than the $0\nu\beta\beta$ -decay NME, since in the latter case the intermediate neutrino can transfer several

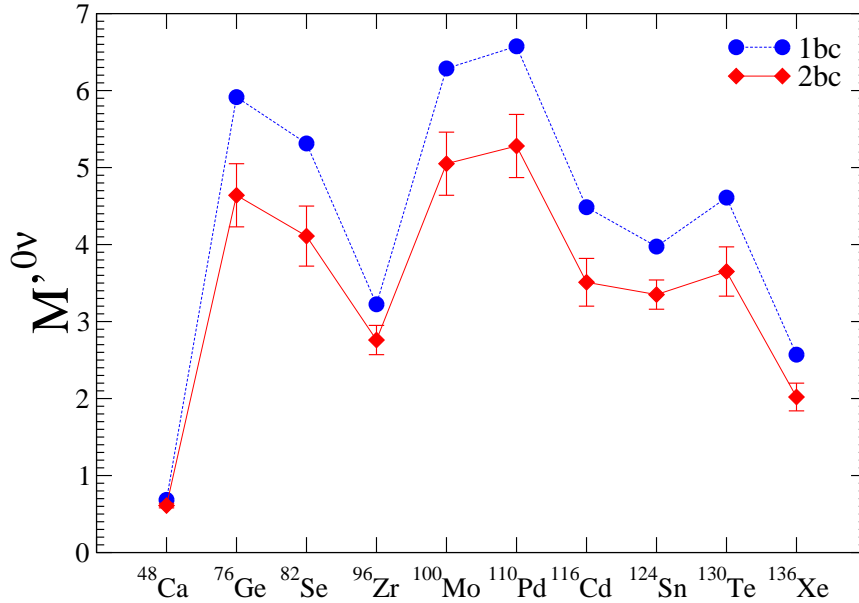


Fig. 10. (Color online) Nuclear matrix element $M_{\nu}^{0\nu}$. The blue circles represent the results with the one-body current (1bc) only, and the red diamonds the average of the results with two-body currents (2bc) included. The error bars represent the dispersion in those values.

hundred MeV of momentum from one decaying nucleon to the other. Later this finding was also confirmed within the QRPA.²⁹⁷ The conclusion is that, if most of the quenching is due to two-body currents, as effective field theory suggests, the $0\nu\beta\beta$ -matrix elements may be quenched by a factor on the order of 30%.^{296,297} The nuclear matrix element $M^{0\nu}$ calculated for the nuclei of experimental interest, obtained by consideration both one- and two-body currents within the QRPA,²⁹⁷ are displayed in Fig. 10.

Currently, it is difficult to assign both systematic and statistical uncertainties to calculated NMEs.²⁹⁸ The most sophisticated way to do it has been proposed in the framework of the QRPA²⁸² and applied later within the PHFB.²⁷⁶ Further, within the QRPA for a given set of nuclei, it has been shown that the correlations among NME errors are as important as their size.^{299,300} It is desired that also other groups present “statistical samples” of NME calculations as well, in order to provide independent estimates of (co)variances for their NME estimates. A covariance analysis proposed^{299,300} is the way to estimate correctly current or prospective sensitivities to effective Majorana neutrino mass $m_{\beta\beta}$.

The investigation of the quenching of the axial current in double beta decay will

be illuminated by the relevant experimental searches (see section 6.5).

Accurate determination of the NMEs, and a realistic estimate of their uncertainty, remains of great importance. Methods are developed and improved. Increasing computer power should allow them to include all important nuclear physics aspects and to reproduce relevant nuclear physics observables. The ultimate goal is to evaluate Nuclear matrix elements with uncertainty of less than 30% to establish the unknown neutrino mass scale. To this end, it is crucial that the theory groups consider all factors outlined above in order to evaluate NMEs within 15 % uncertainty and the experimental groups provide relevant data to be used in checking these models.

9. Concluding remarks

In this review we analyzed the $0\nu\beta\beta$ -decay process, which is the oldest and perhaps the best to test lepton number violation and at the same time settle the issue of the nature of the neutrino, i.e. whether the neutrino mass eigenstates are of the Majorana or Dirac type. We also have seen that it is the best process to settle the neutrino mass scale in the few meV scale. To achieve these goals first, and most important, some serious experimental problems must be overcome in order to be able measure life times of the order of $\geq 10^{26}$ y. We have discussed the ongoing, planned and future experiments. We have witnessed a great progress in tackling the various background problems, improving the energy resolution and preparing large masses of the needed isotopes.

To encourage and guide the experiments we considered a variety of particle models, which allow the double beta decay to occur at a reasonable level. The most important mechanism involves the light Majorana neutrino, but we considered other competing mechanisms as well.

In order to extract useful information from the data i) the phase space integrals must be reliably calculated. There has been great progress in this direction, but we are haunted by the quenching of the axial current. This is crucial in determining the expected life time. There appears to be hope towards determining its effective value by using other related experimental information. ii) The precise evaluation of the nuclear matrix elements themselves. It is encouraging that all available nuclear models (the Interacting Shell Model, the Quasiparticle Random Phase Approximation, the Interacting Boson Model, the Projected Hartree-Fock-Bogoliubov Method and the Energy Density Fractional Method) are being used in the evaluation of all the needed $0\nu\beta\beta$ -decay nuclear matrix elements. The fact that these vastly different models agree in the predicted values of these ME for various mechanisms and a number of different targets as well as the fact that they reproduce data on other related experiments, such as single beta decay rates and charge exchange reactions, gives us confidence that they are perhaps estimated better than a factor of 2. Admittedly we have not witnessed any great progress during the last few years and this situation must be improved. It is hoped that some constraints may arise by

utilizing experimental input from other processes.

It is clear that the mere observation of double beta decay will be a triumph of physics. The next day, however, the extraction of the most useful parameter, namely the determination of the scale of the neutrino mass, will begin. It has been shown that,²⁴ given adequate information on a number of judiciously chosen targets, the neutrino mass can, in principle, be extracted from the data even in the case that other competing mechanisms may significantly contribute to this process.

Acknowledgements

F. Š acknowledges the support in part by the VEGA Grant Agency of the Slovak Republic under Contract No. 1/0922/16, by Slovak Research and Development Agency under Contract No. APVV-14-0524, and by the Ministry of Education, Youth and Sports of the Czech Republic under Contract No. LM2011027. J.D.V acknowledges that part of this work was supported by IBS-R017-D1-2016-a00 in the Republic of Korea and by the ARC Centre of Excellence in Particle Physics (CoEPP), University of Adelaide, Australia. He is indebted to Professors A. Thomas and Y. Semertzidis for support and hospitality.

References

References

1. M. Goeppert-Mayer *Phys. Rev.*, vol. 48, p. 512, 1035.
2. E. Majorana *Nuovo Cim.*, vol. 14, p. 171, 1937.
3. H. Primakoff *Phys. Rev.*, vol. 85, p. 888, 1952.
4. J. R. Davis *Phys. Rev.*, vol. 97, p. 766, 1955.
5. M. G. Ingram and J. H. Reynolds *Phys. Rev.*, vol. 78, p. 822, 1950.
6. T. Kirsten, W. Gentner, and O. Schaeffer *Z. Physik*, vol. 202, p. 273, 1967.
7. T. Kirsten, W. Gentner, and O. Miller *Z. Naturf. A*, vol. 22, p. 1783, 1967.
8. N. Takaota and K. Ogata *Z. Naturf. A*, vol. 21, p. 84, 1966.
9. B. Srinivasan, O. E.C. Alexander, and Manuel *J. Inorg. Nucl. Chem.*, vol. 34, p. 2381, 1972.
10. M. Doi, T. Kotani, N. Nishiura, K. Okuda, and E. Takasugi *Phys. Lett. B.*, vol. 103, p. 219, 1981.
11. J. Schechter and J. W. F. Valle *Phys. Rev. D*, vol. 25, p. 2951, 1982.
12. M. Hirsch, H.V. Klapdor-Kleingrothaus, and S.G. Kovalenko *Phys. Lett. B*, vol. 372, p. 181, 1996.
13. A. Faessler, S. Kovalenko, F. Šimkovic, and J. Schwieger *Phys. Rev. Lett.*, vol. 78, p. 183, 1997.
14. A. Faessler, S. Kovalenko, and F. Šimkovic *Phys. Rev. D*, vol. 58, p. 055004, 1998.
15. A. Wodecki, W. A. Kamiński, and F. Šimkovic *Phys. Rev. D*, vol. 60, p. 115007, 1999.
16. V. I. Tretyak and Y. G. Zdesenko *At. Dat. Nucl. Dat. Tabl.*, vol. 80, p. 83, 2002.
17. H. Ejiri *J. Phys. Soc. Jap.*, vol. 74, p. 2101, 2005.
18. F. Avignone, S. Elliott, and J. Engel *Rev. Mod. Phys.*, vol. 80, p. 481, 2008.
19. L. Camilleri, E. Lisi, and J. F. Wilkerson *Ann. Rev. Nucl. Part. Sci.*, vol. 58, p. 343, 2008.

20. S. R. Elliott, A. A. Hahn, and M. Moe *Phys. Rev. Lett.*, vol. 59, p. 2020, 1987.
21. Y. Fukuda *et al.* (The Super-Kamiokande Collaboration) *Phys. Rev. Lett.*, *ibid* vol. 81, p. 1562 & 1158, 1998; *ibid* vol. 82, p. 1810, 1999; *ibid* vol. 85, p. 3999, 2000; vol. 86, p. 5651, 2001.
22. Q.R. Ahmad *et al.* (The SNO Collaboration) *Phys. Rev.Lett.*, vol. 89, p. 011302; *ibid* vol. 89, p. 011301, 2002; *ibid* vol. 87, p. 071301, 2001;
K. Lande *et al.* (The Homestake Collaboration) *Astrophys. J.*, vol. 496, p. 505, 1998;
W. Hampel *et al.* (The Gallex Collaboration) *Phys. Lett.B*, vol. 447, p. 127, 1999;
J.N. Abdurashitov *et al.* (The Sage Collaboration) *Phys. Rev. C*, vol. 80, p. 056801, 1999;
G.L Fogli *et al.*, *Phys. Rev. D*, vol. 66, p. 053010, 2002.
23. K. Eguchi *et al.* (The KamLAND Collaboration) *Phys. Rev. Lett.*, vol. 90, p. 021802, 2003.
24. J. D. Vergados, H. Ejiri, and F. Šimkovic *Rep. Prog. Phys.*, vol. 75, 2012.
25. A. Gando *et al.* (The KamLAND-Zen Collaboration) *Phys. Rev. Lett.*, vol. 117, p. 082503, 2016.
26. R. Winter *Phys. Rev.*, vol. 100, p. 142, 1955.
27. J. Vergados *Nuc. Phys. B*, vol. 218, p. 109, 1983.
28. J. Bernabeu, A. de Rujula, and C. Jarlskog *Phys. Rev. C*, vol. 223, p. 15, 1983.
29. M. Doi and T. Kotani *Prog. Theor. Phys.*, vol. 89, p. 139, 1993.
30. Z. Sujkowski and S. Wycech *Phys. Rev. C*, vol. 70, p. 052501, 2004.
31. L. Lukaszuk, Z. Sujkowski, and S. Wycech *Eur. Phys. J. A*, vol. 27, p. 63, 2006.
32. M. Krivoruchenko, F. Šimkovic, D. Frekers, and A. Faessler *Nucl. Phys. A*, vol. 859, p. 140, 2011.
33. F. Šimkovic and M. Krivoruchenko *Phys. Part. Nuc.*, vol. 6, p. 298, 2009.
34. J. Vergados *Phys. Rev. C*, vol. 84, p. 044328, 2011.
35. G. Audi *et al. Nucl. Phys. A*, vol. 729, p. 3, 2003.
36. K. Blaum *Phys. Rep.*, vol. 425, p. 1, 2006.
37. G. Douysset *et al. Phys. Rev. Lett.*, vol. 86, p. 4259, 2001.
38. K. Blaum, Y. Novikov, and G. Werth *Contemp. Phys.*, vol. 51, p. 149, 2010.
39. S. Eliseev *et al. Phys. Rev. Lett.*, vol. 106, p. 052504, 2011.
40. M. Redshaw *et al. Phys. Rev. Lett.*, vol. 98, p. 053003, 2007.
41. M. Redshaw *et al. Phys. Rev. Lett.*, vol. 102, p. 212502, 2009.
42. N. Scielzo *et al. Phys. Rev. C*, vol. 80, p. 0225501, 2009.
43. S. Rahaman *et al. Phys. Rev. Lett.*, vol. 103, p. 042501, 2009.
44. V. Kolhinen *et al. Phys. Lett. B*, vol. 684, p. 17, 2010.
45. B. Mount, M. Redshaw, , and E. G. Myers *Phys. Rev. C*, vol. 81, p. 032501, 2010.
46. S. Eliseev *et al. Phys. Rev. C*, vol. 83, p. 038501, 2011.
47. S. Eliseev *et al. Phys. Rev. C*, vol. 84, p. 012501, 2011.
48. M. Goncharov *et al. Phys. Rev. C*, vol. 84, p. 028501, 2011.
49. S. Eliseev *et al. Phys. Rev. Lett.*, vol. 107, p. 152501, 2011.
50. C. Droese *et al. Nucl. Phys. A*, vol. 875, p. 1, 2012.
51. P. Belli *et al. Eur. Phys. J. A*, vol. 47, p. 91, 2011.
52. A. Barabash, P. Hubert, A. Nachab, and V. Umatov *Nucl. Phys. A*, vol. 785, p. 371, 2007.
53. A. Barabash, P. Hubert, A. Nachab, S. Konovalov, I. Vanyushin, and V. Umatov *Nucl. Phys. A*, vol. 807, p. 269, 2008.
54. P. Belli *et al. Nucl. Phys. A*, vol. 824, p. 101, 2009.
55. N.I. Rukhadze *et al.* (TGV Collaboration) *Nucl. Phys. A*, vol. 852, p. 197, 2011.
56. D. Frekers, P. Puppe, J. Thies, P. Povinec, F. Šimkovic, J. Staniček, and I. Sýkora

- Nucl. Phys. A*, vol. 860, p. 1, 2011.
57. P. Belli *et al.* *Nucl. Phys. A*, vol. 859, p. 126, 2011.
 58. J. Vergados *Phys. Rep.*, vol. 133, p. 1, 1986.
 59. W.C. Haxton and G.S. Stephenson, Jr. *Prog. Part. Nucl. Phys.*, vol. 12, p. 409, 1984.
 60. M. Doi, T. Kotani, and E. Tagasugi *Prog. Theor. Phys. (Supp.)*, vol. 83, p. 1, 1985.
 61. T. Tomoda *Rep. Prog. Phys.*, vol. 54, p. 53, 1991.
 62. J. Suhonen and O. Civitarese *Phys. Rep.*, vol. 300, p. 123, 1998.
 63. A. Faessler and F. Šimkovic *J. Phys. G*, vol. 24, p. 2139, 1998.
 64. J. Vergados *Phys. Rep.*, vol. 361, p. 1, 2002.
 65. W. Rodejohann *Int. J. Mod. Phys. E*, vol. 20, p. 1833, 2011.
 66. J. Suhonen, P. Divari, L. Skouras, and I. D. Johnstone *Phys. Rev. C*, vol. 55, p. 714, 1997.
 67. J. Retamosa, E. Caurier, and F. Novacki *Phys. Rev. C*, vol. 51, p. 371, 1995.
 68. E. Caurier, F. Novacki, A. Poves, and J. Retamosa *Phys. Lett. B*, vol. 77, p. 1954, 1996.
 69. J. Sinatkas, L. Skouras, D. Strottman, and J. Vergados *J. Phys. G*, vol. 18, p. 1377, 1992.
 70. E. Caurier, A. Poves, and A. Zucker *Phys. Lett. B*, vol. 252, p. 13, 1990.
 71. B. Aharmin *et al.* *Phys. Rev. C*, vol. 72, p. 055502, 2005.
 72. M. Apollonio *et al.* (The CHOOZ Collaboration) *Phys. Lett. B*, vol. 446, p. 415, 1999.
 73. T. Araki *et al.* *Phys. Rev. Lett.*, vol. 94, p. 081801, 2005.
 74. F.P. An *et al.* (The Daya Bay Collaboration) *Phys. Rev. Lett.*, vol. 108, p. 171803, 2012, arXiv:1203.1669[hep-ex].
 75. J.K. Ahn *et al.* (The RENO Collaboration), *Phys. Rev. Lett.*, vol. 108, p. 191802, 2012, arXiv:1204.0626[hep-ex].
 76. T. Schwetz, M. Tórtola, and J. Valle *New J. Phys.*, vol. 10, p. 113011, 2008.
 77. F. Capozzi, G. Fogli, E. Lisi, A. Marrone, D. Montanino, and A. Palazzo *Phys. Rev. D*, vol. 89, p. 093018, 2014.
 78. M. Gonzales-Garcia and M. Maltoni *Phys. Rep.*, vol. 460, p. 1, 2008.
 79. H. Päs and W. Rodejohann *New J. Phys.*, vol. 17, p. 115010, 2015.
 80. J. Helo, M. Hirsch, T. Ota, and F. P. dos Santos *JHEP*, vol. 1505, p. 092, 2015.
 81. M. Gerbino, M. Lattanzi, and A. Melchiorri *Phys. Rev. D*, vol. 93, p. 033001, 2016.
 82. A. Lewis and S. Bridle *Phys. Rev. D*, vol. 66, p. 103511, 2002.
 83. J. Vergados *Phys. Rev. C*, vol. 13, p. 865, 1976.
 84. W. C. Haxton, G. S. Stephenson, and D. Strottman *Phys. Rev. D*, vol. 25, p. 2360, 1982.
 85. L. Skouras and J. Vergados *Phys. Rev. C*, vol. 28, p. 2122, 1983.
 86. L. Zhao, B. Brown, and W. Richter *Phys. Rev. C*, vol. 42, p. 1120, 1990.
 87. L. Zhao and B. Brown *Phys. Rev. C*, vol. 47, p. 2641, 1993.
 88. R. Radha *et al.* *Phys. Rev. Lett.*, vol. 76, p. 2642, 1996.
 89. T. S. H. Nakada and K. Muto *Nucl. Phys. A*, vol. 607, p. 235, 1996.
 90. S. Koonin, D. Dean, and K. Langanke *Phys. Rep.*, vol. 278, p. 1, 1997.
 91. T. Rodriguez and G. Martinez-Pinedo *Phys. Rev. Lett.*, vol. 105, p. 252503, 2010.
 92. P. Vogel and M. Zirnbauer *Phys. Rev. Lett.*, vol. 57, p. 3148, 1986.
 93. O. Civitarese, A. Faessler, and T. Tomoda *Phys. Lett. B*, vol. 194, p. 11, 1987.
 94. K. Muto and H. Klapdor *Phys. Lett. B*, vol. 208, p. 53, 1988.
 95. J. Engel, P. Vogel, X. Ji, and S. Pittel *Phys. Lett. B*, vol. 225, p. 5, 1989.
 96. A. A. Raduta, A. Faessler, S. Stoica, and W. A. Kamiński *Phys. Lett. B*, vol. 254, p. 7, 1991.

97. A. Griffiths and P. Vogel *Phys. Rev. C*, vol. 46, p. 181, 1992.
98. J. Suhonen and O. Civitarese *Phys. Lett. B*, vol. 308, p. 212, 1993.
99. O. Civitarese and J. Suhonen *Nuc. Phys. A*, vol. 575, p. 251, 1994.
100. F. Šimkovic, J. Schwieger, M. Veselský, G. Pantis, and A. Faessler *Phys. Lett. B*, vol. 393, p. 267, 1997.
101. F. Šimkovic, G. Pantis, and A. Faessler *Prog Part. Phys.*, vol. 40, p. 285, 1998.
102. M. Cheoun, A. Bobyk, A. Faessler, F. Šimkovic, and G. Teneva *Nucl. Phys. A*, vol. 561, p. 74, 1993.
103. K. Muto *Phys. Lett. B*, vol. 391, p. 243, 1997.
104. F. Šimkovic, V. Rodin, A. Faessler, and P. Vogel *Phys. Rev. C*, vol. 87, p. 045501, 2013.
105. J. Toivanen and J. Suhonen *Phys. Rev. Lett.*, vol. 75, p. 410, 1995.
106. J. Schwieger, F. Šimkovic, and A. Faessler *Nuc. Phys. A*, vol. 600, p. 179, 1996.
107. F. Šimkovic, V. Rodin, A. Faessler, and P. Vogel *Phys. Rev. C*, vol. 87, p. 045501, 2013.
108. P. Rath, R. Chandra, K. Chaturvedi, P. Raina, and J. Hirsch *Phys. Rev. C*, vol. 82, p. 064310, 2010.
109. J. Barea and F. Iachello *Phys. Rev. C*, vol. 79, p. 044301, 2009.
110. J. Barea, J. Kotila, and F. Iachello *Phys. Rev. C*, vol. 91, p. 034304, 2015.
111. J. Yao, L. Song, K. Hagino, P. Ring, and J. Meng *Phys. Rev. C*, vol. 91, p. 024316, 2015.
112. A.Yu. Smirnov, arXiv: hep-ph/0411194.
113. S. Weinberg *Phys. Rev. Lett.*, vol. 43, p. 1566, 1979.
114. A. Abada, C. Biggio, F. Bonnet, M. Gavela, and T. Hambye *JHEP*, vol. 0712, p. 061, 2007. arXiv:0707.4058 (hep-ph).
115. J. Lopez-Pavon, E. Molinaro, S. T. Petcov, Radiative Corrections to Light Neutrino Masses in Low Scale Type I Seesaw Scenarios and Neutrinoless Double Beta Decay, arXiv:1506.05296 (hep-ph).
116. P. Humbert, M. Lindner and J. Smirnov, arXiv:1503.03066 (hep-ph); P. Humbert, M. Lindner, S. Patra and J. Smirnov, arXiv:1505.07453 (hep-ph).
117. F. Bonnet, M. Hirsch, T. Ota, and W. Winter *JHEP*, vol. 1303, p. 055, 2013. [Erratum: *J. High Energy Phys.* 1404, 090 (2014)].
118. C. Boehm, Y. Farzan, T. Hambye, S. Palomares-Ruiz, and S. Pascoli *Phys. Rev. D*, vol. 77, p. 043516, 2008.
119. M. Gózdź, W. Kamiński, F. Šimkovic, and A. Faessler *Phys. Rev. D*, vol. 74, p. 055007, 2006.
120. E. Witten *Phys. Lett. B*, vol. 91, p. 81, 1980.
121. C-Q Geng and L-H Tsai, *Annals of Physics*, vol. 365, p. 210, 2016; C-Q Geng, D. Huang and L-H Tsai *Phys. Rev. D*, vol. 90, p. 113005, 2014.
122. G. K. Leontaris and J. D. Vergados *Phys. Lett. B*, vol. 258, p. 111, 1991.
123. Z.-Z. Xing *Phys. Rev. D*, vol. 85, p. 013008, 2012.
124. E. Ma and G. Rajasekaran *Phys. Rev. D*, vol. 64, p. 113012, 2001.
125. F. Bjoerkeroth, F. de Anda, I. de Medeiros Varzielas, and S. F. King *JHEP*, vol. 06, p. 141, 2015. arXiv:1503.03306 (hep-h).
126. G.J. Ding, S.F. King and T. Neder *JHEP*, vol. 12, p. 007, 2014, arXiv:1409.8005[hep-ph]; Y. Shimizu and M. Tanimoto *JHEP* vol. 12, p. 132, 2015, arXiv:1507.06221 [hep-ph].
127. G. Altarelli and F. Feruglio *Rev. Mod. Phys.*, vol. 82, p. 2701, 2010. arXiv:1002.0211[hep-h].
128. S. Dell’Oro, S. Marcocci, M. Viel, and F. Vissani *Adv.High Energy Phys.*, vol. 2016,

- p. 2162659, 2016. arXiv:1601.07512v2 [hep-ph].
129. C. Arbeláez, A. E. Cárcamo Hernández, S. Kovalenko, and I. Schmidt *Phys. Rev. D*, vol. 92, p. 115015, 2015, arXiv:1507.03852[hep-ph]; P. Ballett, S. Pascoli and J. Turner *Phys. Rev. D*, vol. 92, p. 093008, 2015, arXiv:1503.07543 [hep-ph].
 130. R. Fonseca and M. Hirsch *Phys. Rev. D*, vol. 92, p. 015014, 2015. arXiv:1505.06121[hep-ph].
 131. V. Vien, H. Long, and D. P. Khoi *Int. J. Mod. Phys. A*, vol. 30, p. 1550102, 2015. arXiv:1506.06063[hep-h].
 132. J. D. Vergados, Reduction of $SU_f(3) \supset SO(3) \supset A_4$ -The scalar potential, arXiv:1604.00678 [phys.gen-ph].
 133. R. Mohapatra *et al. Rep. Prog. Phys.*, vol. 70, p. 1757, 2007.
 134. F. Capozzi, E. Lisi, A. Maronne, D. Montanino, and A. Palazzo *Nucl. Phys. B*, vol. 908, p. 218, 2016.
 135. M. Gonzalez-Garcia, M. Maltoni, and T. Schwetz *Nucl. Phys. B*, vol. 908, p. 199, 2016.
 136. S. Pascoli, S. Petcov, and T. Schwetz *Nucl. Phys. B*, vol. 734, p. 24, 2006.
 137. A. Osipowicz *et al.* (The KATRIN Collaboration) 2001, hep-ex/0109033; J. Angrik *et al.* (The KATRIN Collaboration) 2004, KATRIN Design Report <http://bibliothek.fzk.de/zb/berichte/FZKA7090.pdf>.
 138. E. Otten and C. Weinheimer *Rep. Prog. Phys.*, vol. 71, p. 086201, 2008.
 139. E. Andreotti (The MARE Collaboration) *Nucl. Instrum. Meth.*, vol. 572, p. 208, 2007.
 140. K. N. Abazajian *et al. Astropart. Phys.*, vol. 35, p. 177, 2011.
 141. S. A. Thomas, F. B. Abdalla, and O. Lahav *Phys. Rev. Lett.*, vol. 105, p. 031301, 2010.
 142. U. Seljak *et al.* (The SDSS Collaboration) *Phys. Rev. D*, vol. 71, p. 103515, 2005.
 143. S. Riemer, S. Sorensen, D. Parkinson, and T. Davis *Phys. Rev. D*, vol. 89, p. 103505, 2014.
 144. M. Costanzi, B. Sartoris, M. Viel, and S. Borgani *JCAP*, vol. 1410, p. 081, 2014.
 145. P. Ade *et al.* (The Planck Collaboration) *Astron. Astrophys.*, vol. 594, p. A13, 2016, arXiv:1502.01589[astro-ph.CO].
 146. S. Dell’Oro, S. Marcocci, M. Viel, and F. Vissani *JCAP*, vol. 1512, p. 023, 2015. arXiv:1505.02722[astro-ph.CO].
 147. S. D. Oro, S. Marcocci, M. Viel, and F. Vissani *Adv. High Energy Phys.*, vol. 2016, p. 2162659, 2016.
 148. S. Kovalenko, M. Krivoruchenko, and F. Šimkovic *Phys. Rev. C*, vol. 112, p. 142503, 2014.
 149. K.N. Abazajian *et al.* arXiv:1204.5379[hep-ph].
 150. J. Helo, S. Kovalenko, and I. Schmidt *Nucl. Phys. B*, vol. 853, p. 80, 2011.
 151. A. Atre, T. Han, S. Pascoli, and B. Zhang *JHEP*, vol. 0905, p. 030, 2009.
 152. J. Beringer *et al.* (The Particle Data Group) *Phys. Rev. D*, vol. 86, p. 010001, 2012.
 153. J. C. Pati and A. Salam *Phys. Rev. D*, vol. 10, p. 275, 1974.
 154. R. N. Mohapatra and J. C. Pati *Phys. Rev. D*, vol. 11, p. 2558, 1975.
 155. V. Tello, M. Nemevšek, F. Nesti, G. Senjanović, and F. Vissani *Phys. Rev. Lett.*, vol. 106, p. 151801, 2011.
 156. M. Nemevšek, F. Nesti, G. Senjanović and V. Tello, arXiv:1112.3061 [hep-ph].
 157. J. Barry and W. Reodejohann *JHEP*, vol. 1309, p. 153, 2013.
 158. H. Ejiri *Prog. Part. Nucl. Phys.*, vol. 64, p. 249, 2010.
 159. H. Ejiri and S. Elliott *Phys. Rev. C*, vol. 89, p. 055501, 2014.
 160. A. Gando *et al.* (The KamLAND-Zen Collaboration) *Phys. Rev. C*, vol. 85, p. 045504, 2012, arXiv:1201.4664 [hep-ex].

161. V. Lozza *et al.* (The SNO-collaboration) *EPJ Web. Conf.*, vol. 65, p. 010003, 2014.
162. V. Gehman, P. Doe, R. Robertson, D. Will, H. Ejiri, and R. Hazama *Nuc. Phys. Proc. Suppl.*, vol. 622, p. 602, 2010.
163. J. Maneira *et al.* (The SNO Collaboration) *Nuc. Phys. Proc. Suppl.*, vol 217, p. 50, 2011.
164. N. Borros and K. Zuber *J. Phys.*, vol. 38, p. 10521, 2011.
165. H. Ejiri and K. Zuber *J. Phys. G: Nucl. Part. Phys.*, vol. 43, p. 045201, 2016.
166. H. V. Klapdor-Kleingrothaus *et al. Phys. Rev. D*, vol. 63, p. 073005, 2001.
167. C. E. Aalseth *et al. Phys. Rev.*, vol. D 65, p. 092007, 2002.
168. C. Arnaboldi *et al. Phys. Rev. Lett.*, vol. 95, p. 142501, 2005.
169. C. Arnaboldi *et al. Astropart. Phys.*, vol. 34, p. 822, 2011.
170. M. Auger *et al.* (The EXO Collaboration) *Phys. Rev. Lett.*, vol.109, p. 032505, 2012, arXiv:1205.5608v1 [hep-ex].
171. N. Ackermann *et al. Phys. Rev. Lett.*, vol. 107, p. 212501, 2011.
172. E. Ejiri *et al. Phys. Rev. C*, vol. 63, p. 065501, 2001.
173. R. Arnold *et al.* (The NEMO-3 Collaboration) *Phys. Rev. Lett.*, vol. 95, p. 182302, 2005.
174. R. Arnold *et al.* (The NEMO-3 Collaboration), *Nucl. Phys.*, vol. 765, p. 483, 2006.
175. M. Agostini (The GERDA Collaboration), NEUTRINO 2016 conf., <http://neutrino2016.iopconfs.org>.
176. R. Arnold *et al.* (The NEMO-3 Collaboration) *Phys. Rev. D*, vol. 89, p. 111101, 2014.
177. K. Alfonso *et al.* (The CUORE Collaboration) *Phys. Rev. Lett.*, vol. 102502, p. 115, 2015, arXiv:1504.02454v1[nucl-exp].
178. J.B. Albert *et al.* (The EXO Collaboration), *Nature*, vol. 510, p. 229, 2014.
179. M. Agostini *et al. Phys. Rev. Lett.*, vol. 111, p. 122503, 2013.
180. H. Klapdor-Kleingrothaus *et al. Phys. Lett. B*, vol. 586, p. 198, 2004.
181. M. Agostini *et al.* (The GERDA Collaboration) *Eur. Phys. J. C*, vol. 75, p. 416, 2015.
182. The EXO Collab. (J.B. Albert et al.) *Phys. Rev. D* 90 (2014) 092004.
183. J. Albert *et al.* (The EXO collaboration) *Phys. Rev. C*, vol. 89, p. 015502, 2014.
184. A. Gando *et al.* (The KamLAND-Zen Collaboration) *Phys. Rev. Lett.*, vol. 110, p. 002502, 2013.
185. A. Gando *et al.* (The KamLAND-Zen Collaboration) *Phys. Rev. C*, vol. 86, 021601R, 2012.
186. H. V. Klapdor-Kleingrothaus and I. Krivosheina *Mod. Phys. Lett. A*, vol. 21, p. 1547, 2006.
187. A. Gando *et al.* (The KamLAND-Zen Collaboration) *Nucl. Phys. A*, vol. 935, p. 52, 2015.
188. T. Wester for GERDA collaboration *MEDEX15 Proc. AIP conference proc.* (2015).
189. C. Cuesta *et al.* (The Majorana Collaboration) *AIP Conf. Proc.*, vol. 1686, p. 020005, 2015, arXiv:1507.07612[physics.ins-det].
190. H. Ejiri *et al. Phys. Rev. Lett.*, vol. 85, p. 2917, 2000.
191. H. Nakamura *et al. J. Phys. Soc. Japan*, vol. 76, p. 114201, 2007.
192. H. Ejiri *et al. Eur. Phys. J. ST*, vol. 162, p. 239, 2008.
193. R. Arnold *et al.* (The SuperNEMO Collaboration) *Eur. Phys. J. C*, vol. 70, p. 927, 2010.
194. R. Hodák for SuperNEMO collaboration *AIP Conf.Proc.*, vol. 1686, p. 020012, 2015.
195. F. Piquemal Private communication 2016.
196. H. Park for AMoRE Collaboration *AIP Conf.Proc.*, vol. 1686, p. 020016, 2015.

197. A. Barabash *et al.* *Eur. Phys. J. C*, vol. 74, p. 3133, 2014.
198. E. Armengaud *et al.* *JINST*, vol. 10, p. PO5007, 2015.
199. T. B. Becker *et al.* *Astropart. Phys.*, vol. 72, p. 38, 2016.
200. G. Wang *et al.* (The CUPID Collaboration) arXiv:1504.03599 [physics.ins-det]; arXiv:1504.03612 [physics.ins-det].
201. A. Giuliani, Private communication, 2016; L. Canonica, NEUTRINO 2016 conf. , <http://neutrino2016.iopconfs.org>.
202. S. Zatschler for COBRA Collaboration *AIP Conf. Proc.*, vol. 1686, p. 020027, 2015.
203. J. Ebert *et al.* (The COBRA collaboration) *Phys. Rev. C*, vol. 94, p. 024603, 2016, arXiv 1509.04113[nucl-ex].
204. F. A. Danevich *et al.* *J. Phys. Conf. Series*, vol. 718, p. 062009, 2016.
205. L. Gironi *et al.* *AIP Conf. Proc.*, vol. 1686, p. 020011, 2015.
206. Y. Lin, for nEXO collaboration, *APR15 meeting of APS*.
207. J. Shirai for KamLAND-Zen Collaboration *Nucl. Phys. Proc. Suppl.*, vol. 28, p. 237, 2013.
208. K. Inoue, private communication 2016.
209. V. Álvarez *et al.* (The NEXT Collaboration) *JINST*, vol. 7, p. T06001, arXiv:1202.0721v2 [physics.ins-det].
210. D. Lorca for NEXT Collaboration, Proc. 20th Int. Conf. on Part. and Nucl. (PANIC 14): Hamburg, Germany, August 24-29, 2014, DOI:10.3204/DESY-PROC-2014-04/65, arXiv:1411.0475[physics.ins-det].
211. V. Lozza *et al.* (The SNO+ Collaboration) *EPJ Web Conf.*, vol. 65, p. 01003, 2014.
212. J. Maneira *et al.* (The SNO+ Collaboration) *Nucl. Phys. Proc. Suppl.*, vol. 217, p. 50, 2011.
213. T. Iida *et al.* (The CANDLES Collaboration) *J. Phys. Conf. Series*, vol. 718, p. 062026, 2016.
214. K.L.Giboni, Panda X-III collaboration, KEK seminar, Dec. 2015.
215. H. Ejiri *Phys. Rep.*, vol. 338, p. 265, 2000. and refs. therein.
216. H. Ejiri and J. Suhonen *J. Phys. G*, vol. 42, p. 055201, 2015.
217. H. Ejiri, N. Soukouti, and J. Suhonen *Phys. Lett. B*, vol. 729, p. 27, 2014.
218. F. Avignone *Workshop Neutr. Nucl. Phys. Stopped $\pi\mu$ Facility (Oak Ridge)*, 2000.
219. H. Ejiri *Nucl. Instr. Meth. Phys. Research*, vol. 503, p. 276, 2003.
220. H. Ejiri *Czech. J. Phys.*, vol. 56, p. 459, 2006.
221. J. Suhonen and M. Kortelainen *Czech J. Phys.*, vol. 56, p. 519, 2006.
222. I. Hashim, H. Ejiri *et al.* Proc. Neutrino nuclear response workshop Osaka, 2016.
223. H. Ejiri *et al.* *Phys. Rev. Lett.*, vol. 21, p. 373, 1968.
224. H. Ejiri, S. Titov, M. Boswell, and A. Young *Phys. Rev.*, vol. C 88, p. 045610, 2013.
225. C. Guess *et al.* *Phys. Rev. C*, vol. 83, p. 064318, 2011.
226. P. Puppe *et al.* *Phys. Rev. C*, vol. 84, p. 051305, 2011.
227. P. Puppe *et al.* *Phys. Rev. C*, vol. 86, p. 044603, 2012.
228. J. H. Thies *et al.* *Phys. Rev. C*, vol. 86, p. 014304, 2012.
229. J. H. Thies *et al.* *Phys. Rev. C*, vol. 86, p. 044309, 2012.
230. J. H. Thies *et al.* *Phys. Rev. C*, vol. 86, p. 054323, 2012.
231. D. Freckers *et al.* *Phys. Rev. C*, vol. 94, p. 014614, 2016.
232. H. Ejiri and D. Frekers, *J. Phys. G*, vol. 43, p. 11LT01, 2016.
233. H. Ejiri and K. Takahisa Private communication.
234. F. Cappuzzello *et al.* *Eur. Phys. J*, vol. A 51, p. 145, 2015.
235. J. Schiffer *et al.* *Phys. Rev. Lett.*, vol. 100, p. 112501, 2008.
236. H. Ejiri and H. Toki *J. Phys. Soc. Japan*, vol. 65, p. 7, 1996.
237. H. Ejiri *J. Phys. Soc. Japan*, vol. 78, p. 074201, 2009.

238. H. Ejiri *J. Phys. Soc. Japan*, vol. 81, p. 033201, 2012.
239. P. Belli *et al. Phys. Rev.*, vol. C 93, p. 045502, 2016.
240. N.J. Rukhadze *et al. AIP Conf. Proc.*, vol. 1686, p. 020020, 2015.
241. J. Kotila and F. Iachello *Phys. Rev. C*, vol. 85, p. 034316, 2012.
242. F. Šimkovic, A. Faessler, V. Rodin, P. Vogel, and J. Engel *Phys. Rev. C*, vol. 77, p. 045503, 2008.
243. R. Arnold *et al.* (The NEMO-3 Collaboration) *Phys. Rev. D*, vol. 93, p. 112008, 2016.
244. R. Arnold *et al.* (The NEMO-3 Collaboration) *Phys. Rev. D*, vol. 92, p. 072011, 2015, arXiv:1506.05825[nucl-ex].
245. R. Arnold *et al.* (The NEMO-3 Collaboration) *Phys. Rev. D*, vol. 94, p. 072003, 2016, arXiv:1606.08494 [hep-ex].
246. F.A. Danevich *et al.* (The CAMEO Collaboration) *Nucl. Phys. Proc. Suppl.*, vol. 138, p. 230, 2005.
247. K. Alfonso *et al.* (The CUORE Collaboration) *Phys. Rev. Lett.*, vol. 115, p. 102502, 2015.
248. A. Faessler, M. González, S. Kovalenko, and F. Šimkovic *Phys. Rev. D*, vol. 90, p. 096010, 2014.
249. S. Kovalenko, Z. Lu, and I. Schmidt *Phys. Rev. D*, vol. 80, p. 073014, 2009.
250. J. Menendez, A. Poves, E. Caurier, and F. Nowacki *Nucl. Phys. A*, vol. 818, p. 139, 2009.
251. M. Horoi and A. Neacsu *Phys. Rev. C*, vol. 93, p. 024308, 2016.
252. J. Barea, J. Kotila, and F. Iachello *Phys. Rev. C*, vol. 91, p. 034304, 2015.
253. D. Fang, A. Faessler, and F. Šimkovic *Phys. Rev. C*, vol. 92, p. 044301, 2015.
254. J. Hyvärinen and J. Suhonen *Phys. Rev. C*, vol. 91, p. 024613, 2015.
255. P. Rath, R. Chandra, P. Raina, K. Chaturvedi, and J. Hirsch *Phys. Rev. C*, vol. 85, p. 014308, 2012.
256. P. Beneš, A. Faessler, S. Kovalenko, and F. Šimkovic *Phys. Rev. D*, vol. 71, p. 077901, 2005.
257. M. Mitra, G. Senjanovic, and F. Vissani *Nucl. Phys. B*, vol. 856, p. 26, 2012.
258. T. Asaka and M. Shaposhnikov *Phys. Lett. B*, vol. 620, p. 17, 2005.
259. T. Asaka, S. Blanchet, and M. Shaposhnikov *Phys. Lett. B*, vol. 631, p. 151, 2005.
260. D. Štefánik, R. Dvornický, F. Šimkovic, and P. Vogel *Phys. Rev. C*, vol. 92, p. 055502, 2015.
261. P. B. Dev, S. Goswami, and M. Mitra *Phys. Rev. D*, vol. 91, p. 113004, 2015.
262. K. Muto, E. Bender, and H. Klapdor *Z. Phys. A*, vol. 334, p. 177, 1989.
263. R. Mohapatra *Nucl. Phys. B*, vol. 908, p. 423, 2016.
264. F. Šimkovic, G. Pantis, J. Vergados, and A. Faessler *Phys. Rev. C*, vol. 60, p. 055502, 1999.
265. A. Faessler, A. Meroni, S. T. Petcov, F. Šimkovic, and J. D. Vergados *Phys. Rev. D*, vol. 83, p. 113003, 2011.
266. A. Meroni, S. Petcov, and F. Šimkovic *JHEP*, vol. 02, p. 025, 2013.
267. R. Roth, T. Neff, H. Hergert, and H. Feldmeier *Nucl. Phys. A*, vol. 745, p. 3, 2004.
268. R. Sen'kov, M. Horoi, and B. Brown *Phys. Rev. C*, vol. 89, p. 054304, 2014.
269. A. Neacsu and M. Horoi *Phys. Rev. C*, vol. 91, p. 024309, 2015.
270. R. Sen'kov and M. Horoi *Phys. Rev. C*, vol. 93, p. 044334, 2016.
271. M. Mustonen and J. Engel *Phys. Rev. C*, vol. 87, p. 064302, 2013.
272. M. Kortelainen and J. Suhonen *Phys. Rev. C*, vol. 75, p. 051303(R), 2007.
273. M. Kortelainen, O. Civitarese, J. Suhonen, and J. Toivanen *Phys. Lett. B*, vol. 647, p. 128, 2007.

274. M. Kortelainen and J. Suhonen *Phys. Rev. C*, vol. 76, p. 024315, 2007.
275. J. Terasaki *Phys. Rev. C*, vol. 93, p. 024317, 2016.
276. P. Rath, R. Chandra, K. Chaturvedi, P. Lohani, P. Raina, and J. Hirsch *Phys. Rev. C*, vol. 88, p. 064322, 2013.
277. T. Rodriguez and G. Martinez-Pinedo *Phys. Rev. Lett.*, vol. 105, p. 252503, 2010.
278. S. Stroberg, H. Hergert, J. Holt, S. Bogner, and A. Schwenk *Phys. Rev. C*, vol. 93, p. 051301, 2016.
279. H. Hergert, S. K. Bogner, T. D. Morris, A. Schwenk, and K. Tsukiyama *Phys. Rept.*, vol. 621, p. 165, 2016.
280. M. Schuster, S. Quaglioni, C. Johnson, E. Jurgenson, and P. Navratil *Phys. Rev. C*, vol. 90, p. 011301, 2014.
281. P. Navratil, S. Quaglioni, G. Hupin, C. Romero-Redondo, and A. Calci *Physica Scripta*, vol. 91, p. 053002, 2016.
282. V. Rodin, A. Faessler, F. Šimkovic, and P. Vogel *Phys. Rev. C*, vol. 68, p. 044302, 2003.
283. V. Rodin, A. Faessler, F. Šimkovic, and P. Vogel *Nucl. Phys. A*, vol. 766, p. 107, 2006.
284. S. Freeman and J. Schiffer *J. Phys. G*, vol. 39, p. 124004, 2012.
285. B. Kay *et al.* *Phys. Rev. C*, vol. 79, p. 121301, 2009.
286. J. Thomas *et al.* *Phys. Rev. C*, vol. 86, p. 047304, 2012.
287. B. Kay *et al.* *Phys. Rev. C*, vol. 87, p. 011302(R), 2013.
288. J. Entwisle *et al.* *Phys. Rev. C*, vol. 93, p. 064312, 2016.
289. K. Yako *et al.* *Phys. Rev. Lett.*, vol. 103, p. 012503, 2009.
290. P. Vogel and M. Zirnbauer *Phys. Rev. C*, vol. 37, p. 731, 1988.
291. D. Štefánik, F. Šimkovic, and A. Faessler *Phys. Rev. C*, vol. 91, p. 064311, 2015.
292. E. Caurier and F. Nowacki *Phys. Lett. B*, vol. 711, p. 62, 2012.
293. J. Barea, J. Kotila, and F. Iachello *Phys. Rev. C*, vol. 87, p. 014315, 2013.
294. A. Faessler, G. Fogli, E. Lisi, V. Rodin, A. Rotunno, and F. Šimkovic *J. Phys. G*, vol. 35, p. 075104, 2008.
295. F.F. Deppisch and J. Suhonen, arXiv:1606.02908 [nucl-th].
296. J. Menéndez, D. Gazit, and A. Schwenk *Phys. Rev. Lett.*, vol. 107, p. 062501, 2011.
297. J. Engel, F. Šimkovic, and P. Vogel *Phys. Rev. C*, vol. 89, p. 064308, 2014.
298. J. Engel *J. Phys. G*, vol. 42, p. 034017, 2015.
299. A. Faessler, G. Fogli, E. Lisi, V. Rodin, and F. Šimkovic *Phys. Rev. D*, vol. 79, p. 053001, 2009.
300. E. Lisi, A. Rotunno, and F. Šimkovic *Phys. Rev. D*, vol. 92, p. 093004, 2015.